Climate Forcing

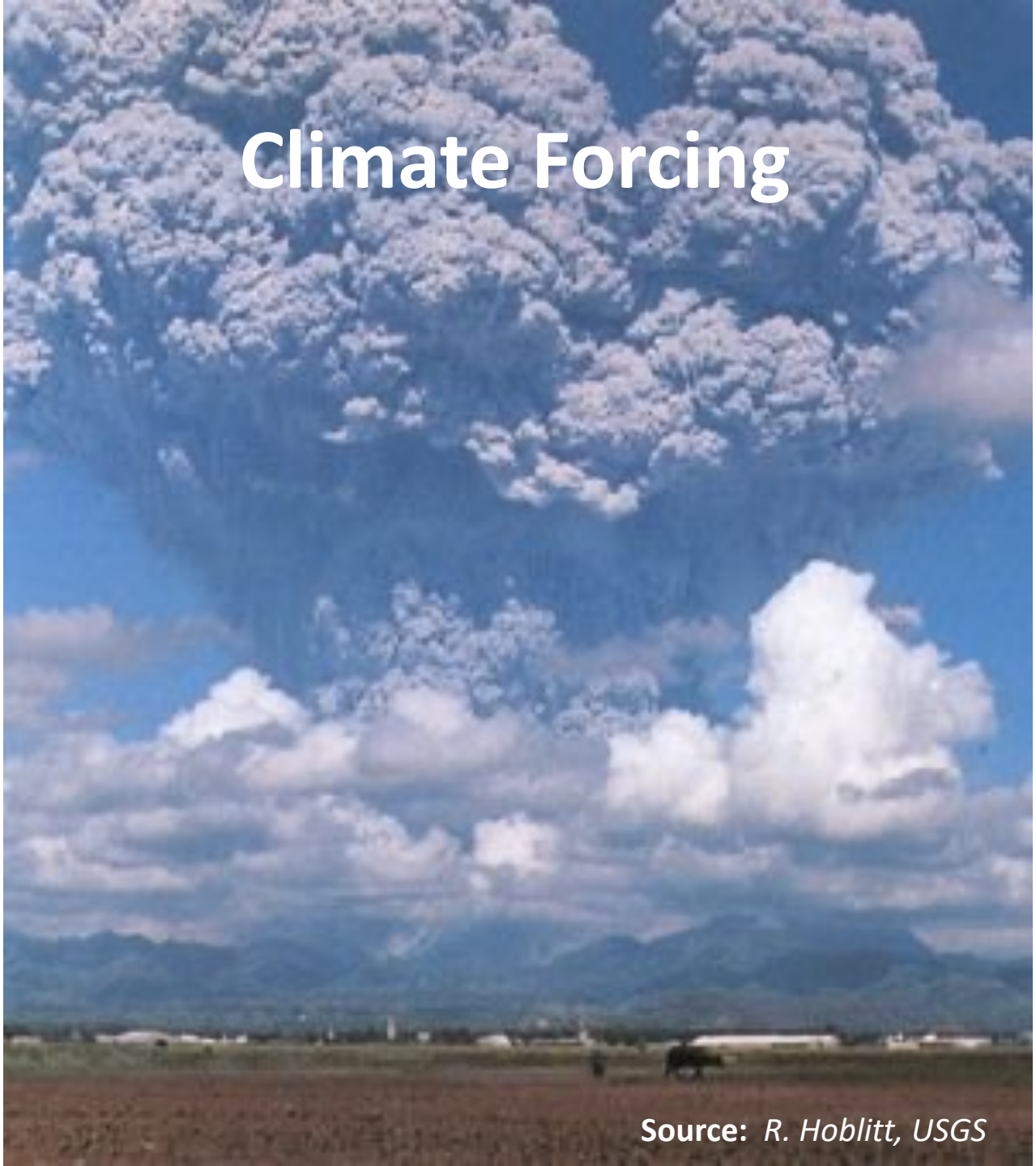

Source: *R. Hoblitt, USGS*

Forcing can be considered on several timescales:

"Tectonic" (orogenic/eustatic/glacio-isostatic)

Orbital or glacial-interglacial –Milankovic (eccentricity/obliquity/precession)

~100,000; 40,000; 23,000/19,000 years

Millennial to centennial

solar irradiance

thermohaline oscillations ("internal" variability?)

Decadal-to-interannual

volcanic

ENSO/NAO/PDO ("internal" variability?)

Feedbacks? Vegetation/hydrological changes; snow/sea-ice cover

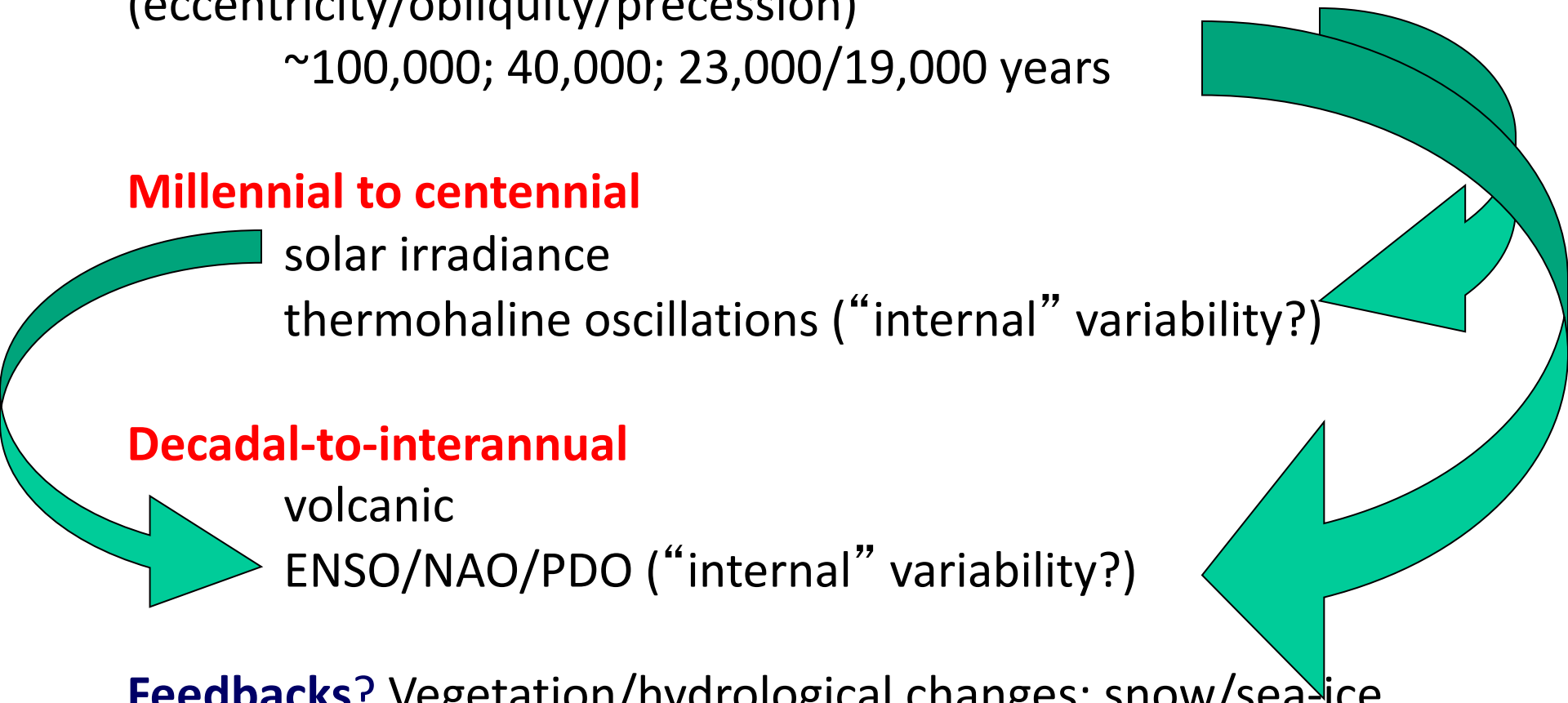

Forcing can be considered on several timescales:

"Tectonic" (orogenic/eustatic/glacio-isostatic)

Orbital –Milankovic (eccentricity/obliquity/precession)
~100,000; 40,000; 23,000/19,000 years

Millennial to centennial
solar irradiance
thermohaline oscillations ("internal" variability?)

Decadal-to-interannual
ENSO/NAO/PDO ("internal" variability?)
volcanic

Feedbacks? Vegetation/hydrological changes; snow/sea-ice cover

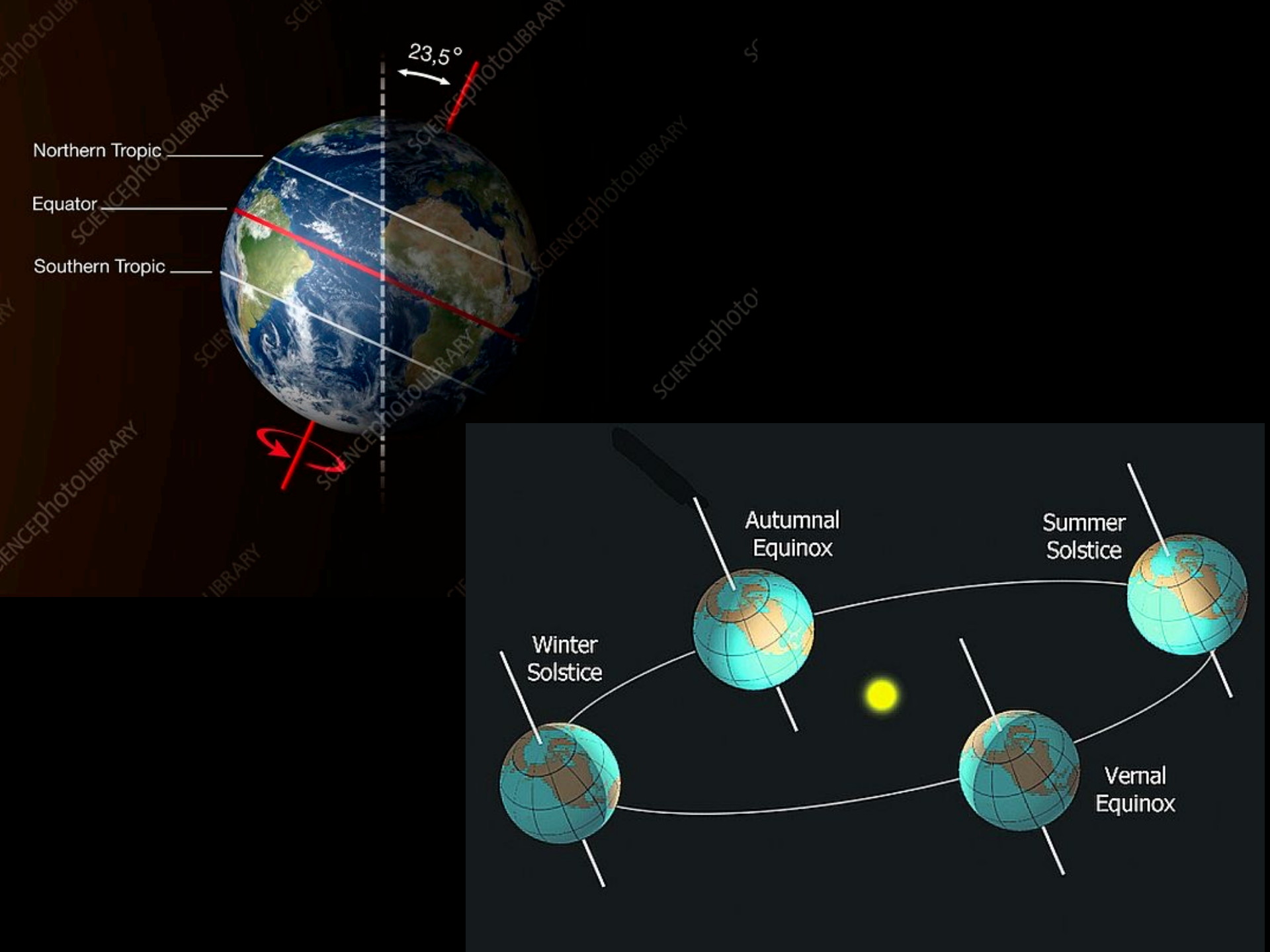
23,5°
Northern Tropic
Equator
Southern Tropic
Autumnal Equinox
Summer Solstice
Winter Solstice
Vernal Equinox

Theory of the astronomical cause of the Ice Age (known as Milankovitch theory)

Milutin Milankovitch (1989-1958)

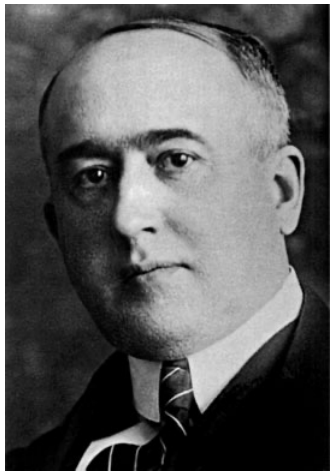

Wladimir Peter Koppen (1846-1940)

Alfred Wegener (1880-1930)

Milankovitch Theory :

Astronomical Control of *Insolation*

- La órbita de la Tierra es variable, ¿y qué?
  Un control importante sobre el clima.
  Escalas de tiempo de decenas a cientos de miles de años.

¿Hipótesis de Milankovitch? La insolación del verano en el hemisferio norte controla el crecimiento de las capas de hielo.

-

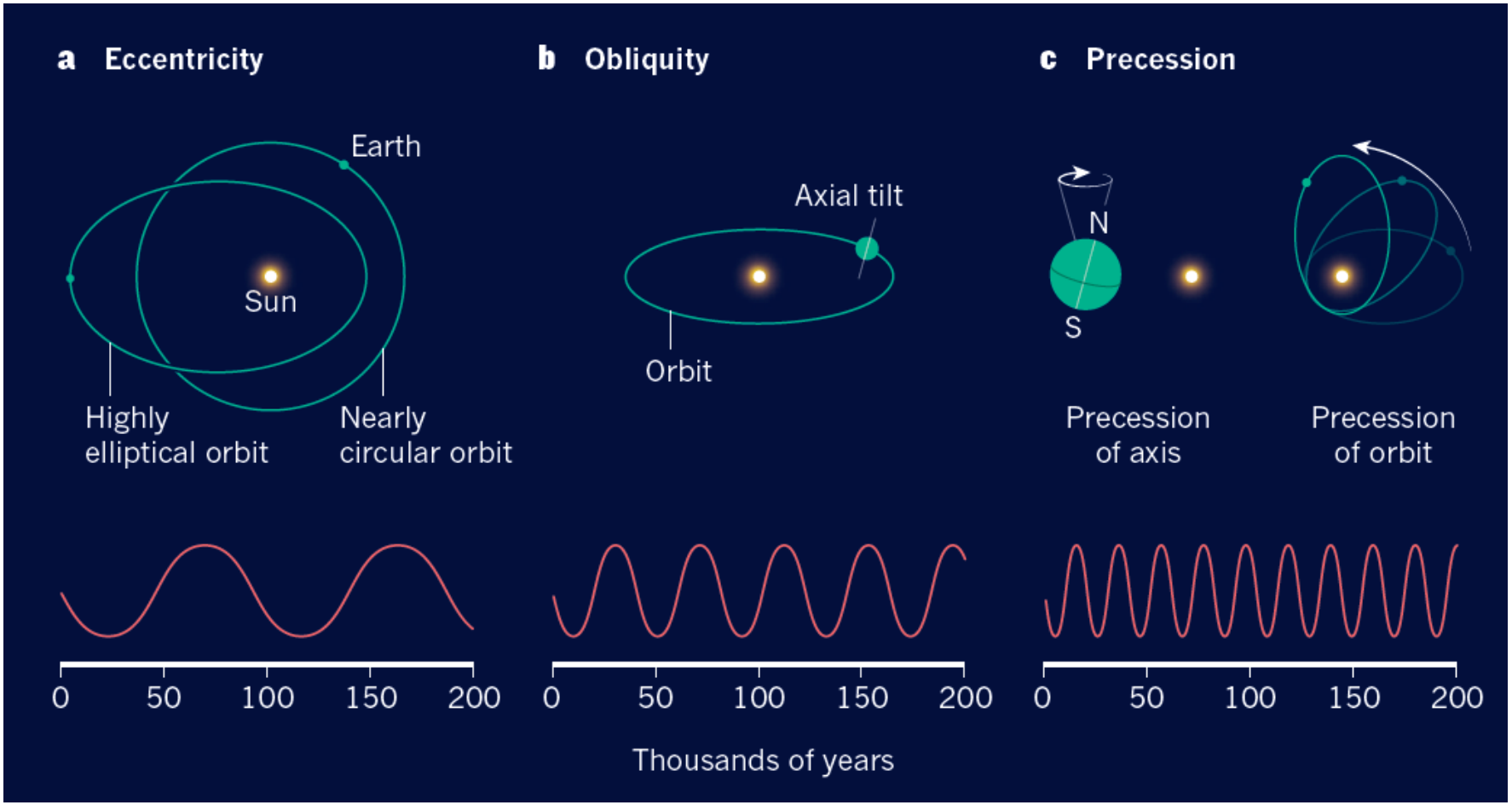
a Eccentricity
Earth
Sun
Highly elliptical orbit
Nearly circular orbit
b Obliquity
Axial tilt
Orbit
c Precession
N
S
Precession of axis
Precession of orbit
0 50 100 150 200
0 50 100 150 200
0 50 100 150 200
Thousands of years

Maslin, 2016

Earth's Eccentric Orbit: Distance Between Earth and Sun

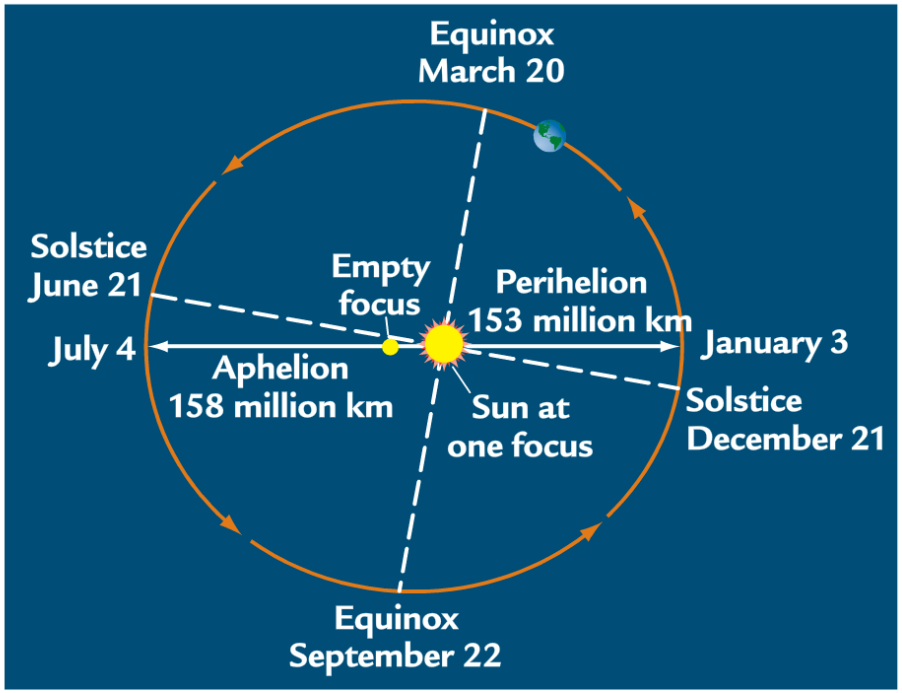

FIGURE 8-2

Earth's eccentric orbit

Earth's orbit around the Sun is slightly elliptical. Earth is most distant from the sun at aphelion, on July 4, just after the June 21 solstice, and closest to the Sun at perihelion, on January 3, just after the December 21 solstice. (MODIFIED FROM J. IMBRIE AND K. P. IMBRIE, *ICE AGES: SOLVING THE MYSTERY* [SHORT HILLS, NJ: ENSLOW, 1979].)

- **Effect on insolation is small (~3%)**
- **Seasons mostly due to tilt**
- **Timing of equinoxes not symmetric**

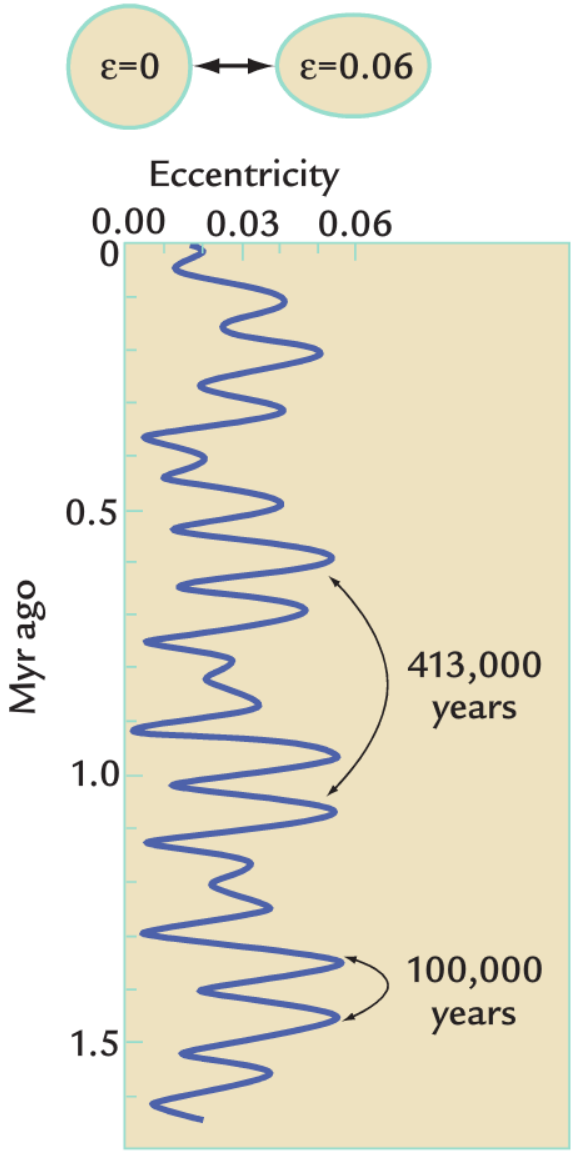

FIGURE 8-7

Long-term changes in eccentricity

The eccentricity (ε) of Earth's orbit varies at periods of 100,000 and 413,000 years.

Tilt of Earth's Spin Axis, II

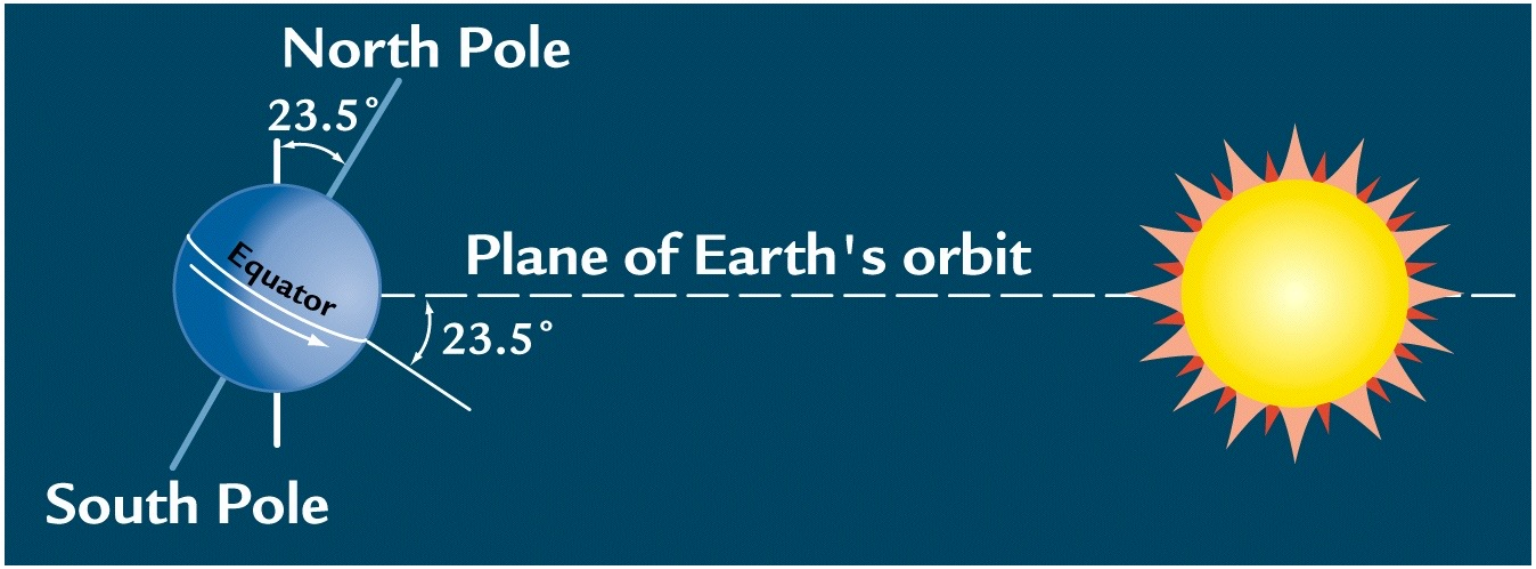

- **Ángulo y Dirección de la Inclinación de la Tierra**
- **Ángulo y Dirección**: Constantes a corto plazo.
- **Variabilidad**: Cambian a largo plazo, en miles de años.
- **Estaciones**: Responsable de las estaciones.
- **Solsticios**:
  - Días más cortos y más largos del año.
  - Fechas: 21/6 y 21/12.
- **Equinoccios**:
  - Duración igual de días y noches.
  - Fechas: 20/3 y 22/9.

Tilt of Earth's Spin Axis, I

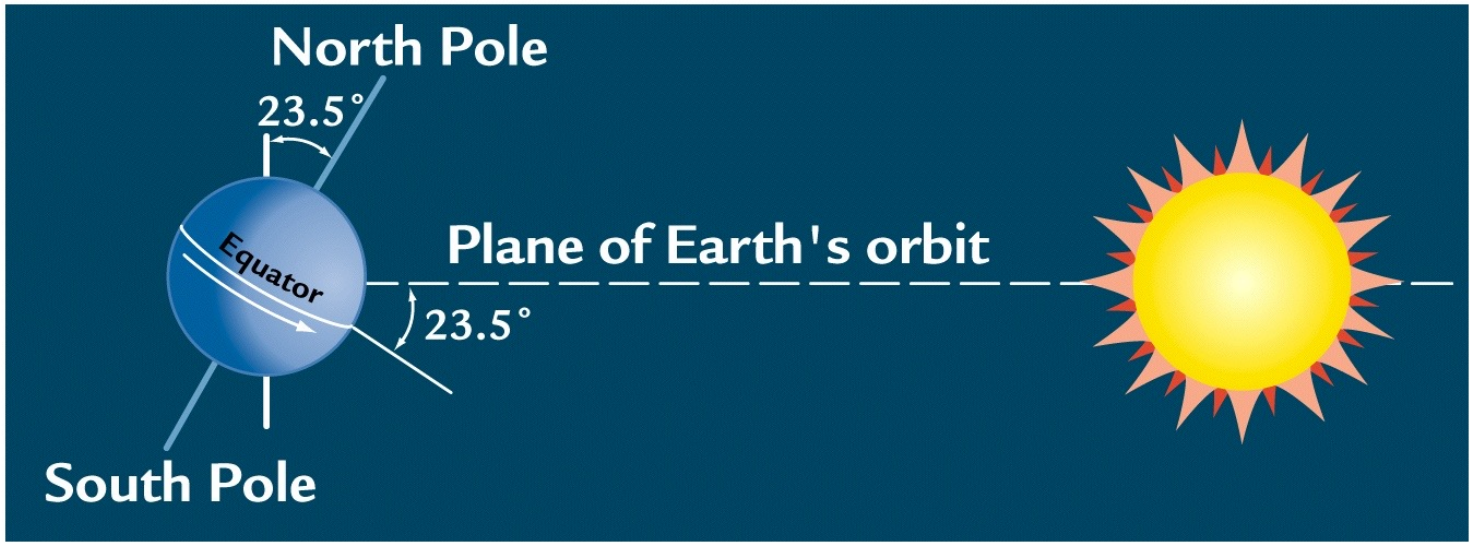

- **Trópicos y Círculos Polares**
- **Trópico de Cáncer y Trópico de Capricornio**:
  - Latitudes de ±23.5˚.
  - Son las líneas donde el sol está directamente sobre la cabeza al mediodía en el día más largo del año.
- **Círculos Ártico y Antártico**:
  - Latitudes de ±66.5˚.
  - Son las líneas donde no hay luz solar en latitudes más altas durante el día más corto del invierno.

In Summary, changes in tilt mainly amplify or suppress the seasons, particularly at the poles.

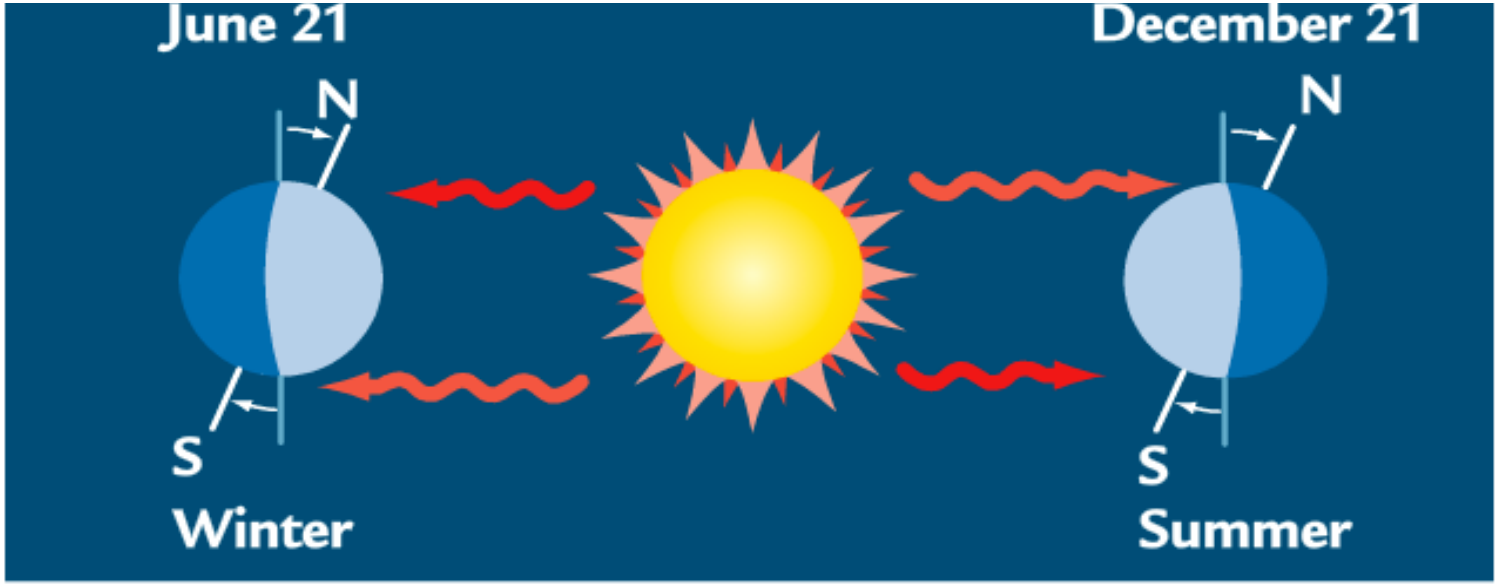

FIGURE 8-5

Effects of increased tilt on polar regions

Increased tilt brings more solar radiation to the poles in the

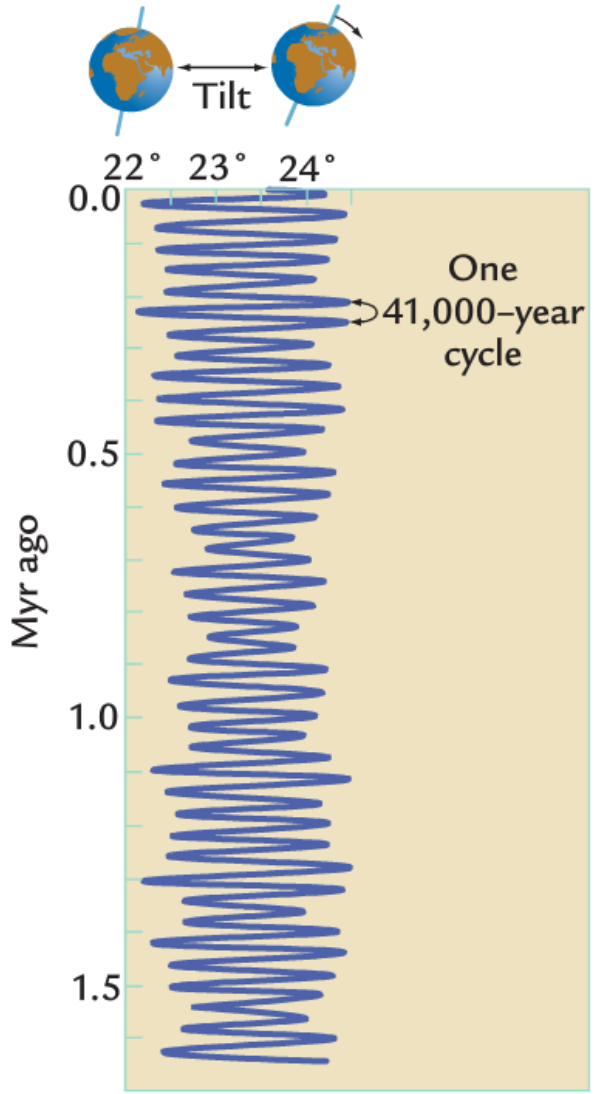

FIGURE 8-4

Long-term changes in tilt

Changes in the tilt of Earth's axis have occurred in a regular 41,000-year cycle.

8-5 Precession of the Solstices and Equinoxes Around Earth's Orbit

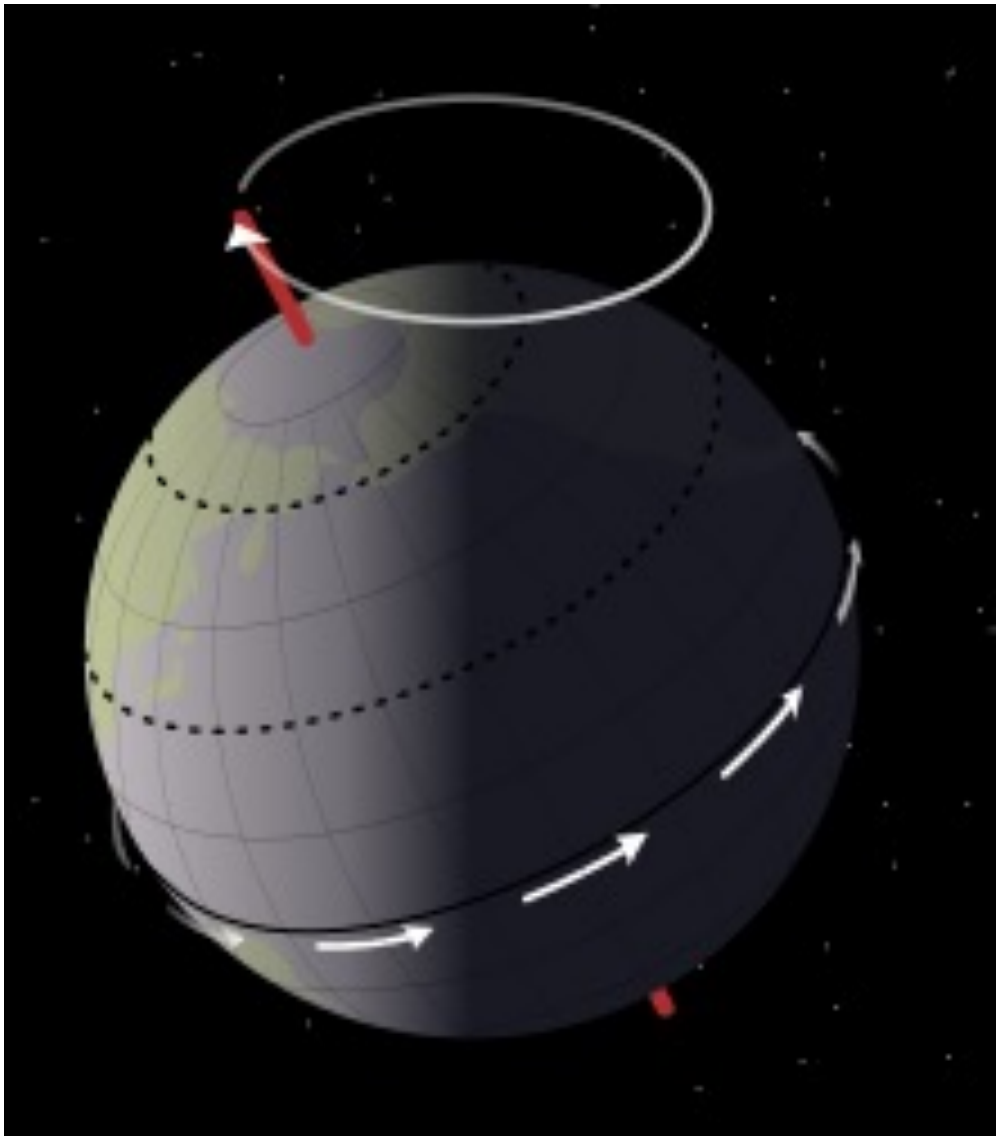

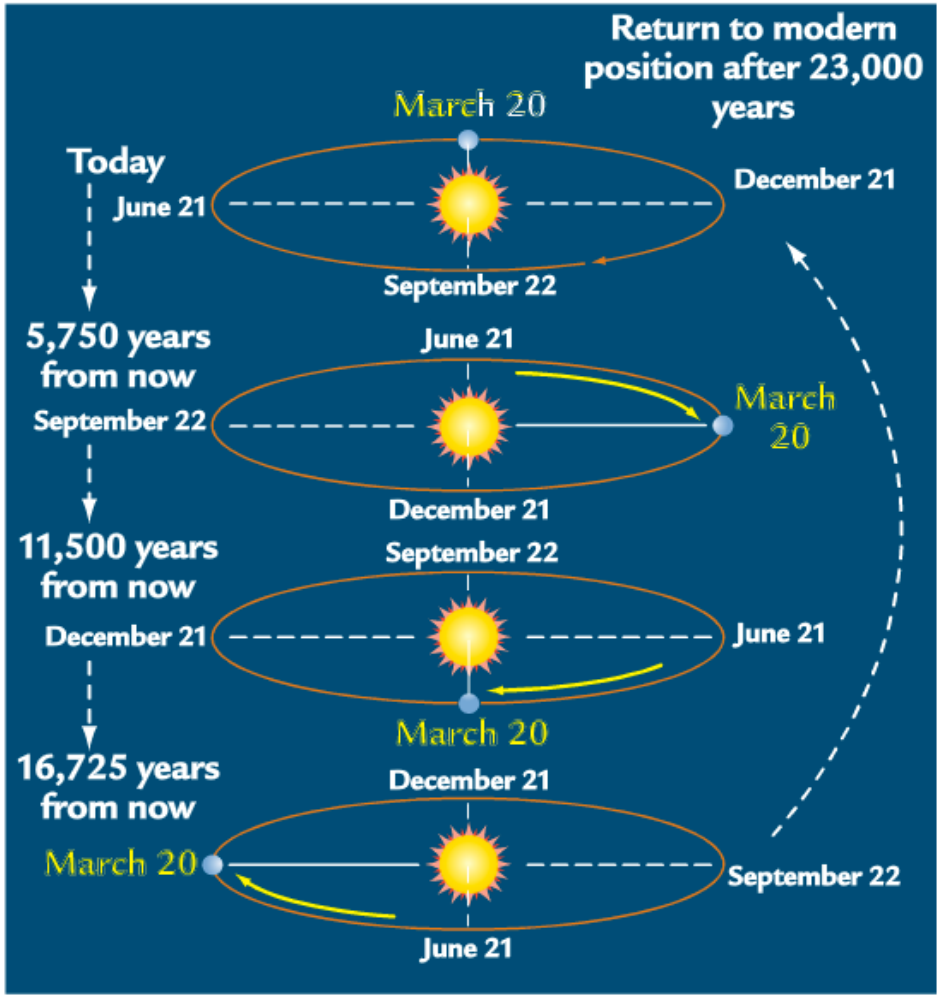

FIGURE 8-11

Precession of the equinoxes

Earth's wobble and the slow turning of its elliptical orbit combine to produce the precession of the equinoxes. Both the solstices and equinoxes move slowly around the eccentric orbit in cycles of 23,000 years. (ADAPTED FROM J. IMBRIE AND K. P. IMBRIE, *ICE AGES: SOLVING THE MYSTERY* [SHORT HILLS, NJ: ENSLOW, 1979].)

June and December insolation changes at different latitudes over the last 300 thousand years

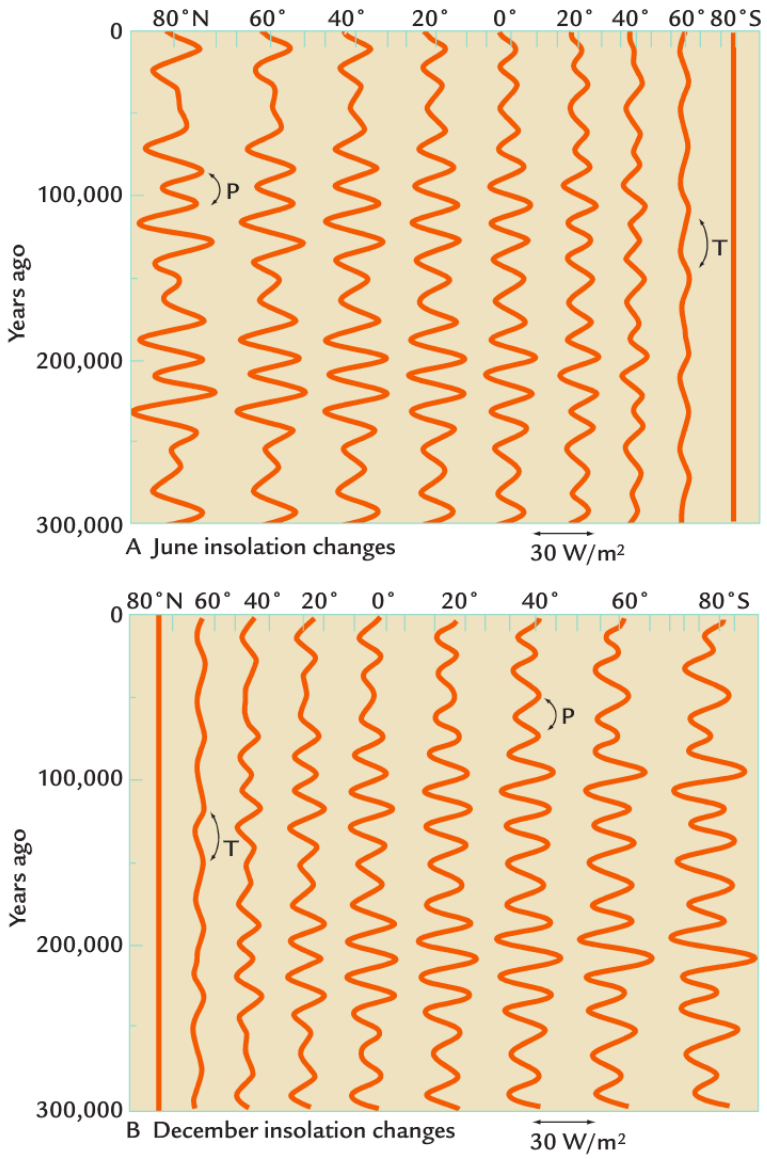

In Summary, monthly seasonal insolation changes are dominated by precession at low and middle latitudes, with the effects of tilt evident only at higher latitudes.

FIGURE 8-16

June and December insolation variations

June and December monthly insolation values show the prevalence of precessional changes at low and middle latitudes and the presence of tilt changes at higher latitudes. Cycles of tilt and precession are indicated by *T* and *P*. The double arrows indicate variations of 30 W/m^2 for these signals.

Ice volume

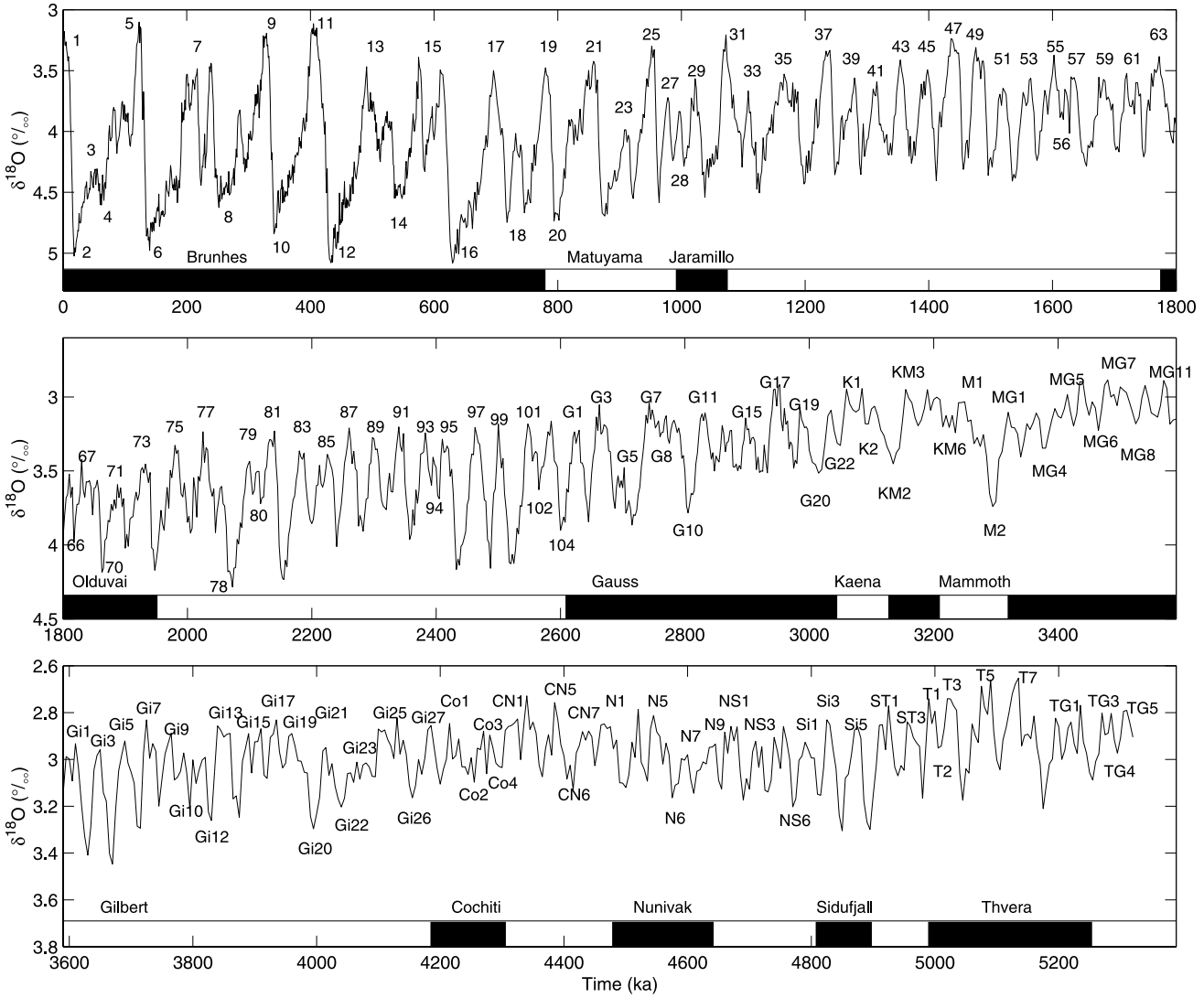

Figure 4. The LR04 benthic $\delta^{18}O$ stack constructed by the graphic correlation of 57 globally distributed benthic $\delta^{18}O$ records. The stack is plotted using the LR04 age model described in section 5 and with new MIS labels for the early Pliocene (section 6.2). Note that the scale of the vertical axis changes across panels.

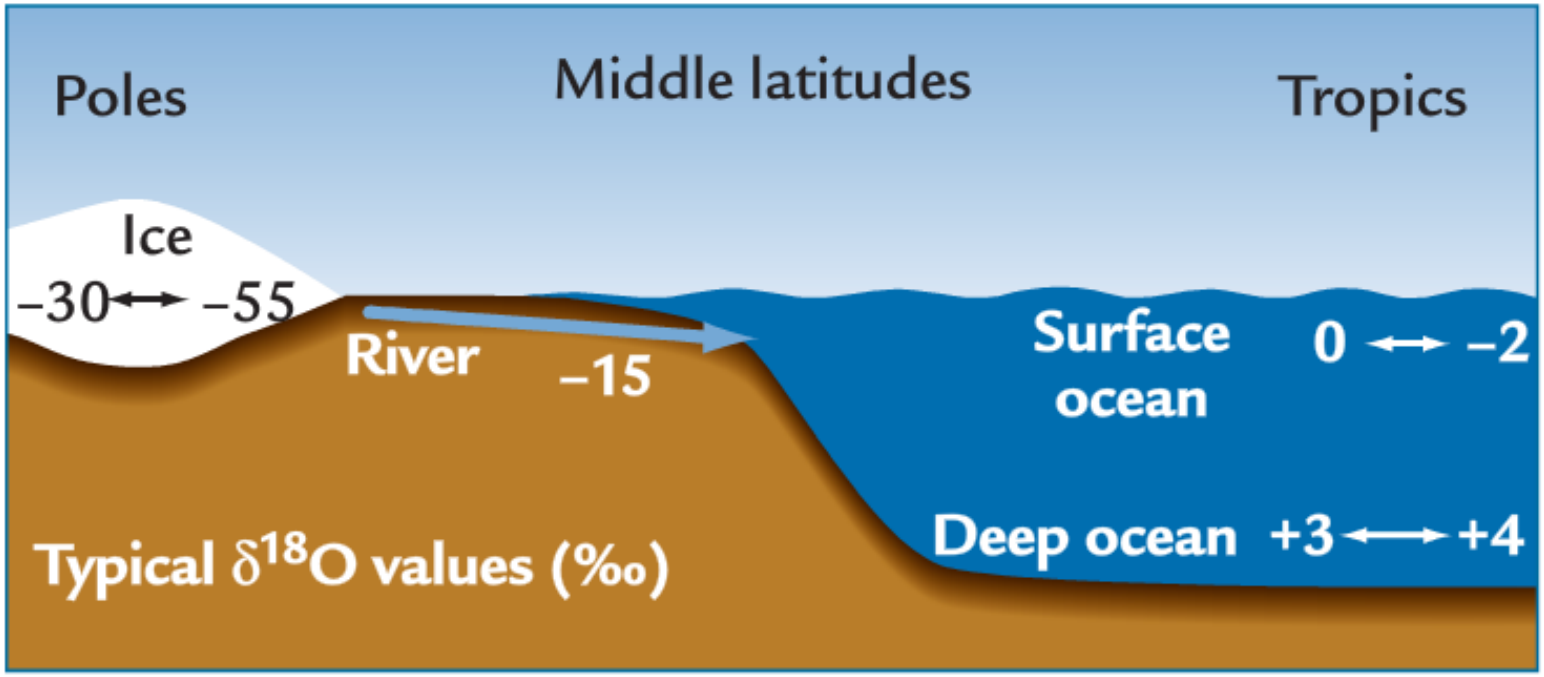

FIGURE-1

$\delta^{18}O$ values in the modern world

In the modern ocean, $\delta^{18}O$ values vary from 0 to -2‰ in warm tropical surface waters to as much as $+3$ to $+4$‰ in cold deep-ocean waters. In present ice sheets, typical $\delta^{18}O$ values reach -30‰ in Greenland and -55‰ in Antarctica.

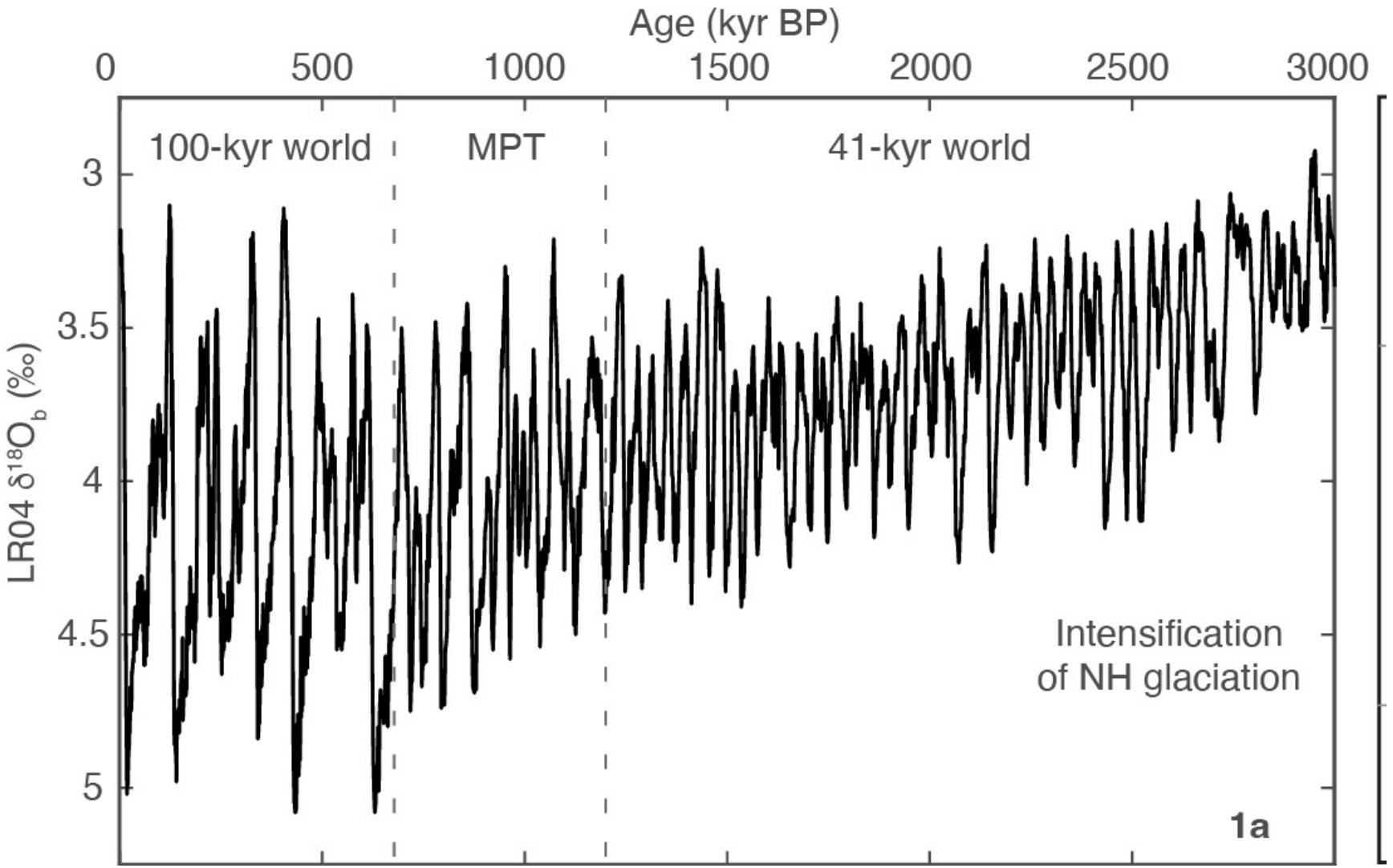
Age (kyr BP)
0
500
1000
1500
2000
2500
3000
100-kyr world
MPT
41-kyr world
3
3.5
4
4.5
5
LR04 δ18Ob (‰)
Intensification
of NH glaciation
1a

Hipótesis sobre el Conductor del MPT:

- **Eliminación de Regolito**:
  - Cambió la dinámica de la capa de hielo, lo que llevó a capas de hielo más grandes y a ciclos glaciares de ~100 mil años (Clark y Pollard 1998).
- **Enfriamiento a Largo Plazo**:
  - El aumento en el umbral de insolación para la desglaciación llevó a ciclos de oblicuidad omitidos y a capas de hielo más grandes (Tzedakis et al. 2017).
- **Efecto Combinado**:
  - Enfriamiento a largo plazo debido a la disminución de CO_2 y eliminación de regolito (Willeit et al. 2019).
- **Crecimiento de la Capa de Hielo Antártica**:
  - Cambió la circulación oceánica y el almacenamiento de carbono, llevando a capas de hielo más grandes en el Hemisferio Norte y al ciclo de 100 mil años (Farmer et al. 2019; Ford y Raymo 2020; Peña y Goldstein 2014).
- **Fortalecimiento del Flujo Atlántico**:
  - Aumentó el transporte de humedad hacia el polo, lo que llevó a capas de hielo más grandes y a un cambio de ~41 a ~100 mil años de periodicidad (Barker et al. 2021).
- **Transicion conducida por el switch de CO_2 de 41 a ~100 mil años** (Medina-Elizalde et al., 2005, 2010, Lawrence et al., 2010)

Science

HOME > SCIENCE > VOL. 289, NO. 5486 >

The 100,000-Year Ice-Age Cycle Identified and Found to Lag Temperature, Carbon Dioxide, and Orbital Eccentricity

Nicholas J. Shackleton

The deep-sea sediment oxygen isotopic composition ($\delta^{18}O$) record is dominated by a 100,000-year cyclicity that is universally interpreted as the main ice-age rhythm. Here, the ice volume component of this $\delta^{18}O$ signal was extracted by using the record of $\delta^{18}O$ in atmospheric oxygen trapped in Antarctic ice at Vostok, precisely orbitally tuned. The benthic marine $\delta^{18}O$ record is heavily contaminated by the effect of deep-water temperature variability, but by using the Vostok record, the $\delta^{18}O$ signals of ice volume, deep-water temperature, and additional processes affecting air $\delta^{18}O$ (that is, a varying Dole effect) were separated. At the 100,000-year period, atmospheric carbon dioxide, Vostok air temperature, and deep-water temperature are in phase with orbital eccentricity, whereas ice volume lags these three variables. Hence, the 100,000-year cycle does not arise from ice sheet dynamics; instead, it is probably the response of the global carbon cycle that generates the eccentricity signal by causing changes in atmospheric carbon dioxide concentration.

Fig. 5. Linear variance spectra obtained by cross-spectral analysis versus ETP (*25*) of (**A**) deep-Pacific temperature, (**B**) ocean $\delta^{18}O$ is, with reference to insolation in the Northern Hemisphere midsummer). Arrows labeled "e," "t," and "p" identify the frequencies associated with eccentricity, obliquity (tilt), and precession. The bar labeled "BW" indicates the bandwidth.

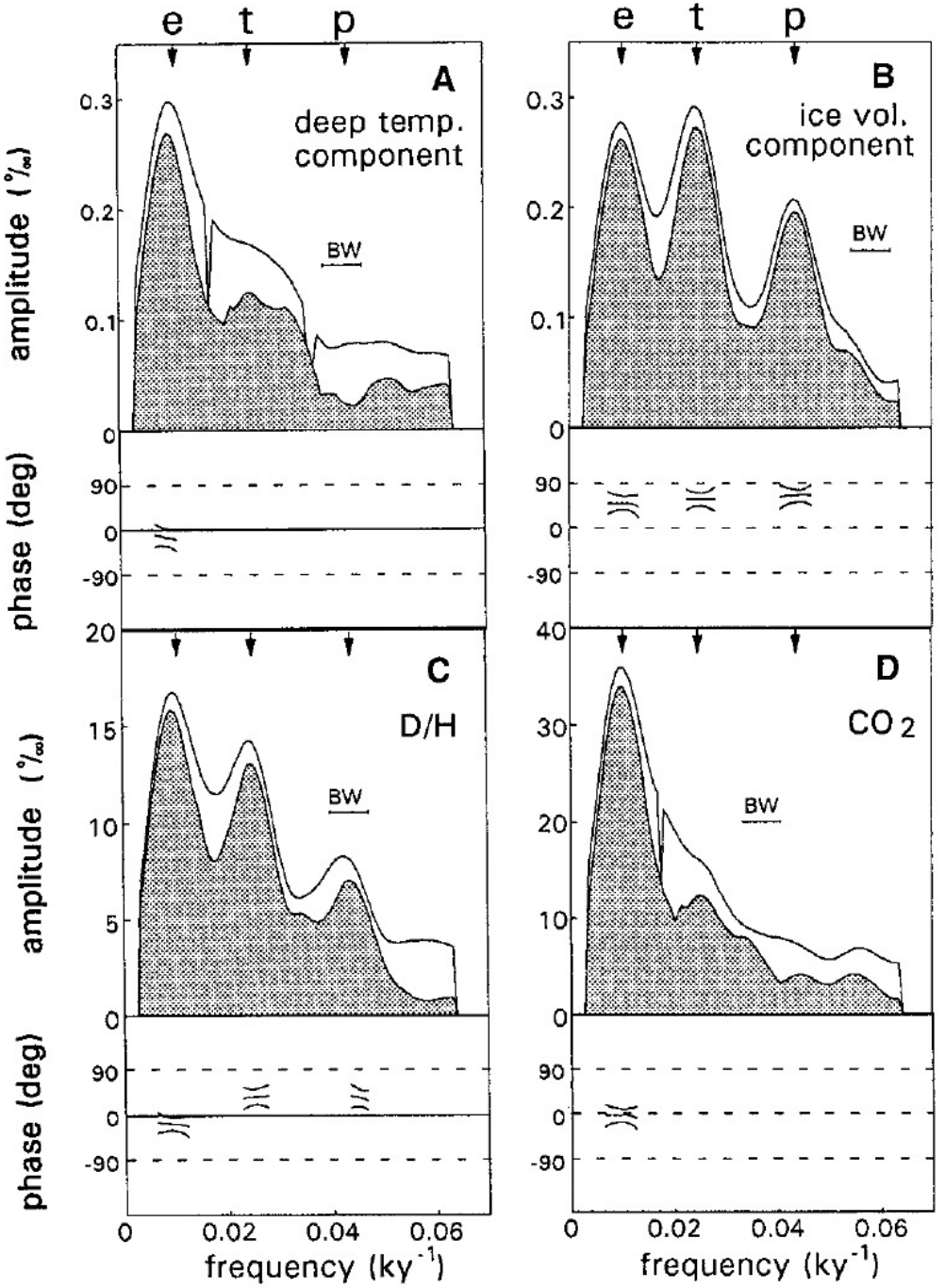

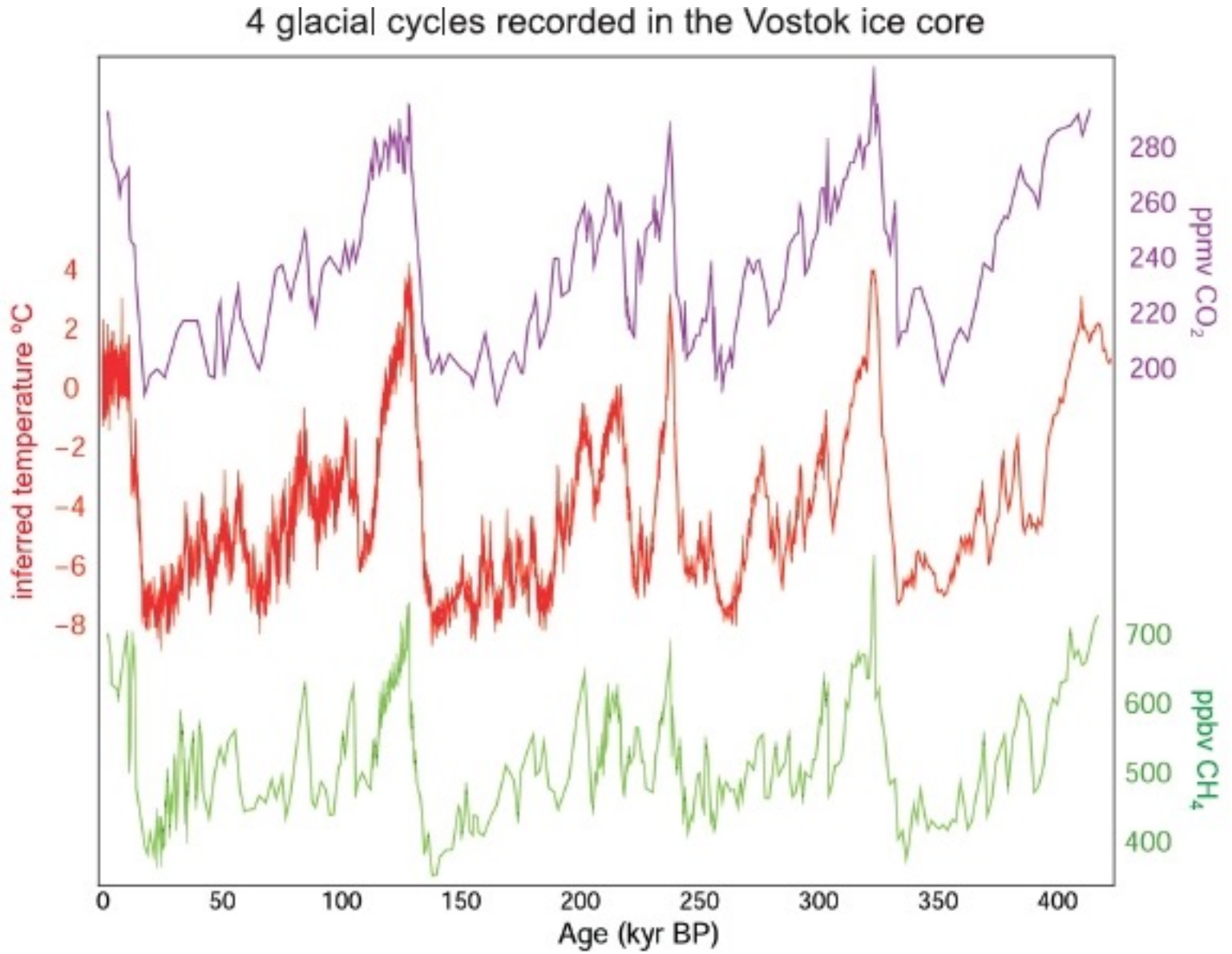

Figure 1. Variations in local Antarctic atmospheric temperature, as derived from oxygen isotope data, as well as concentrations of atmospheric CO_2 and CH_4 from Vostok, Antarctica ice core records. Figure redrawn from Petit et al. (1999).

Climate Feedback

A process internal to the climate system that is triggered by a temperature change, that either reinforces, weakens or cou

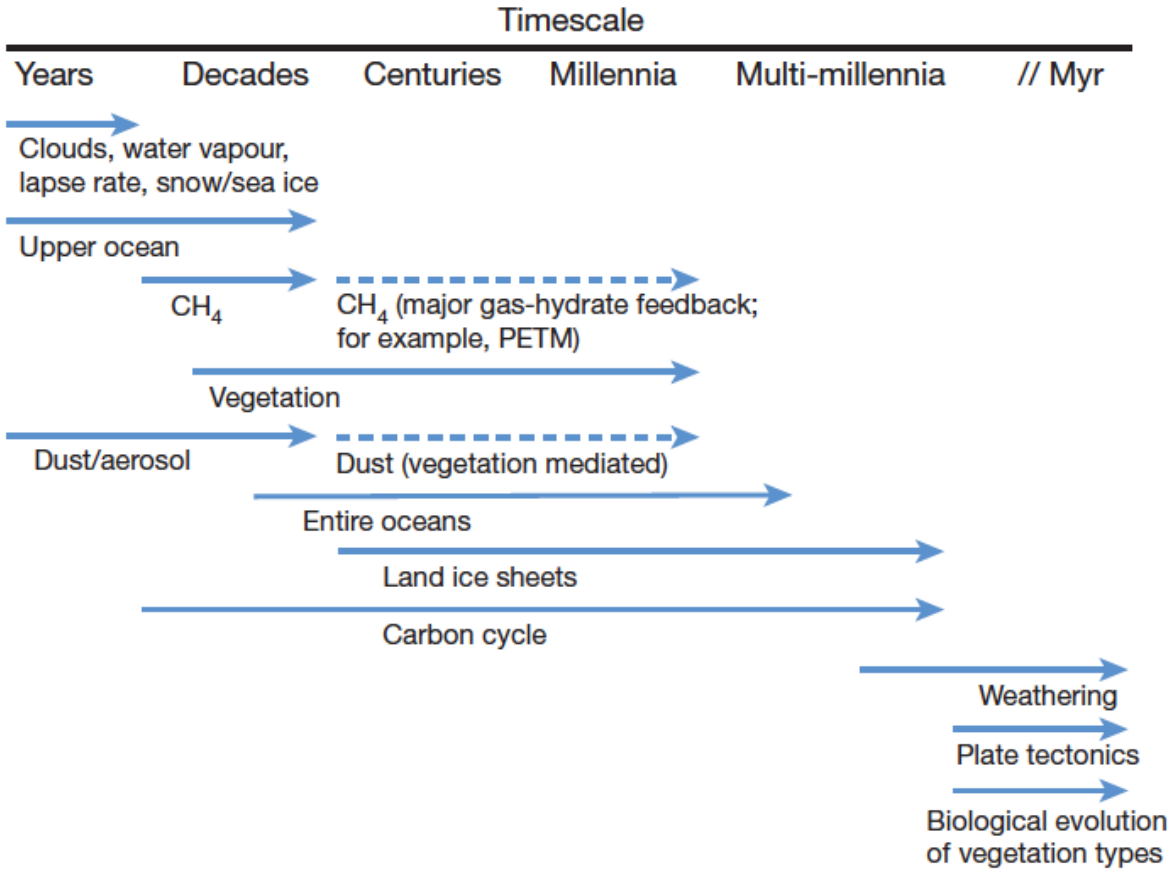

Radiative ‘forcing’ (slow feedbacks)

- GHG based on Antarctic ice-core CO_2 and CH_4 (and N_2O) data, converted to radiative forcing anomalies using equations from IPCC and Hansen et al. (2007, 2008)

- Surface albedo changes based on Red Sea sea-level reconstruction (Rohling et al., 2009, 2010) and conversion to radiative forcing changes after Hansen et al. (2007, 2008)

- Dust/Aerosol data from Antarctic ice-core records, and conversion to radiative forcing anomalies after Köhler et al. (2010)

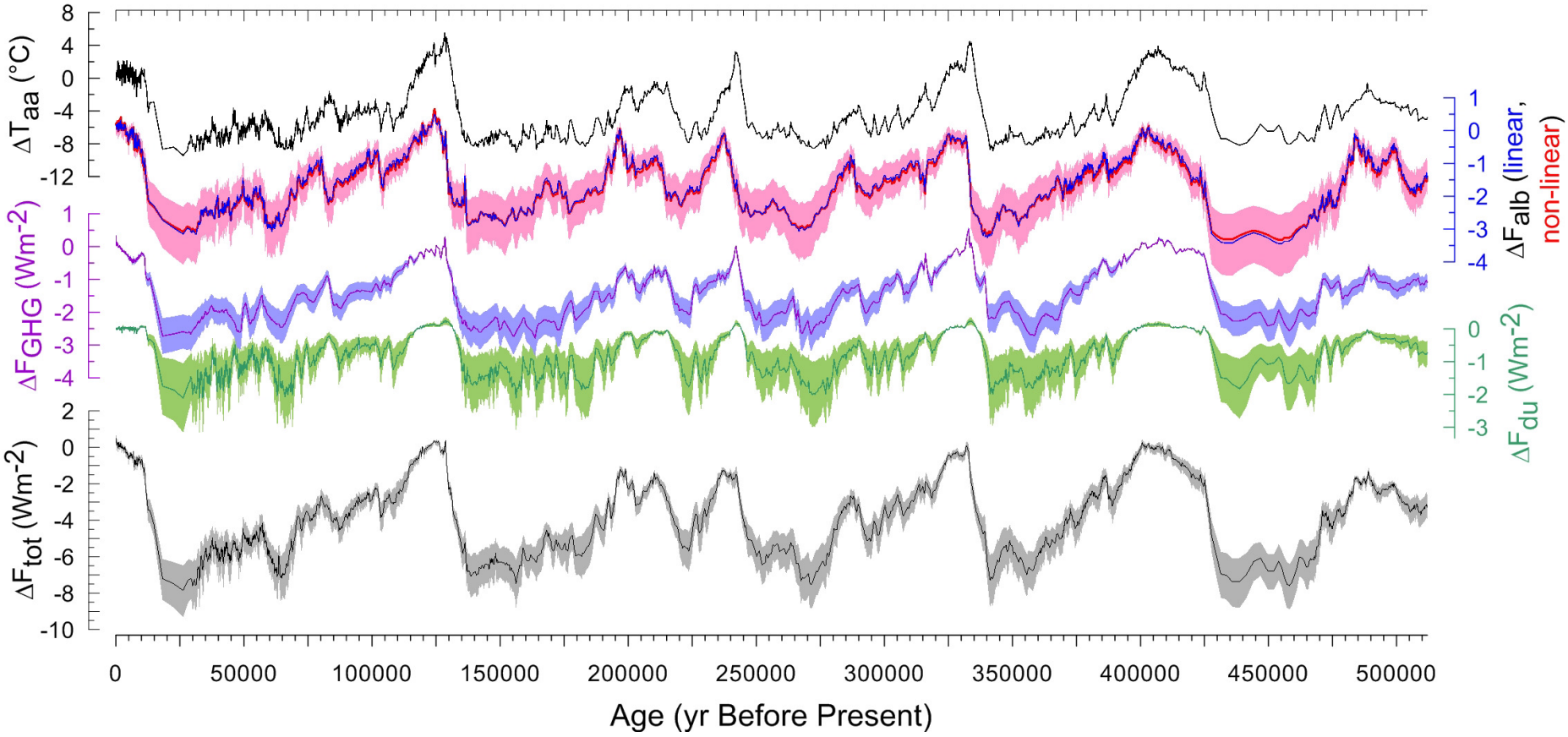

Source: Rohling, Medina-Elizalde et al., J. Climate 2011

Radiative forcings not evenly distributed around the globe

Approach: Global mean influence per type of forcing consists of area-weighted sum of impacts per 10° Latitude band: $\Delta F_{loc} = (m/f)\ \Delta F_{glob\ mean}$

Meridional distribution determined using a muliplier (*m*) for the 'loading' per 10° latitude band, and the fraction of earth's surface per 10° latitude band (*f*).

Meridional distribution for GHG influences from Ramanatan et al. (1979)

Meridional distribution for ice-sheet albedo influences from Broccoli (2001)

Meridional distribution for dust/aerosol forcing influences from Claquin et al. (2003)

Reference albedo distribution (interglacial state) after Fasullo and Trenberth (2008).

Latter is needed, together with the albedo changes through time from ice-sheet effects, to calculate the *absorbed* component of insolation (orbital calculations give Top of Atmosphere)

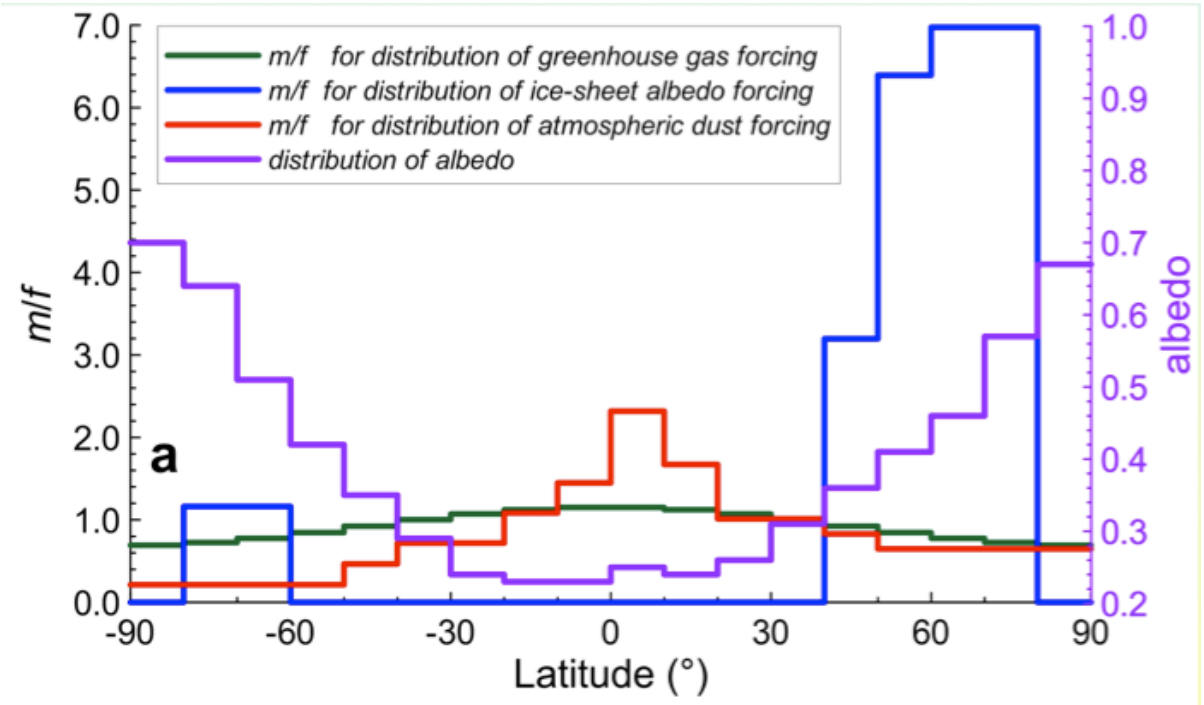

Papel de insolación durante el Holoceno temprano

Radiation at the top of the atmosphere (W m^{-2})

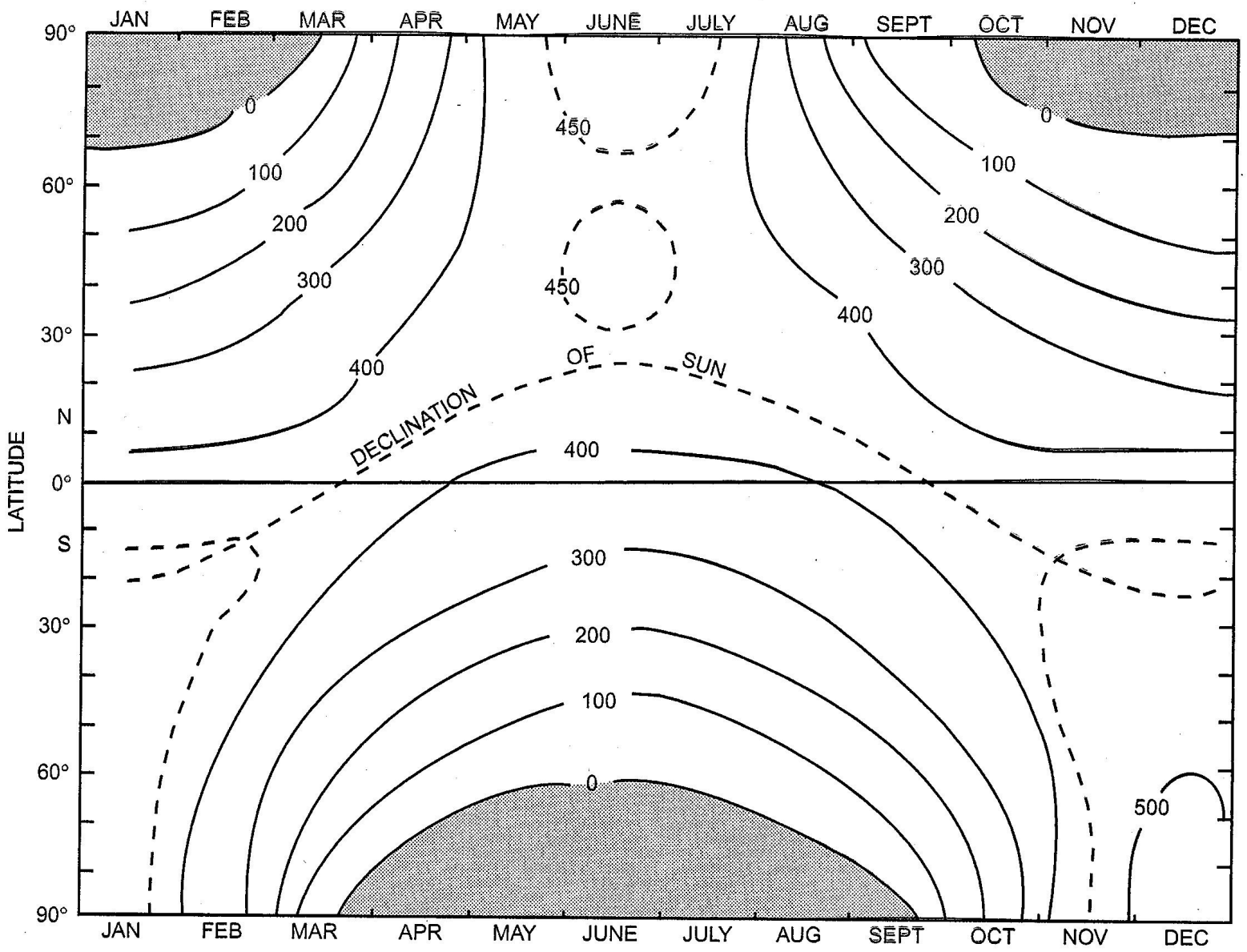

A moment in time……9,000 years B.P.
-- changes with season & latitude

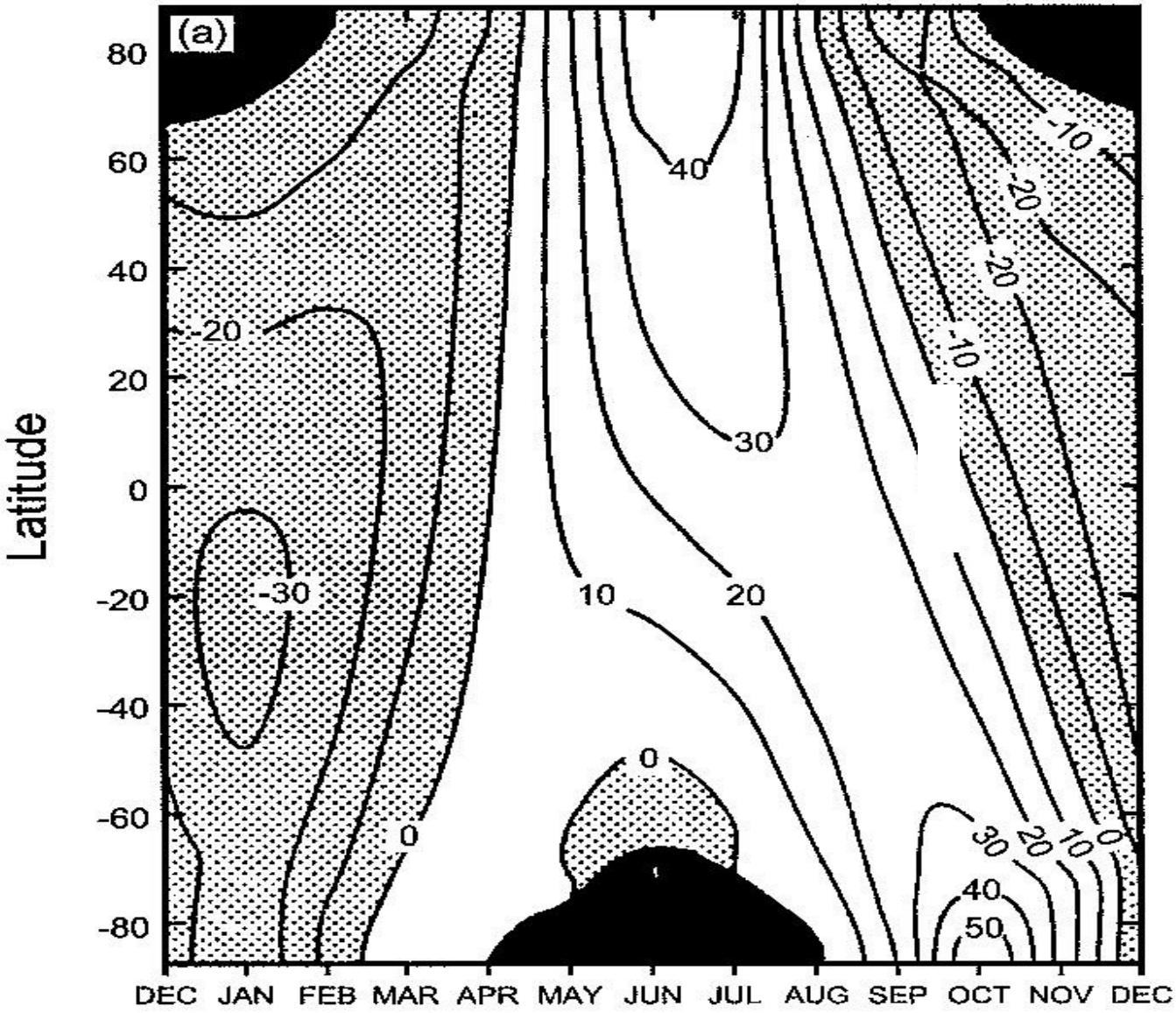

Difference in solar radiation in W m^{-2}, at 9ka B.P. compared to present.

Source: *Mitchell et al, 1988*

A moment in time……9,000 years B.P.
-- changes with season & latitude

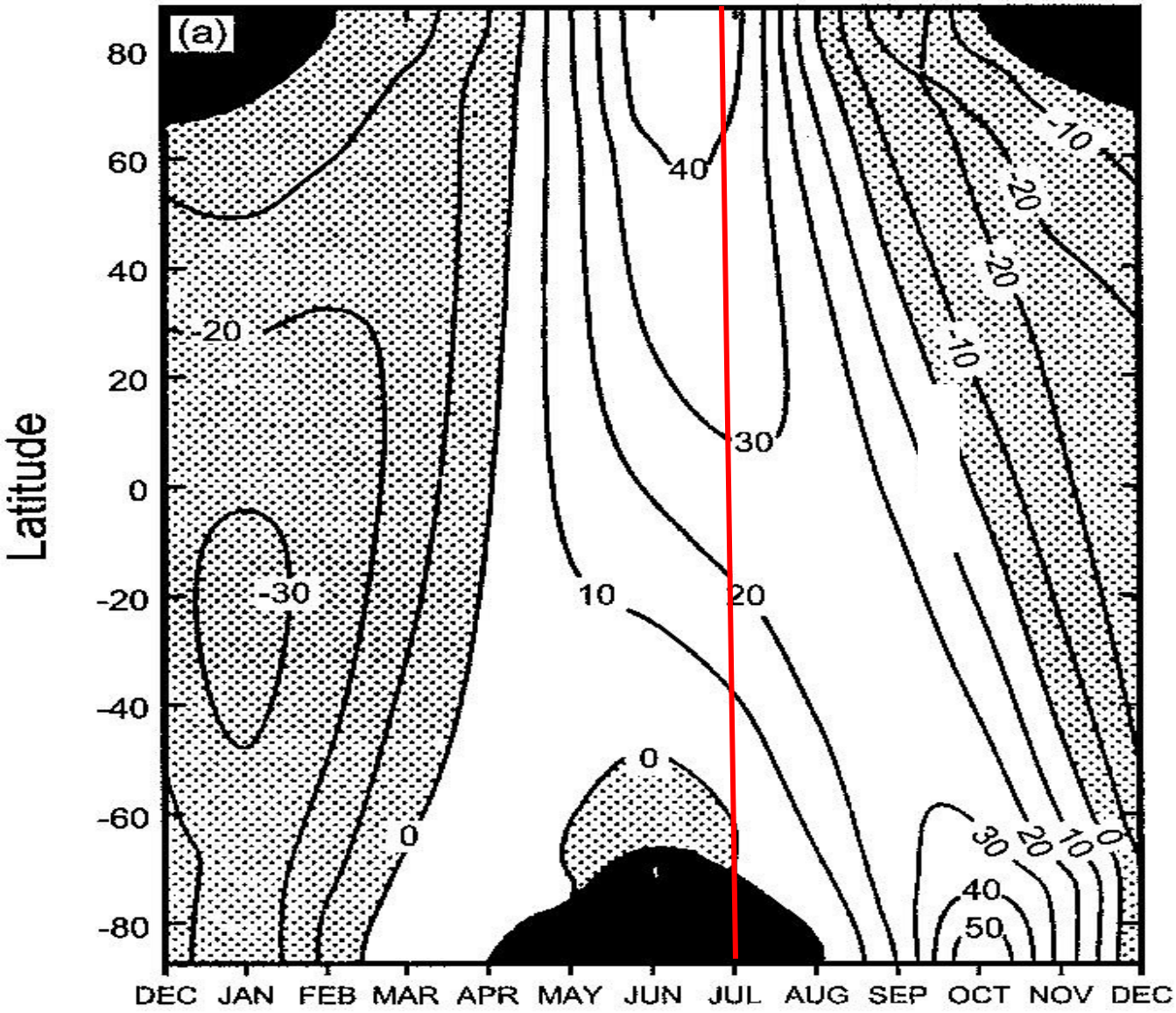

Difference in solar radiation in W m^{-2}, at 9ka B.P. compared to present.

Source: *Mitchell et al, 1988*

Changes in July, over time & space

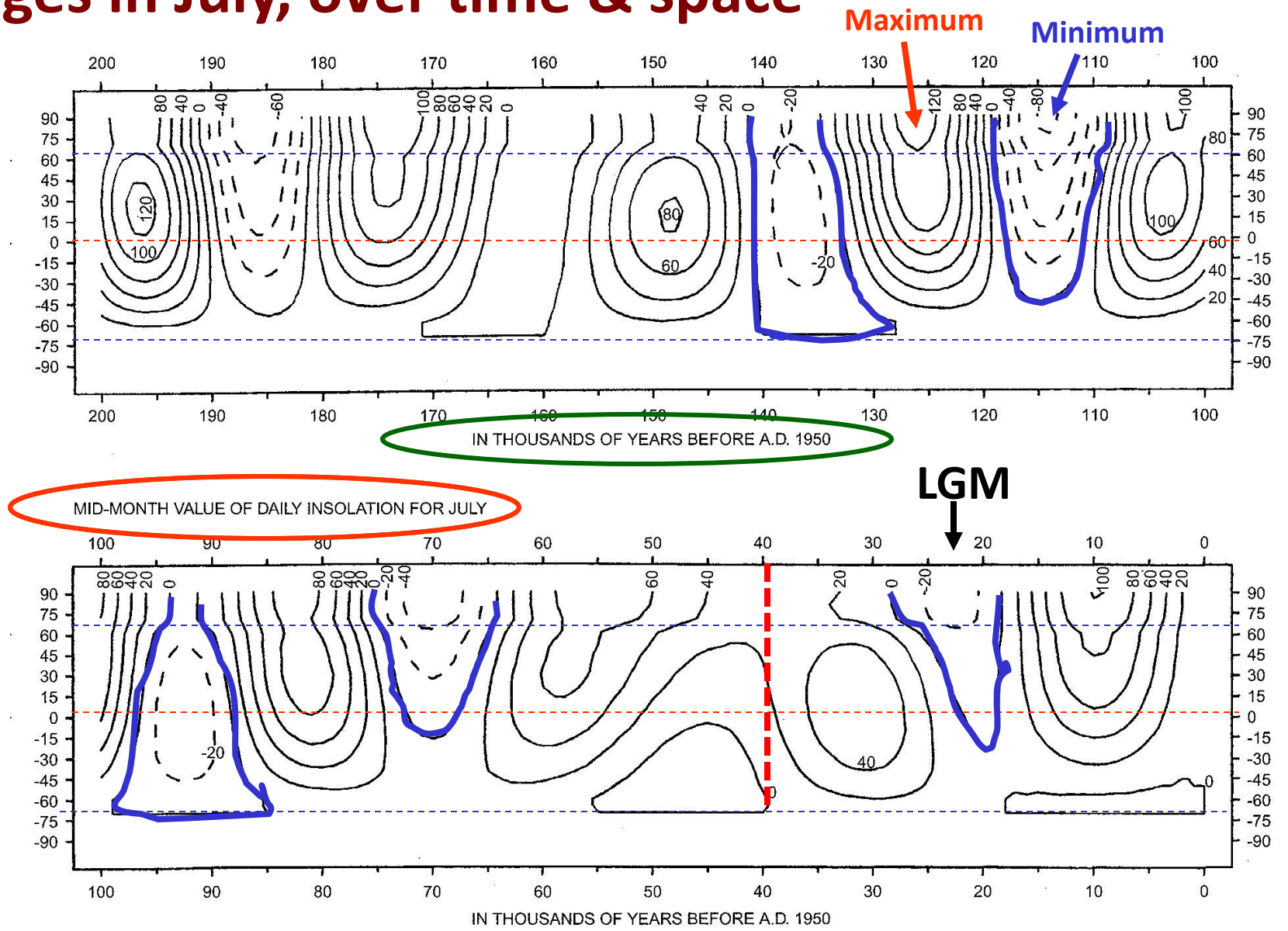

Solar radiation anomalies (top of atmosphere) relative to 1950 values (cal cm^{-2} d^{-1})

Estimated Global Mean Temperature Anomalies*

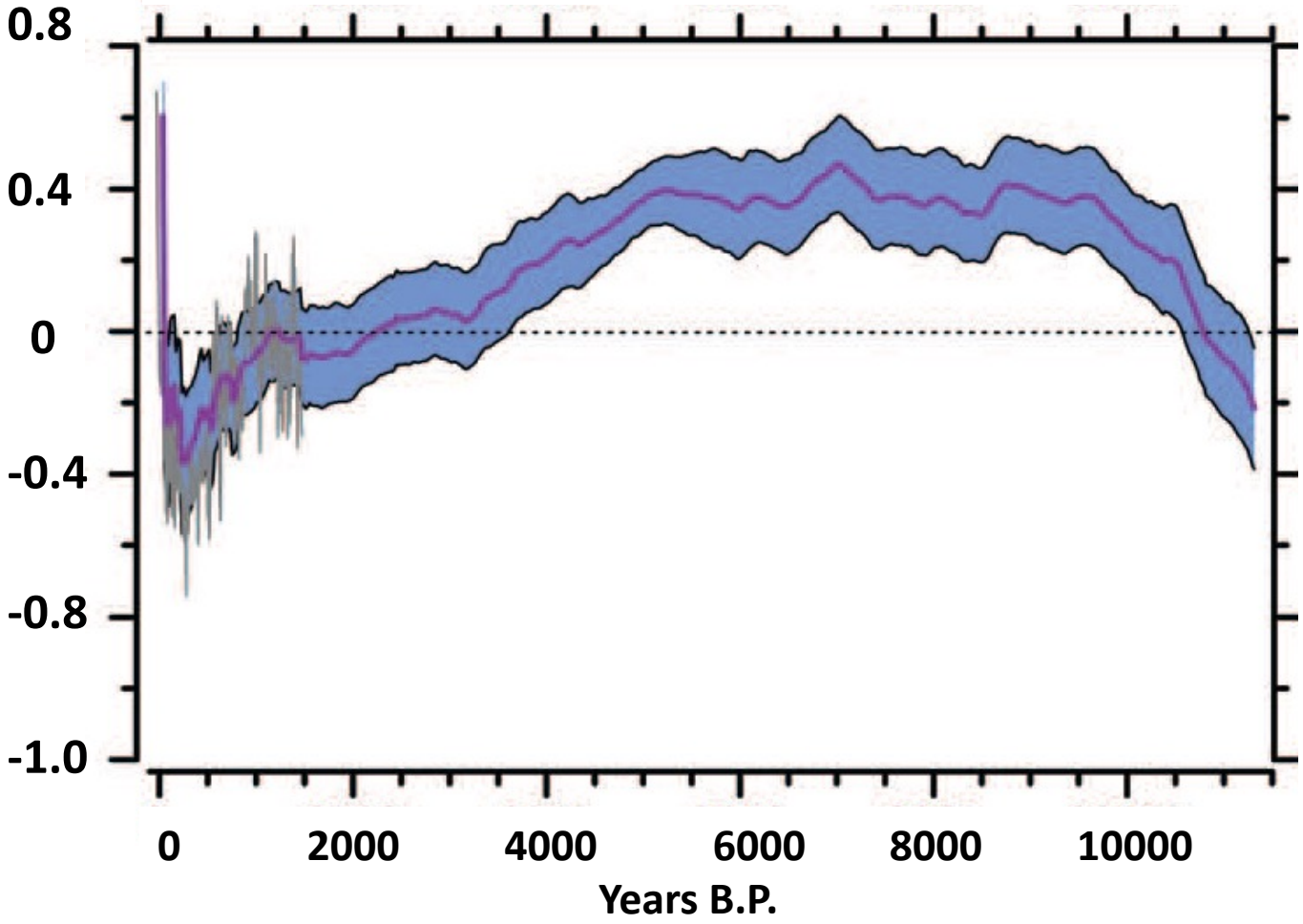

*relative to 1961-90

Source: *Marcott et al. 2013*

UMASS AMHERST
Geosciences

CLIMATE SYSTEM RESEARCH CENTER

Hydroclimate

Regional changes through the Holocene indicate a shift towards drier conditions in the NH…
wetter in the SH

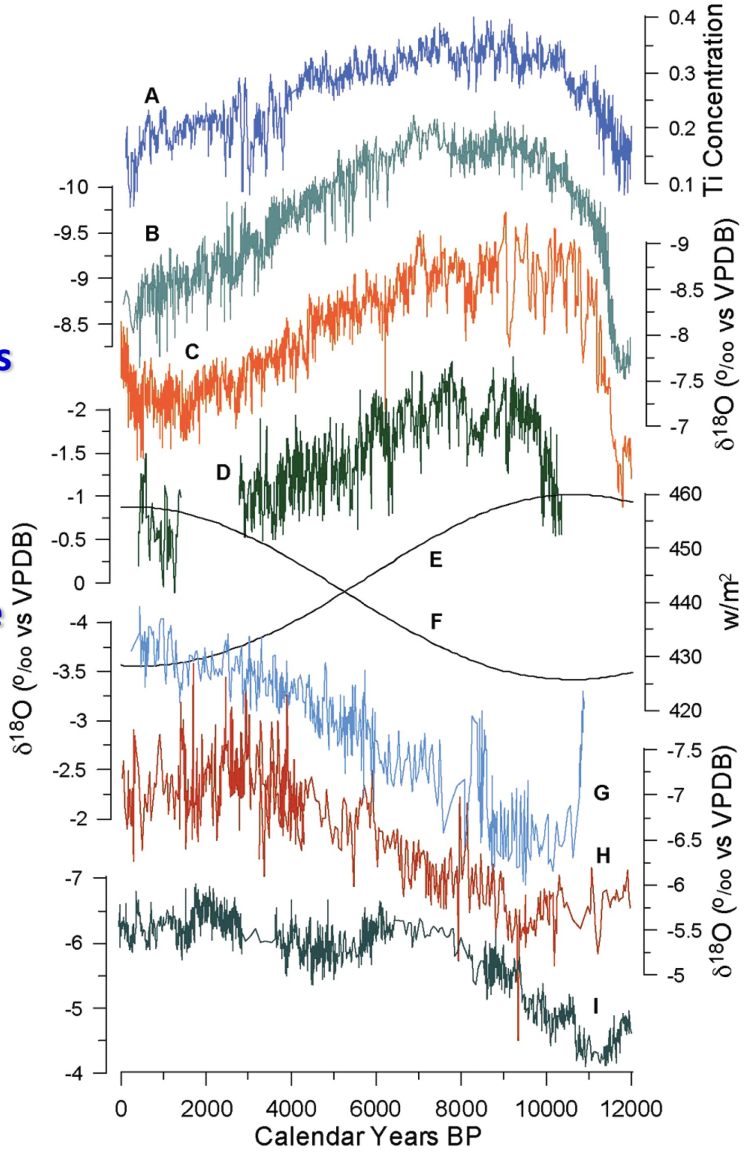

A. Cariaco Basin Ti record (Haug et al., 2001).

B. Southern China, 31° N (Dong et al., 2010)

C. Central China, 25° N (Dykoski et al., 2005; Wang et al., 2005)

D. Southern Oman, 17° N (Fleitmann et al., 2003b)

E. Insolation for July at 10° N

F. Insolation for January at 10° S

G. Southeastern Brazil, 27° S (Wang et al., 2006)

H. Eastern Peru, 7° S (van Breukelen et al., 2008)

I. Indonesia, 8° S (Griffiths et al., 2009).

Source: *Burns 2011*

A High-Resolution Absolute-Dated Late Pleistocene Monsoon Record from Sanbao Cave, China

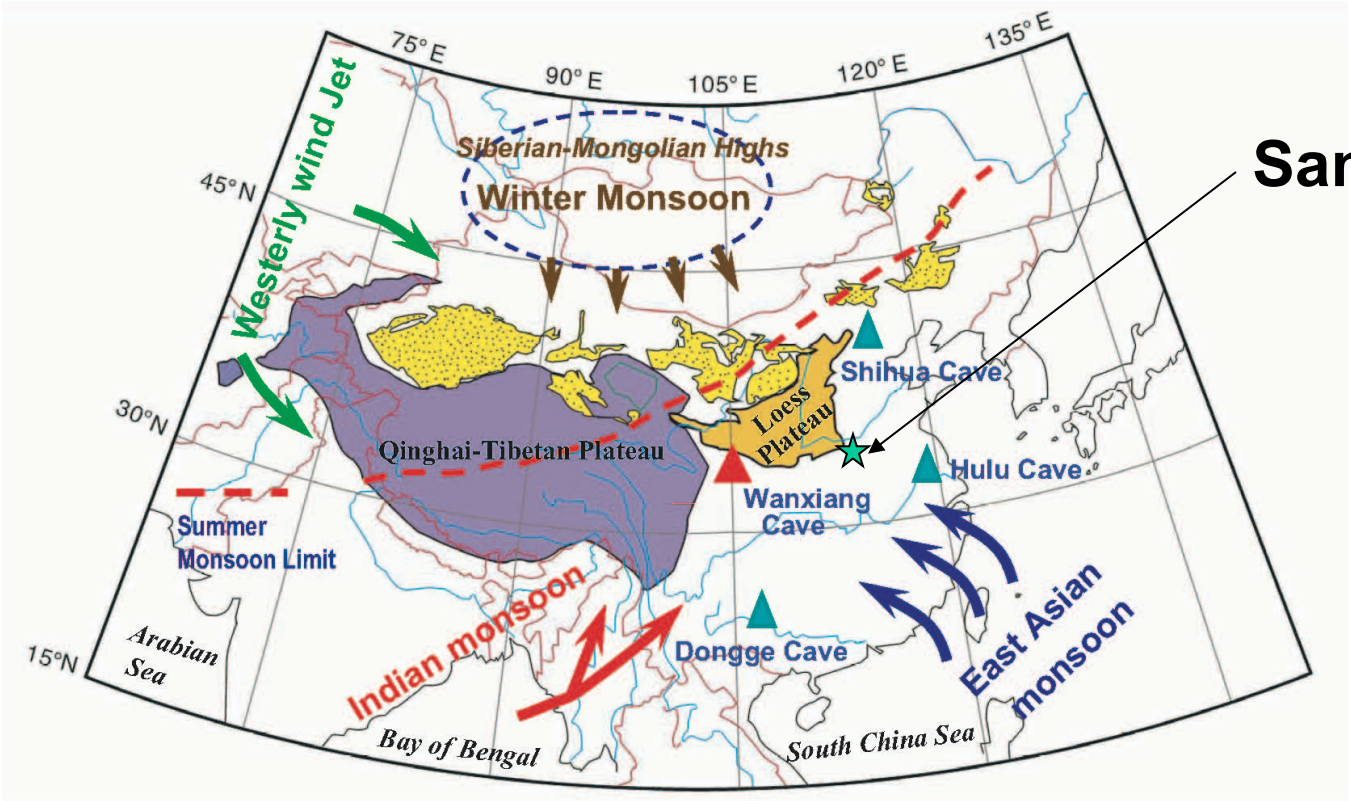

Figure S1. Map of the China and surrounding areas, including the Chinese Loess Plateau and the Qinghai-Tibetan Plateau. The red triangle indicates Wangxiang Cave (33°19' N, 105°00' E, 1200 m a.s.l.). Hulu (32°30'N, 119°10'E), Dongge (25°17'N, 108°5'E) and Shihua Caves (39°47'N, 115°56'E) are also shown with blue triangles. Arrows depict Asian Monsoon (including East Asian Monsoon (dark blue) and Indian Monsoon (red)); Westerly (green) and winter monsoon (dark brown). The dashed red line illustrates the approximate northwestern extent of the Asian summer monsoon.

Published by AAAS

Sanbao stalagmite record, central China

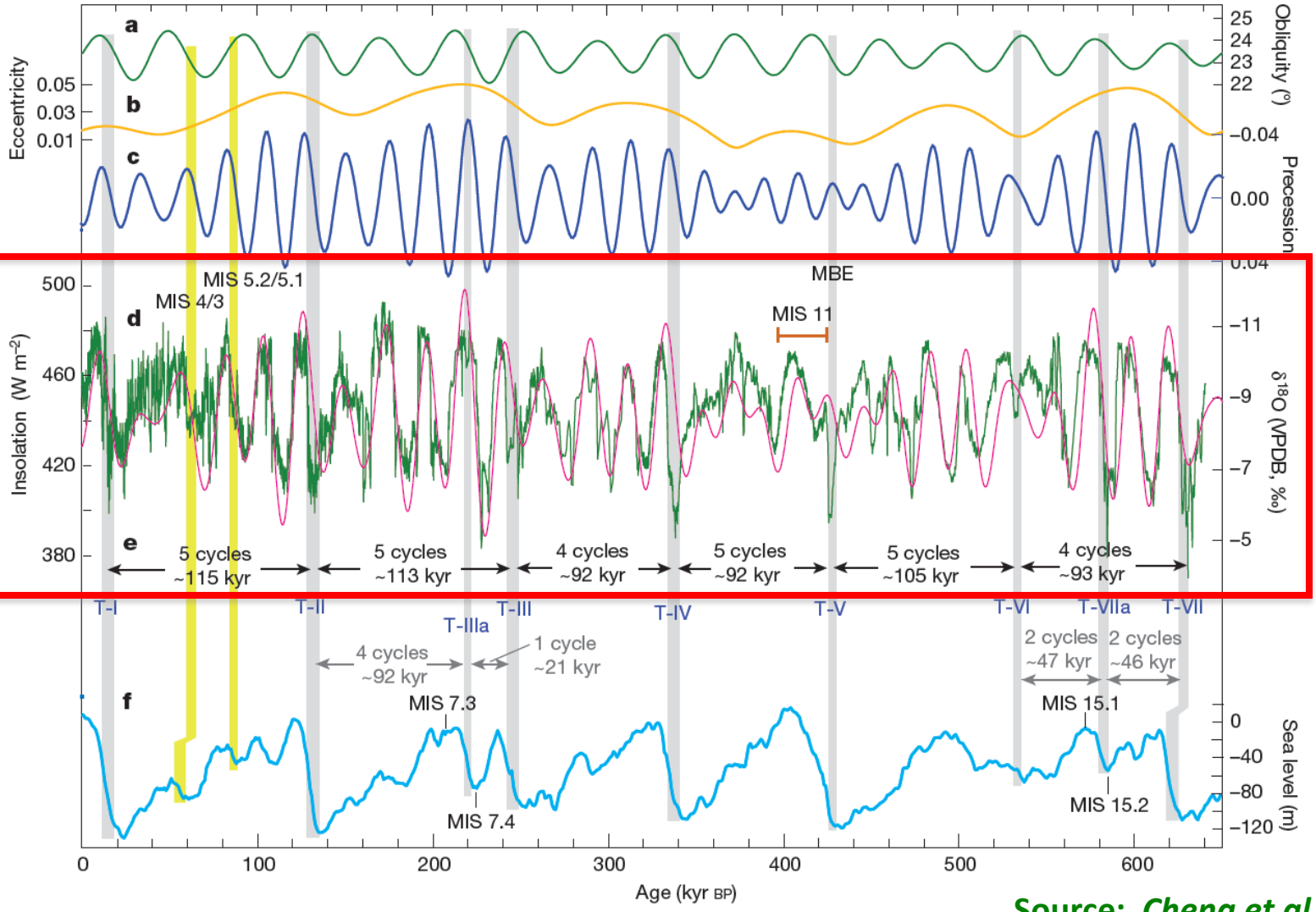

Source: ***Cheng et al. 2016***

UMASS AMHERST

CLIMATE SYSTEM RESEARCH CENTER

Forcing can be considered on several timescales:

Orbital –Milankovic (eccentricity/obliquity/precession)
~100,000; 40,000; 23,000/19,000 years

Millennial to centennial

solar irradiance

thermohaline oscillations ("internal" variability?)

Decadal-to-interannual

ENSO/NAO/PDO ("internal" variability?)

volcanic

Feedbacks? Vegetation/hydrological changes; snow/sea-ice cover

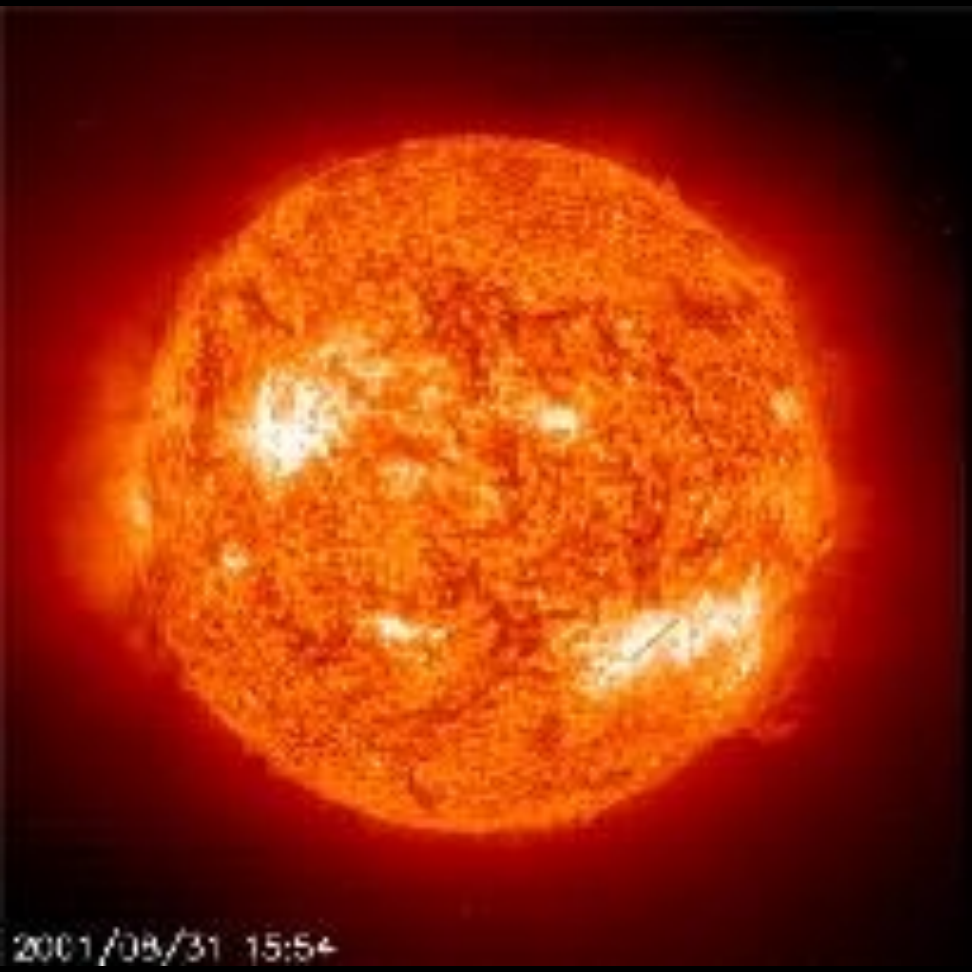

Facular Brightening

solar spots

NASA SOHO image

Actividad Solar (Fuente: NASA)

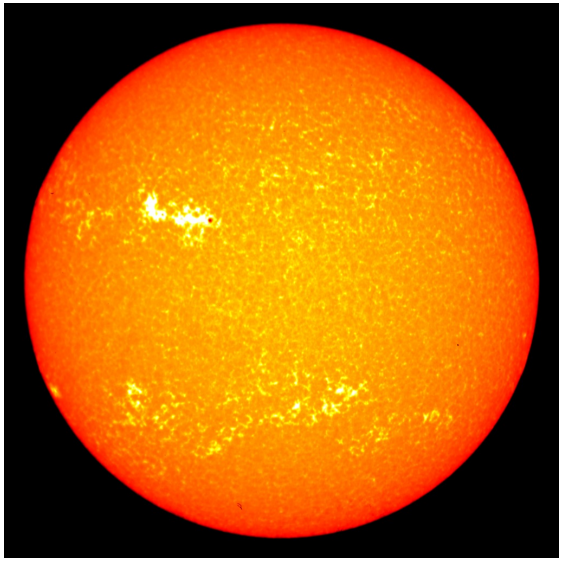

Baja

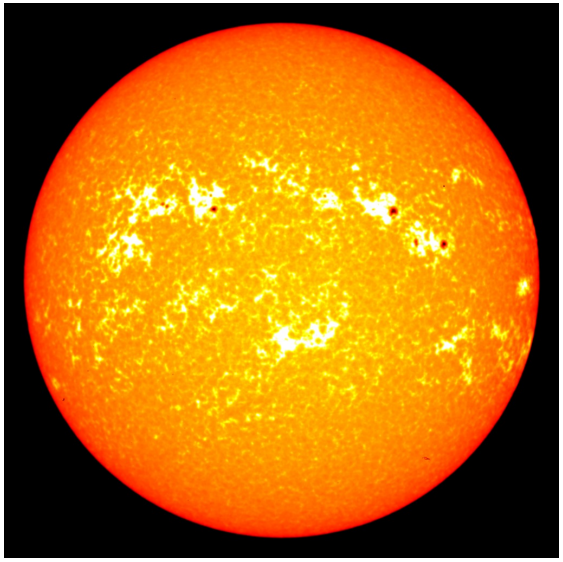

Moderada

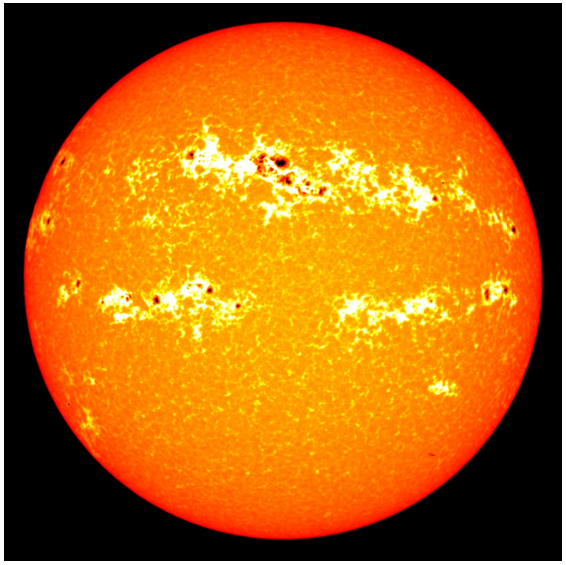

Alta

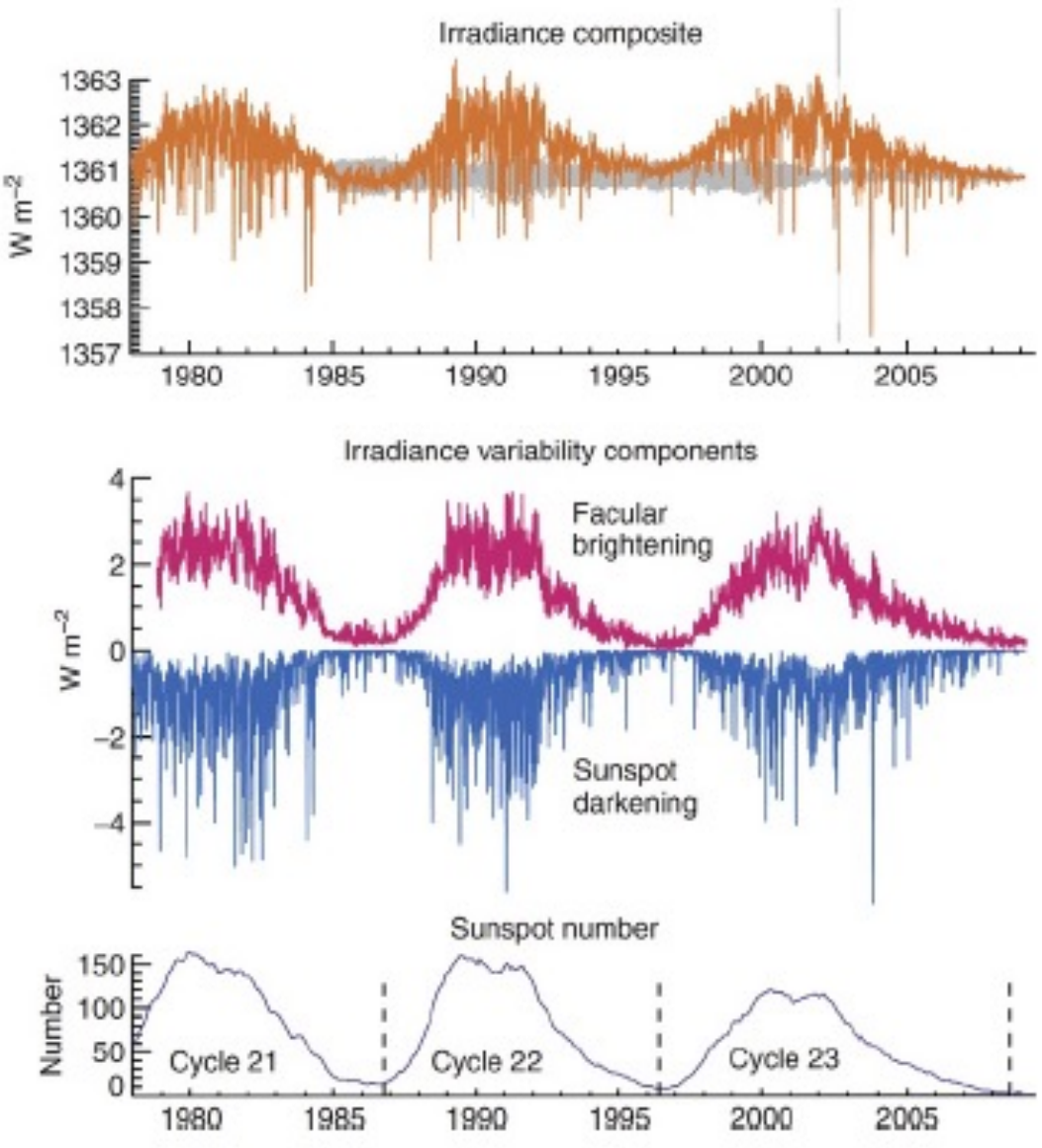

- **Flacular Brightening**:
  - **Definición**: Son áreas brillantes que se forman en la fotosfera solar.
  - **Radiación**: Emiten más radiación que las áreas circundantes.
  - **Temperatura**: Son más calientes que el área solar promedio.
  - **Impacto en la Radiación Solar**: Aumentan la radiación solar total, contribuyendo a su variabilidad.
  - **Duración**: Son temporales pero suelen durar más que las manchas solares.
- **Sunspots (Manchas Solares)**:
  - **Definición**: Son áreas oscuras que se forman en la fotosfera solar.
  - **Radiación**: Emiten menos radiación que las áreas circundantes.
  - **Temperatura**: Son más frías que el área solar promedio.
  - **Impacto en la Radiación Solar**: Disminuyen la radiación solar total, pero su efecto es superado por el de los brillos flaculares.
  - **Duración**: Son temporales, pero pueden durar de días a semanas.

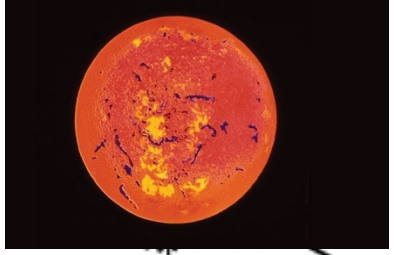

Galactic cosmic rays

Energy radiated by the sun

Electromagnetic emission

Corpuscular emission

Solar luminosity

UV variations

Solar cosmic rays

Solar wind variations

Modulation of cosmic ray fluxes

^{10}Be ^{14}C production

STRATOSPHERE ?

TROPOSPHERE

variations of optical properties and radiation balance of the atmosphere

ozone
aerosols
veil
clouds

Geomagnetic field intensity

Variations of the solar radiation, atmospheric circulation, precipitation and temperature near the Earth's surface

More irradiance=
Stronger solar wind=
Reduced galactic cosmic rays=
Less ^{14}C and ^{10}Be produced in upper armosphere

So, ^{14}C and ^{10}Be variations are *inversely related* to solar irradiance

Sources: *Carslaw et al., 2002*
van Geel et al., 1999

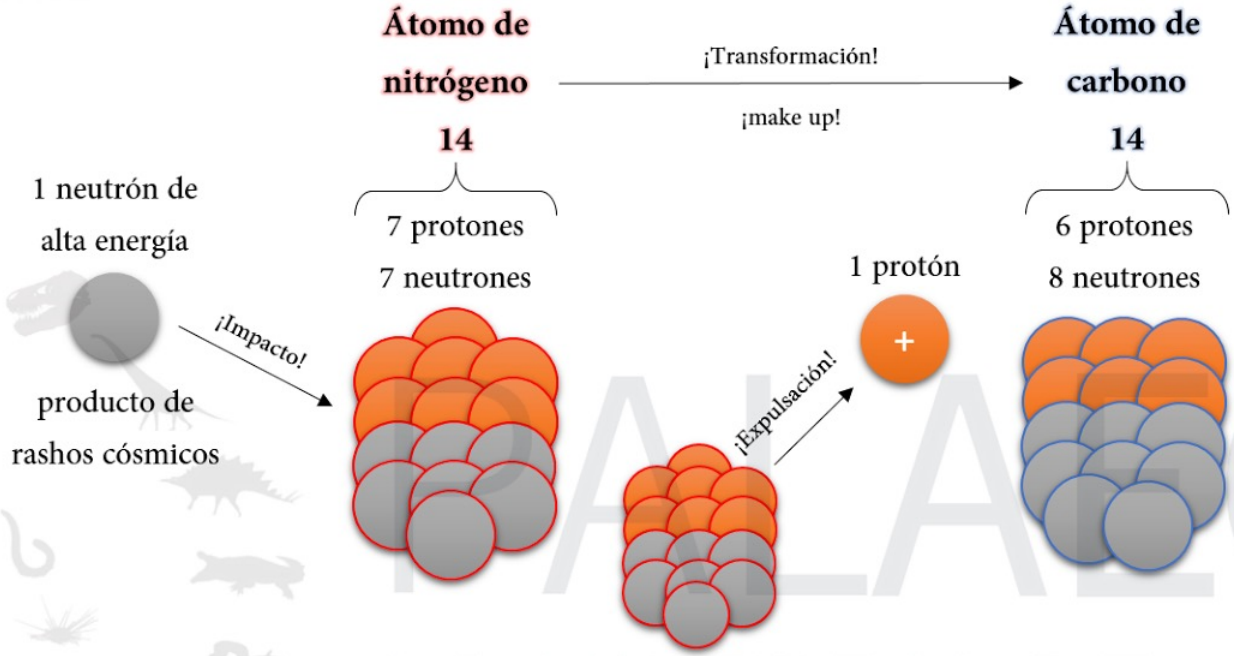

Nitrógeno "mutante", ahora carbono

¿CÓMO LEER ESTO?

Masa atómica

$^{14}_{6}C$

Número atómico

$$^{1}_{0}n + {}^{14}_{7}N \rightarrow {}^{1}_{1}p + {}^{14}_{6}C$$

7	Número atómico
N	
14.01	Masa atómica

Nitrógeno "normal"

6	Número atómico
C	
12.01	Masa atómica

Carbono "normal"

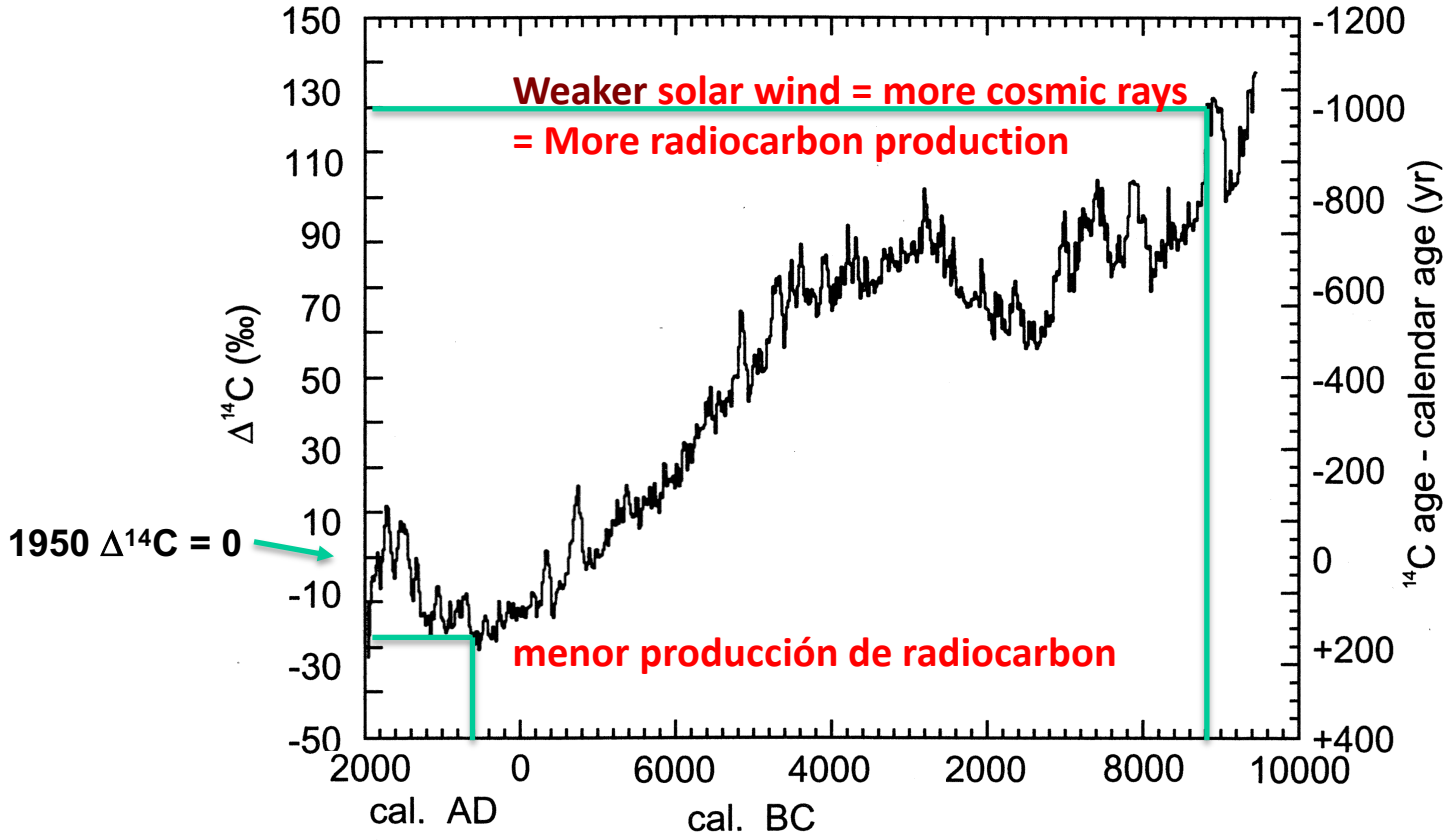

Edad de ^{14}C más joven que la calendárica

Edad de ^{14}C más vieja que la calendárica

$\Delta^{14}C$= Valor de $\delta^{14}C$ de muestra en relación a $\delta^{14}C$ atmósfera en el año 1950

Ejemplo: Una muestra o la atmósfera de hace 11 mil años de antigüedad tenía 130 per mil más ^{14}C que una muestra o la atmósfera en el año 1950. El resultado es que la edad de ^{14}C no corregida te da una edad distinta a la calendárica; 1000 años más joven (porque al no ser corregida es en referencia al año 1950). En este caso la edad de 14C te daría una edad de 8000 años a una edad calendárica (real) de 9000 años

UMASS AMHERST
Geosciences

Source: *Stuiver and Reimer 1993*

CLIMATE SYSTEM RESEARCH CENTER

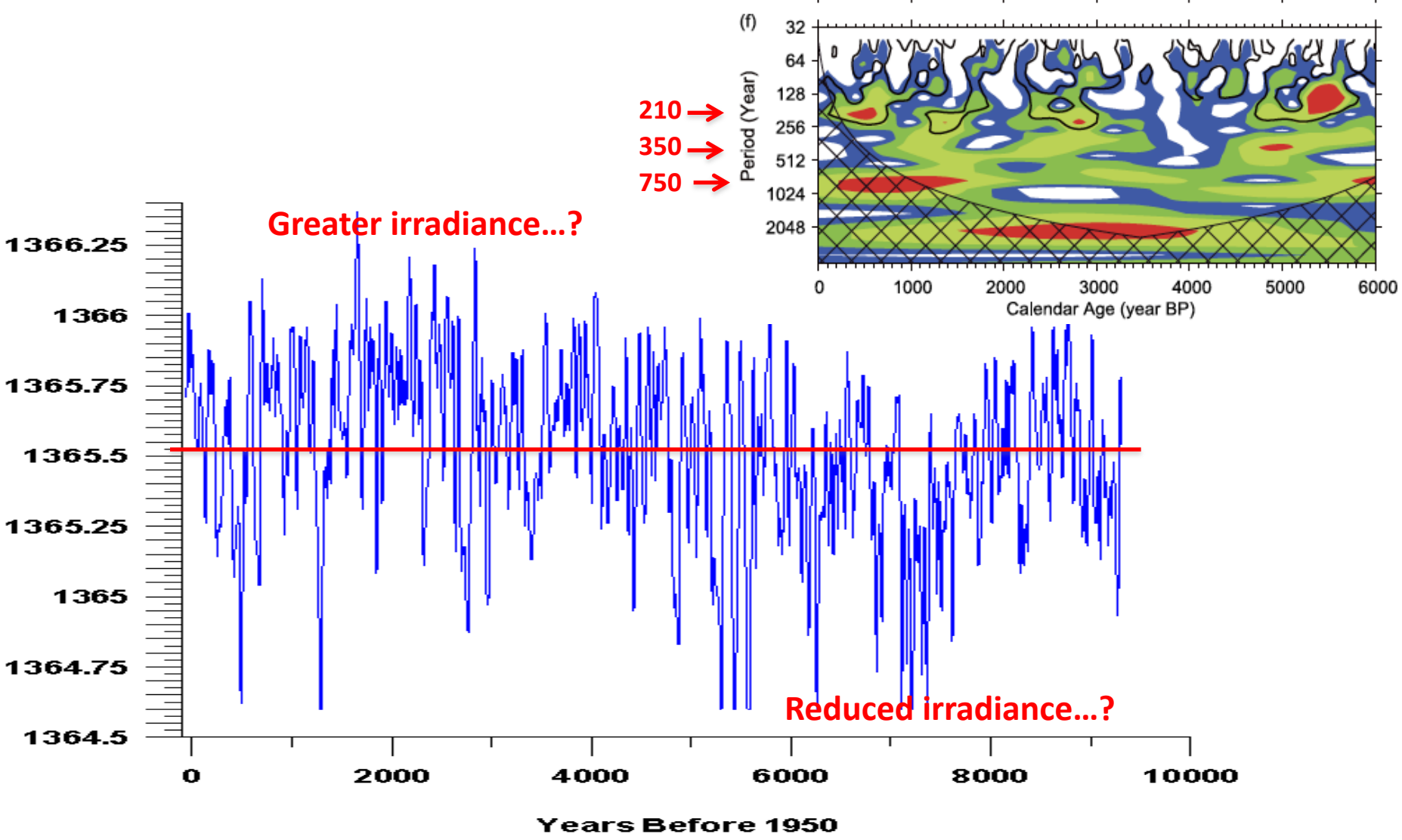

Source: *Steinhilber et al. 2012*

UMASS AMHERST
Geosciences

CLIMATE SYSTEM RESEARCH CENTER

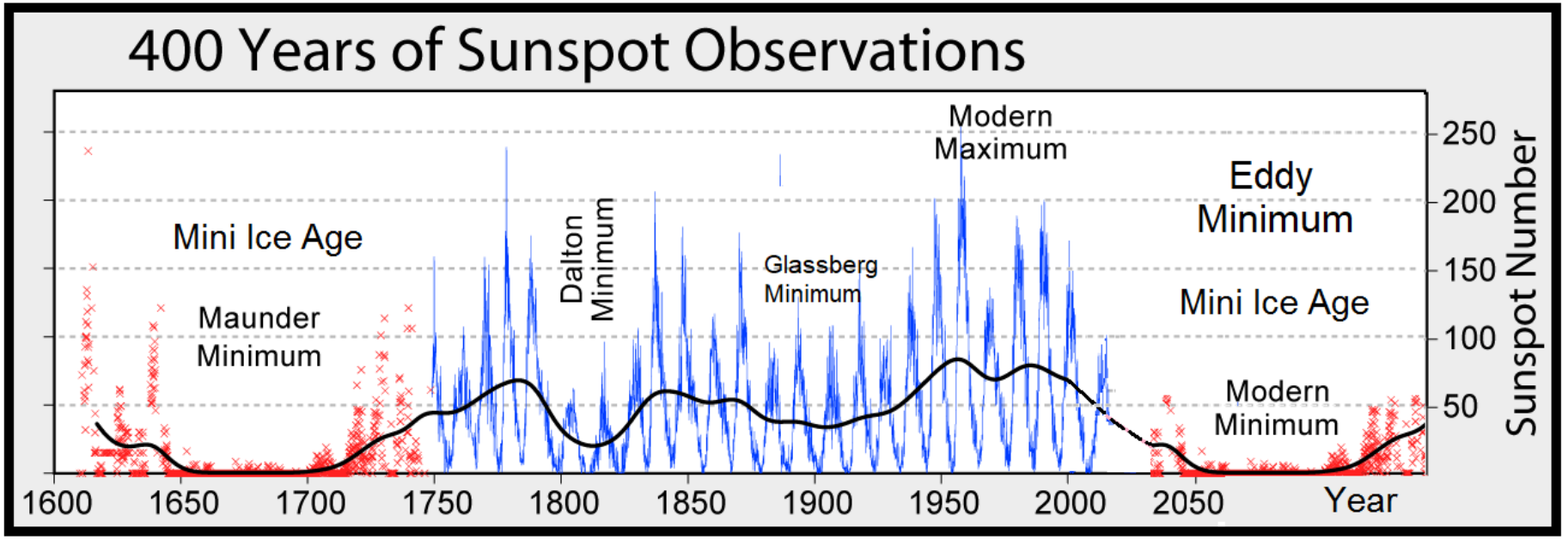
400 Years of Sunspot Observations
Mini Ice Age
Maunder Minimum
Dalton Minimum
Glassberg Minimum
Modern Maximum
Eddy Minimum
Mini Ice Age
Modern Minimum
250
200
150
100
50
Sunspot Number
1600
1650
1700
1750
1800
1850
1900
1950
2000
2050
Year

Dongge Cave, China

Stalagmite oxygen isotope record (25°N)

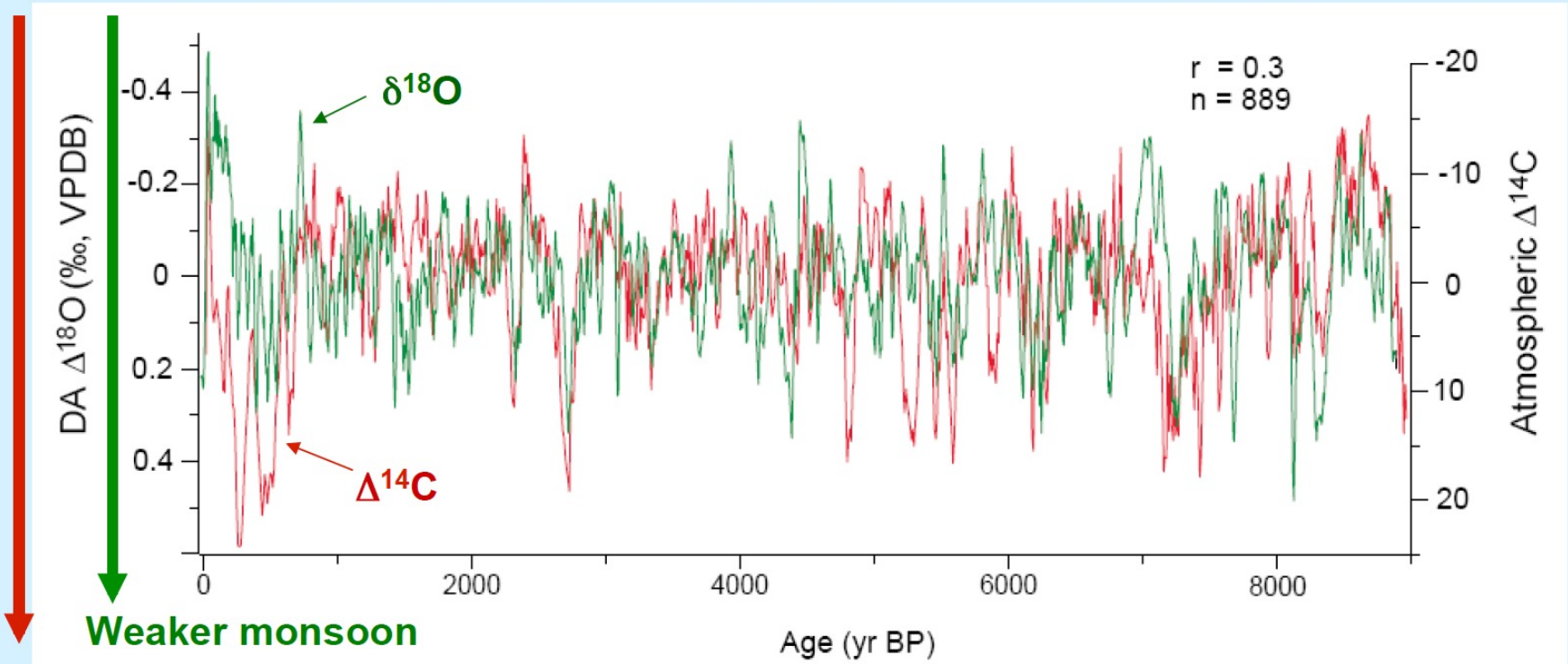

Source: *Wang et a*

UMASS AMHERST
Geosciences

CLIMATE SYSTEM
RESEARCH CENTER

Solar effects
on Arabian monsoon rainfall?

Lower irradiance?

Drier

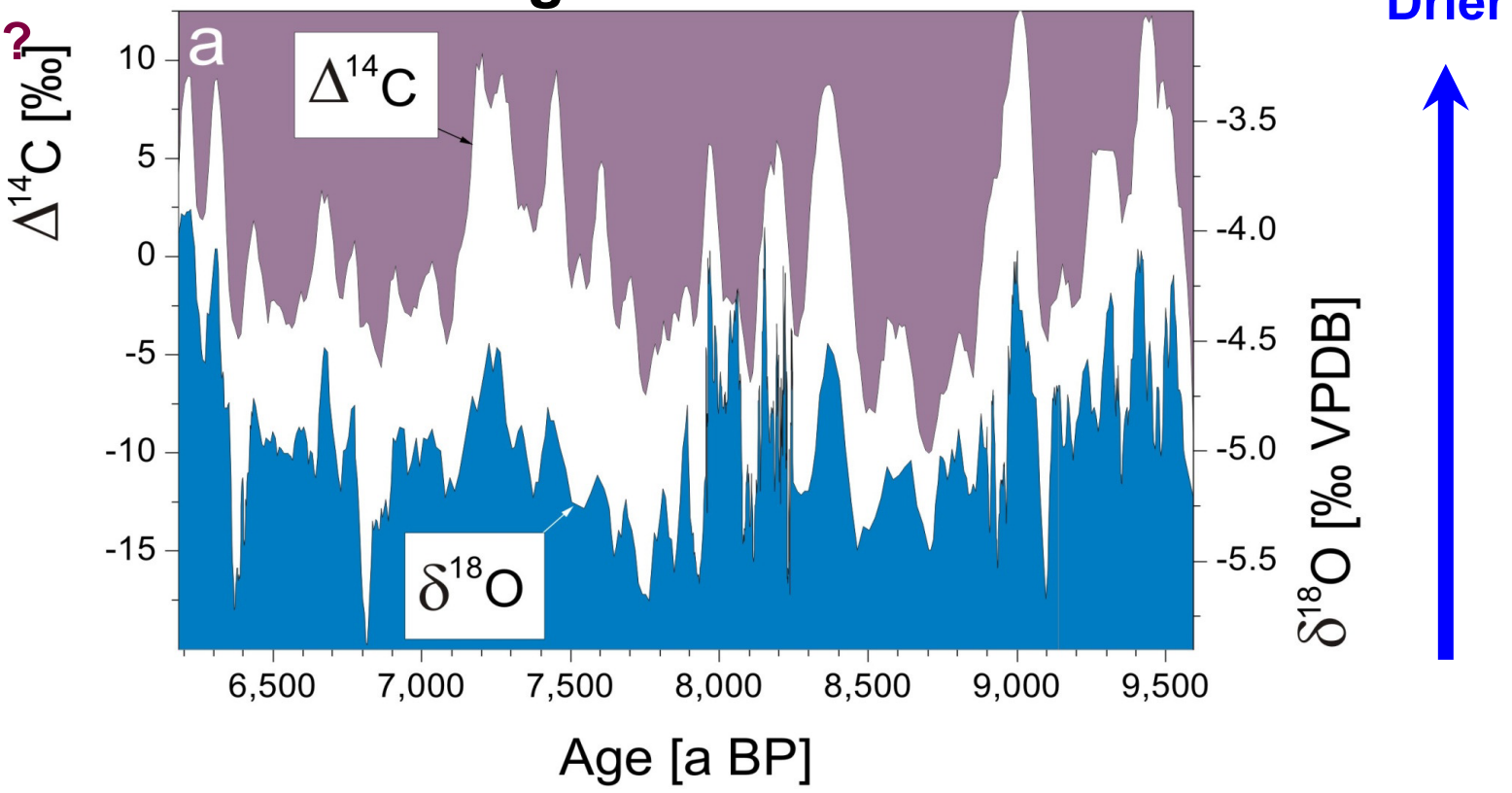

Source: *Neff et al.*

"La excelente correlación entre los dos registros sugiere que uno de los controles principales sobre los cambios en la precipitación tropical y la intensidad del monzón a escala centenaria y decenal durante este tiempo son las variaciones en la radiación solar".

Monsón de la India durante el Verano (Izquierda) y el Invierno (derecha)

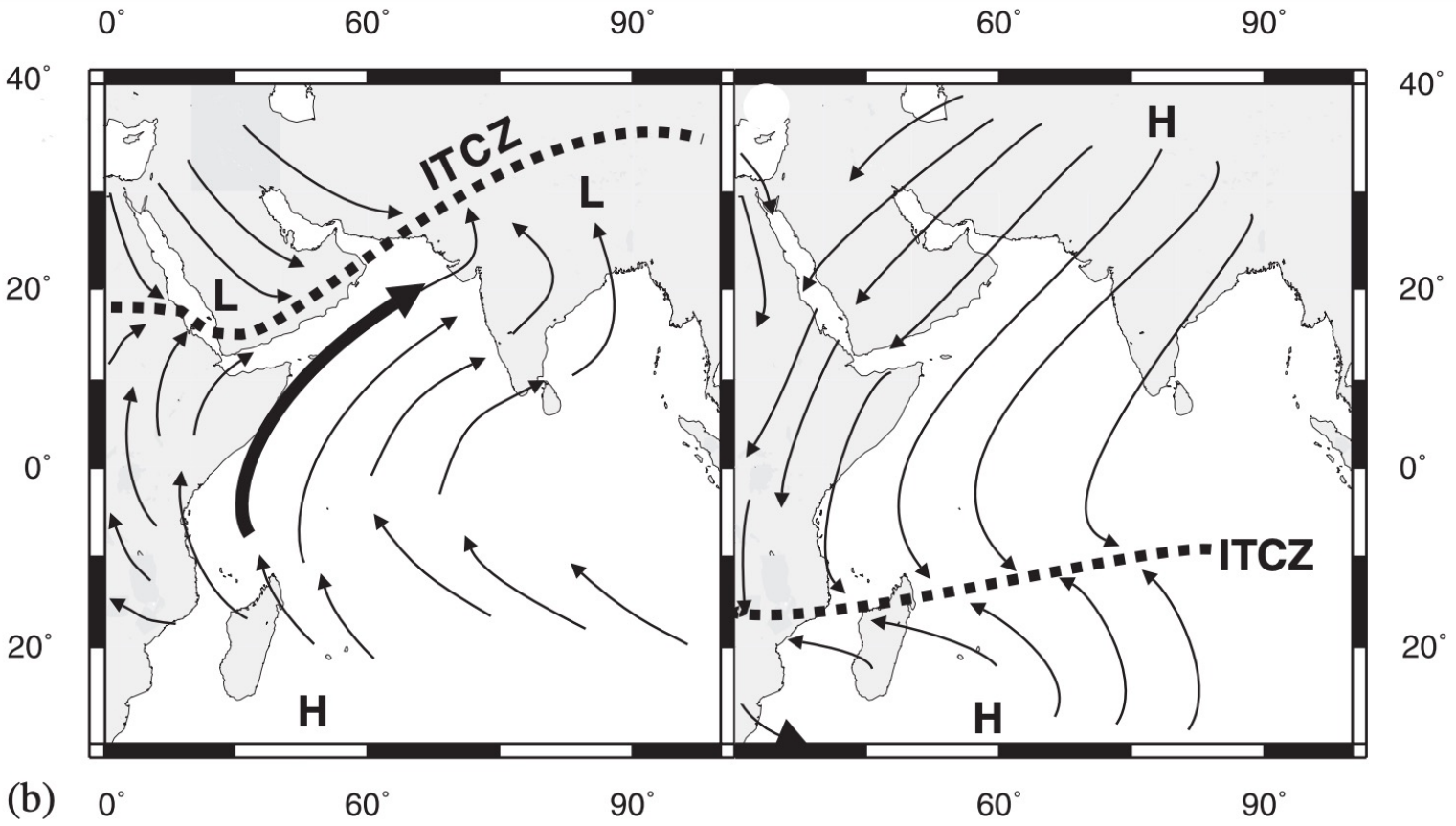

A High-Resolution Absolute-Dated Late Pleistocene Monsoon Record from Hulu Cave, China

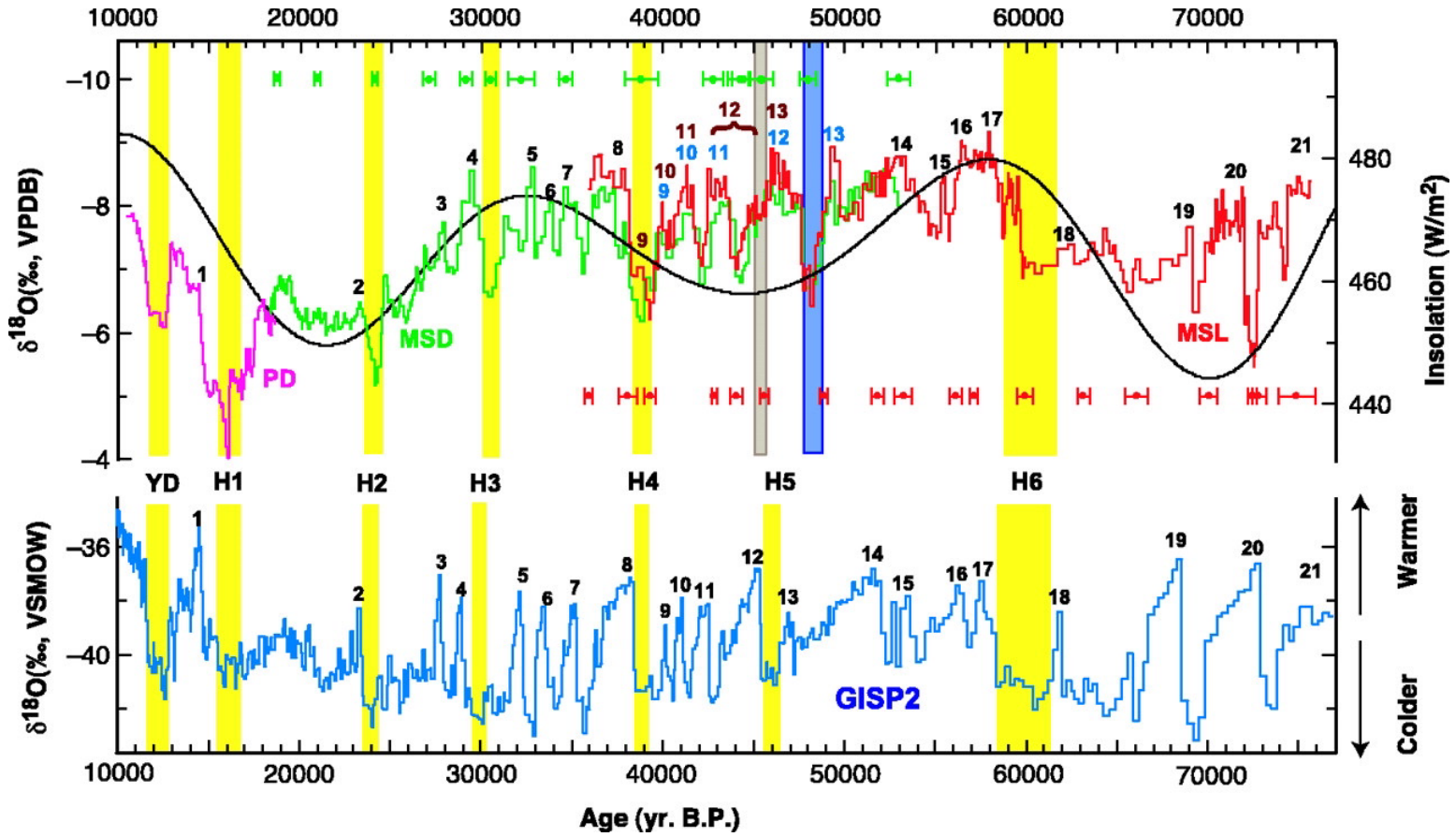

Y. J. Wang et al., Science 294, 2345 -2348 (2001)

Resolución: 130 años

Science
AAAS

Hidroclima de Hemisferios opuestos estan 180 grados fuera de fase

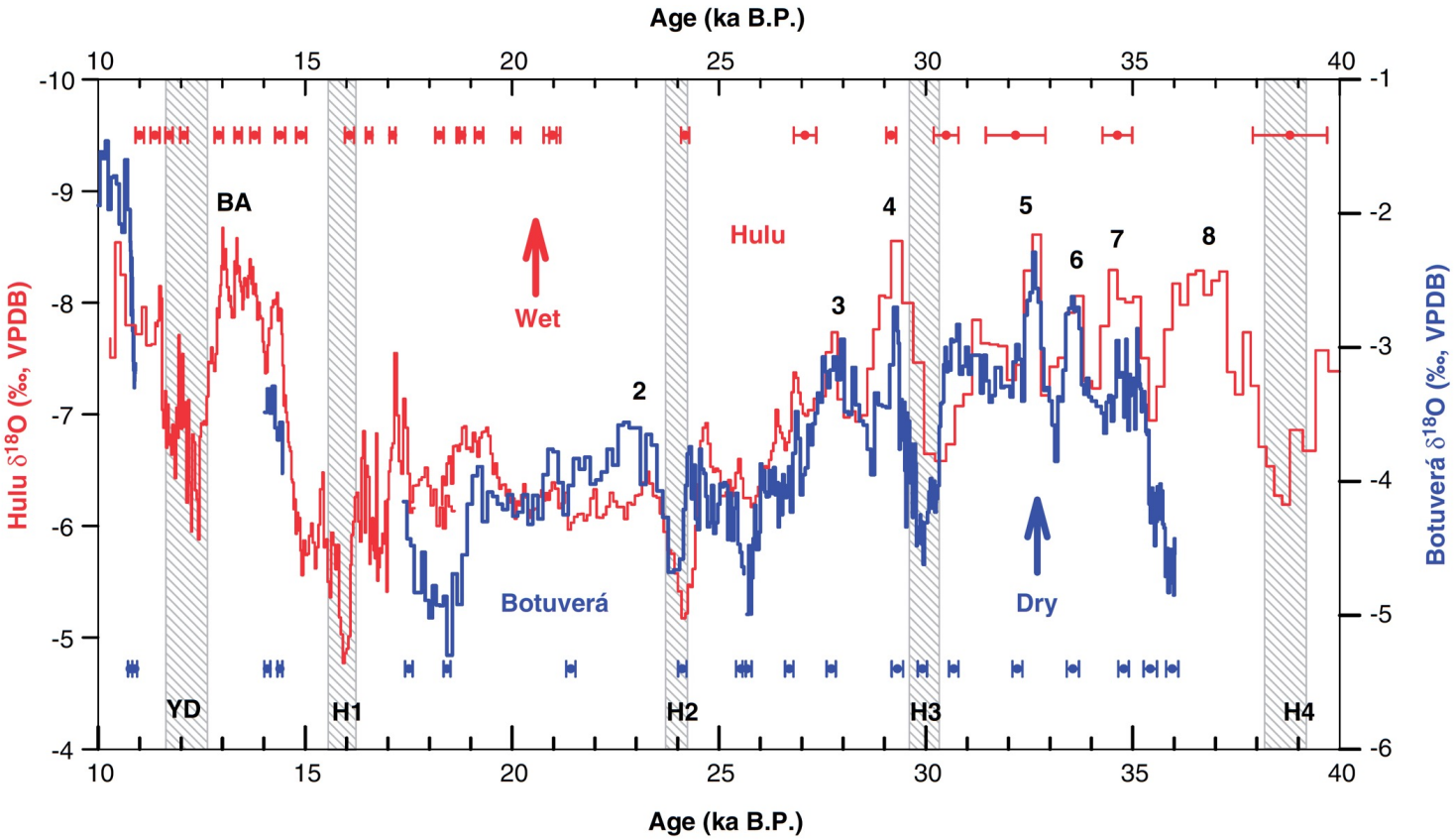

Source: *Wang et al. 2006*

UMASS AMHERST Geosciences

CLIMATE SYSTEM RESEARCH CENTER

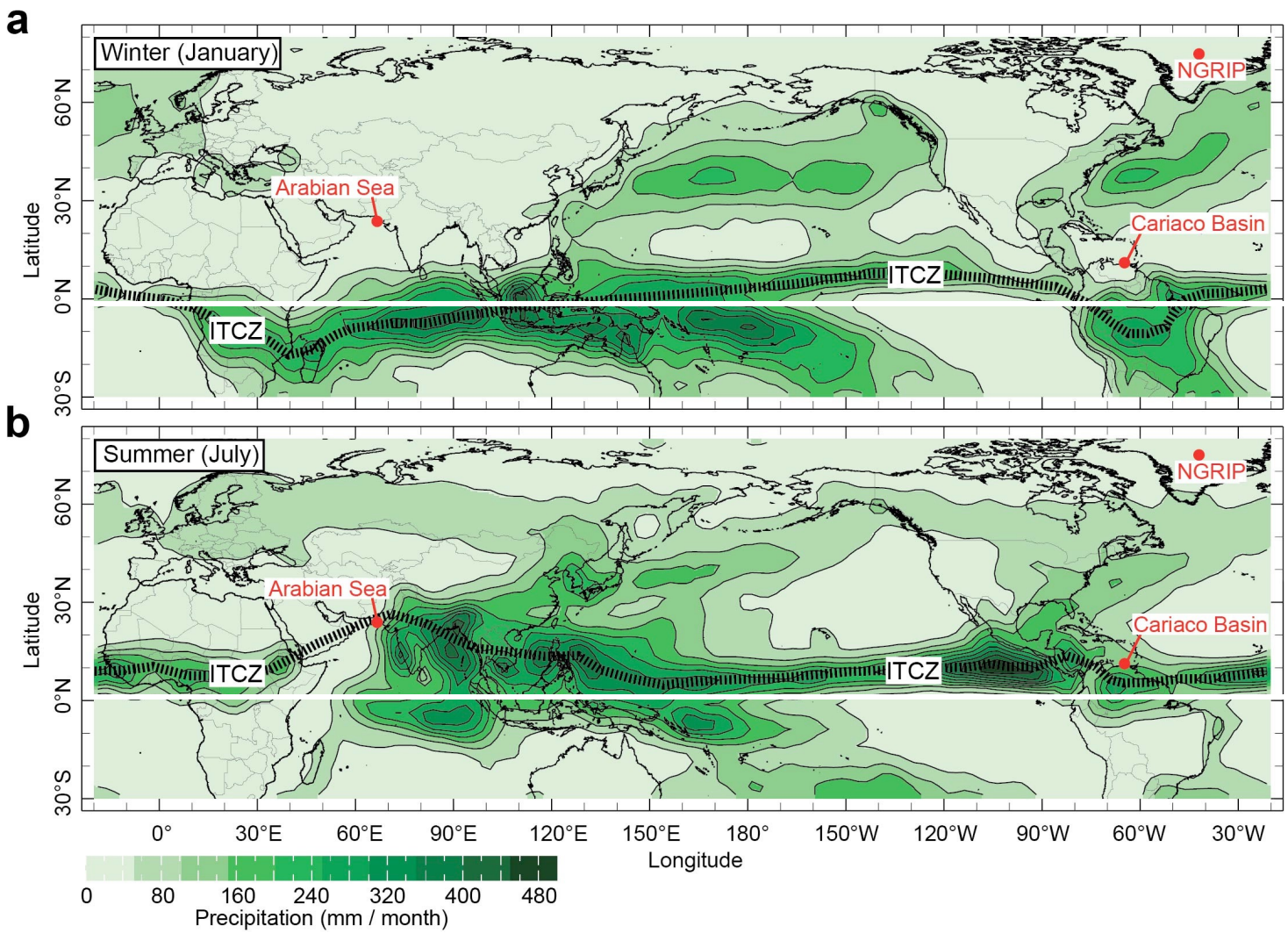

Source: *Deplazes et al. 2013*

UMASS AMHERST
Geosciences

CLIMATE SYSTEM RESEARCH CENTER

Lower solar activity (*decreased* total irradiance?) =

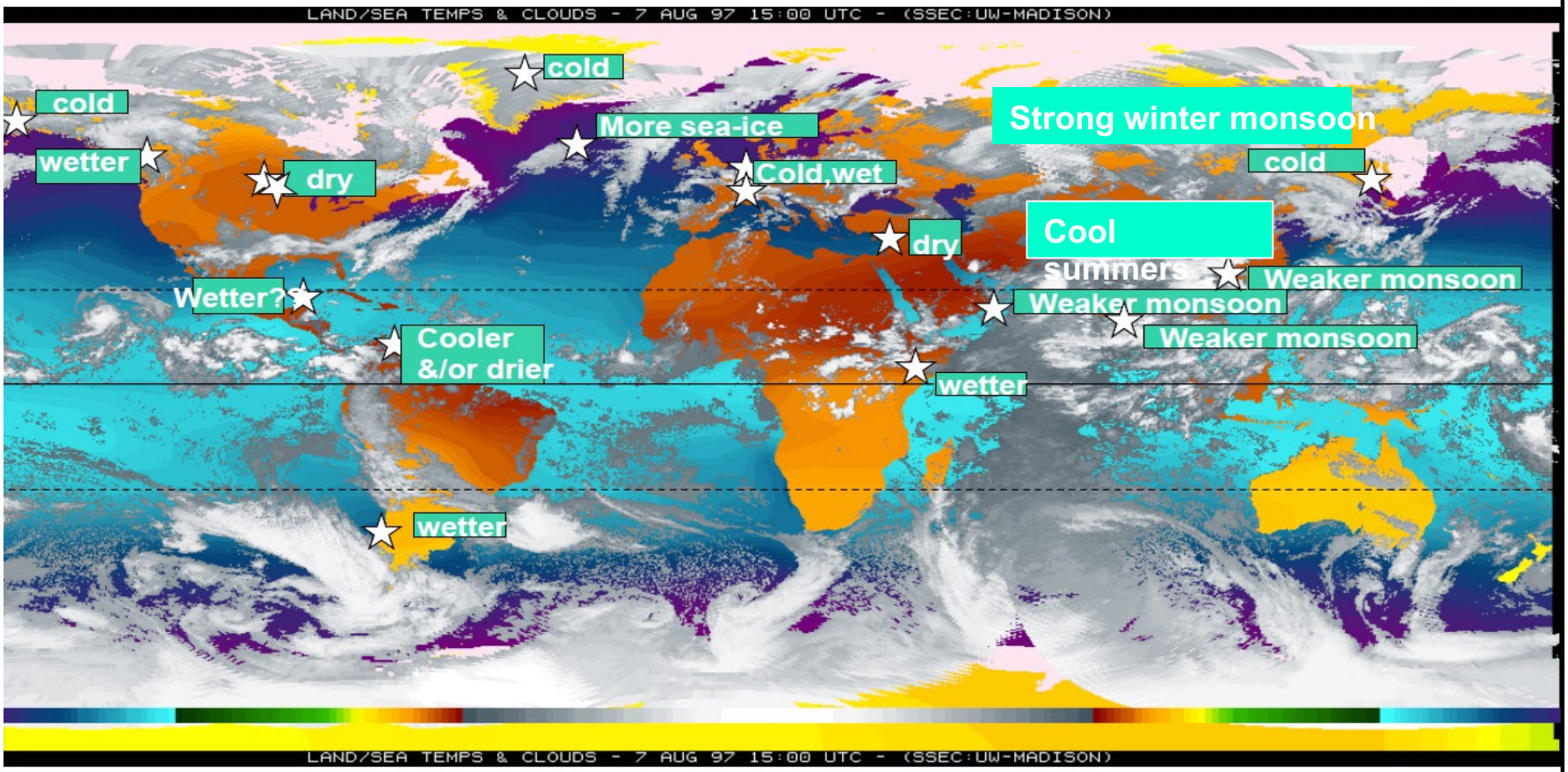

Sources: *Wiles et al., 2004; Hallett et al., 2003; Anderson 1992; Yu & Ito, 1999; Hodell et al., 2001; Black et al., 1999,2004; Verschuren et al., 2000; Neff et al., 2000; Bond et al., 2001; van Geel et al., 1996, 2000; Magny, 1993; Prasad et al., 2004; Agnihotri et al., 2002, 2003; Hong et al., 1999*

Definición Holoceno

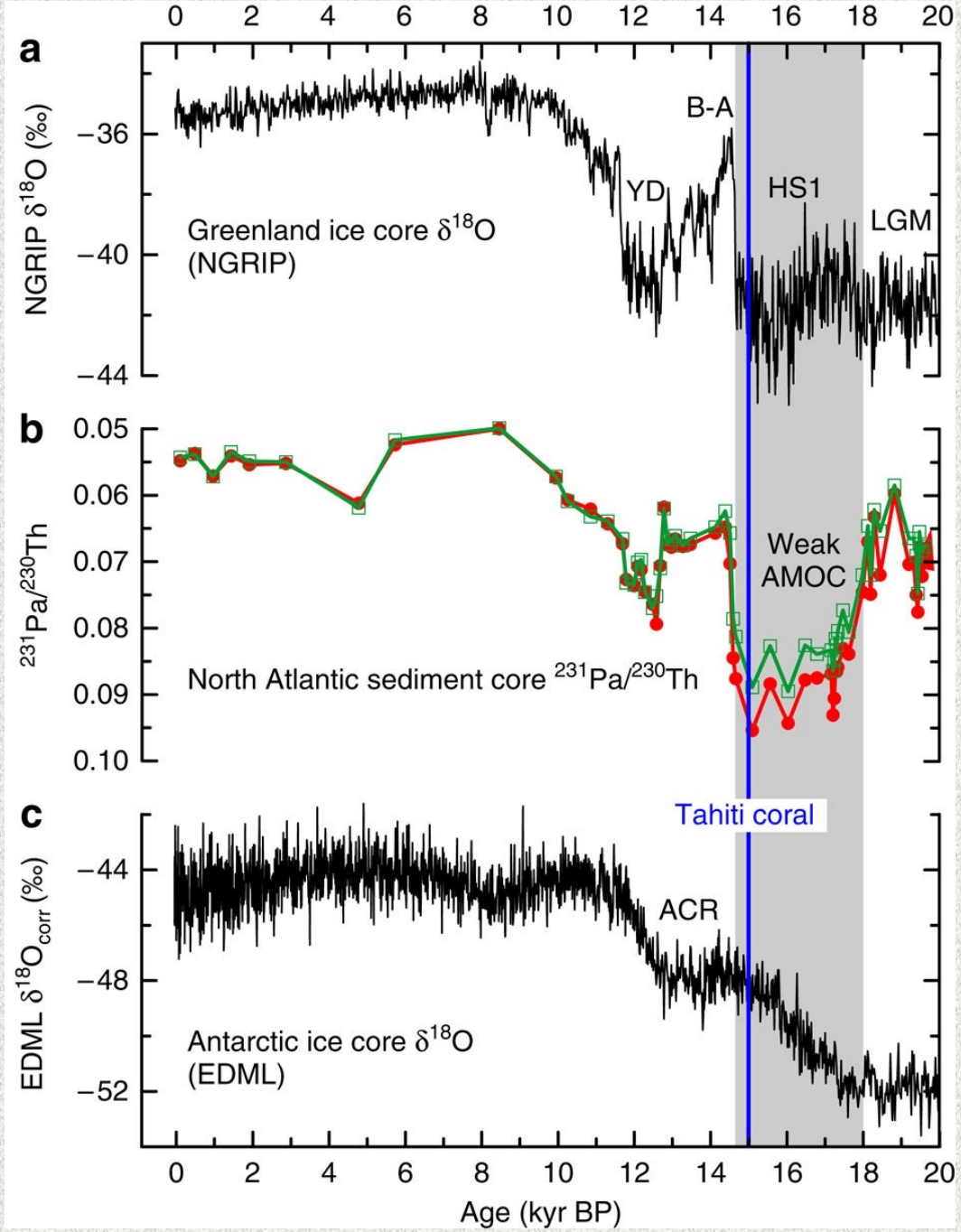

El término "Holoceno" proviene del griego "holos", que significa "entero" o "completo", y "kainos", que significa "nuevo". Por lo tanto, "Holoceno" se puede traducir aproximadamente como "nuevo todo" o "totalmente nuevo".

Propuesto por el geólogo británico Charles Lyell en 1833 para referirse a la época geológica más reciente, que sigue al Pleistoceno.

"El Holoceno se caracteriza por el desarrollo de condiciones climáticas relativamente estables y por el surgimiento y la expansión de la civilización humana".

Source: Felis, T., Merkel, U., Asami, R. *et al.* Pronounced interannual variability in tropical South Pacific temperatures during Heinrich Stadial 1. *Nat Commun* **3**, 965 (2012).

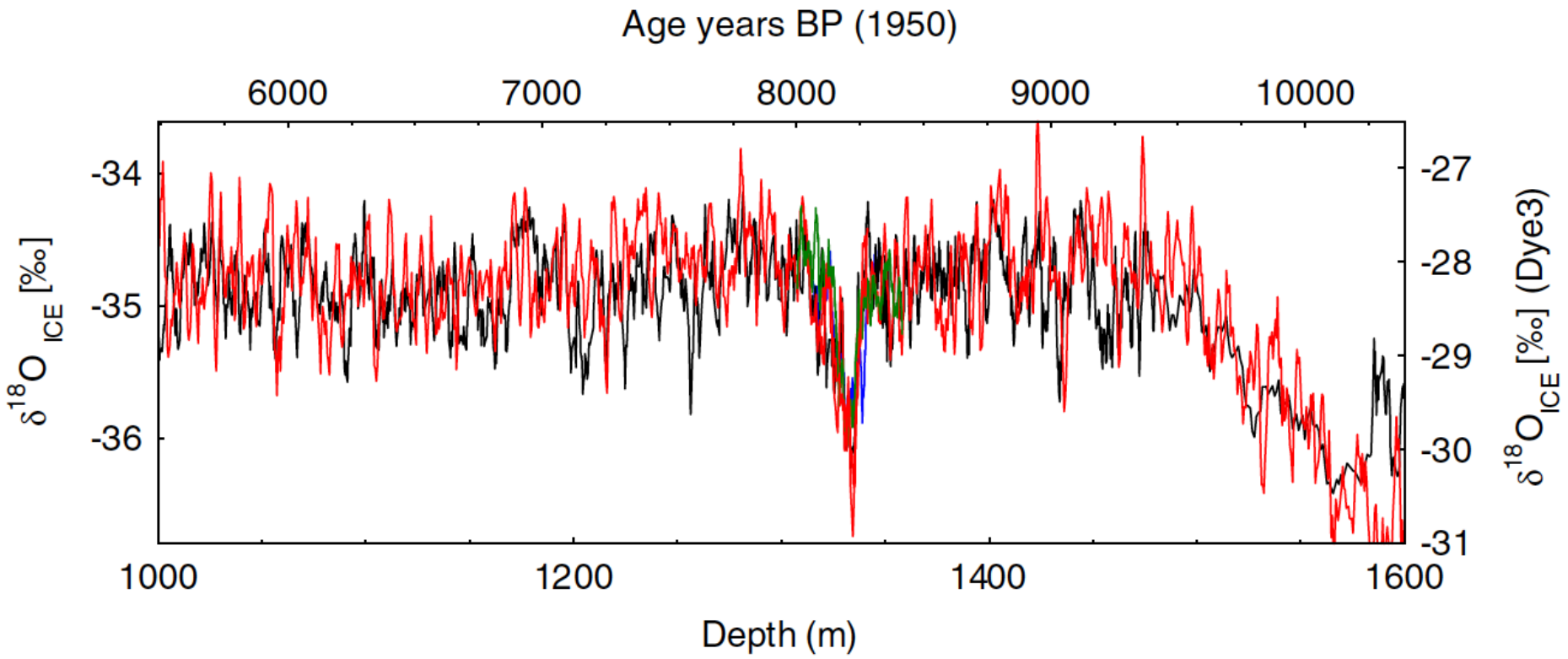

GRIP, GISP2, NGRIP and Dye 3 all plotted on the GRIP depth scale and the GICC05 age scale

Source: *Thomas et al. 2007*

UMASS AMHERST Geosciences

CLIMATE SYSTEM RESEARCH CENTER

Age Model for Hoti Cave, Oman

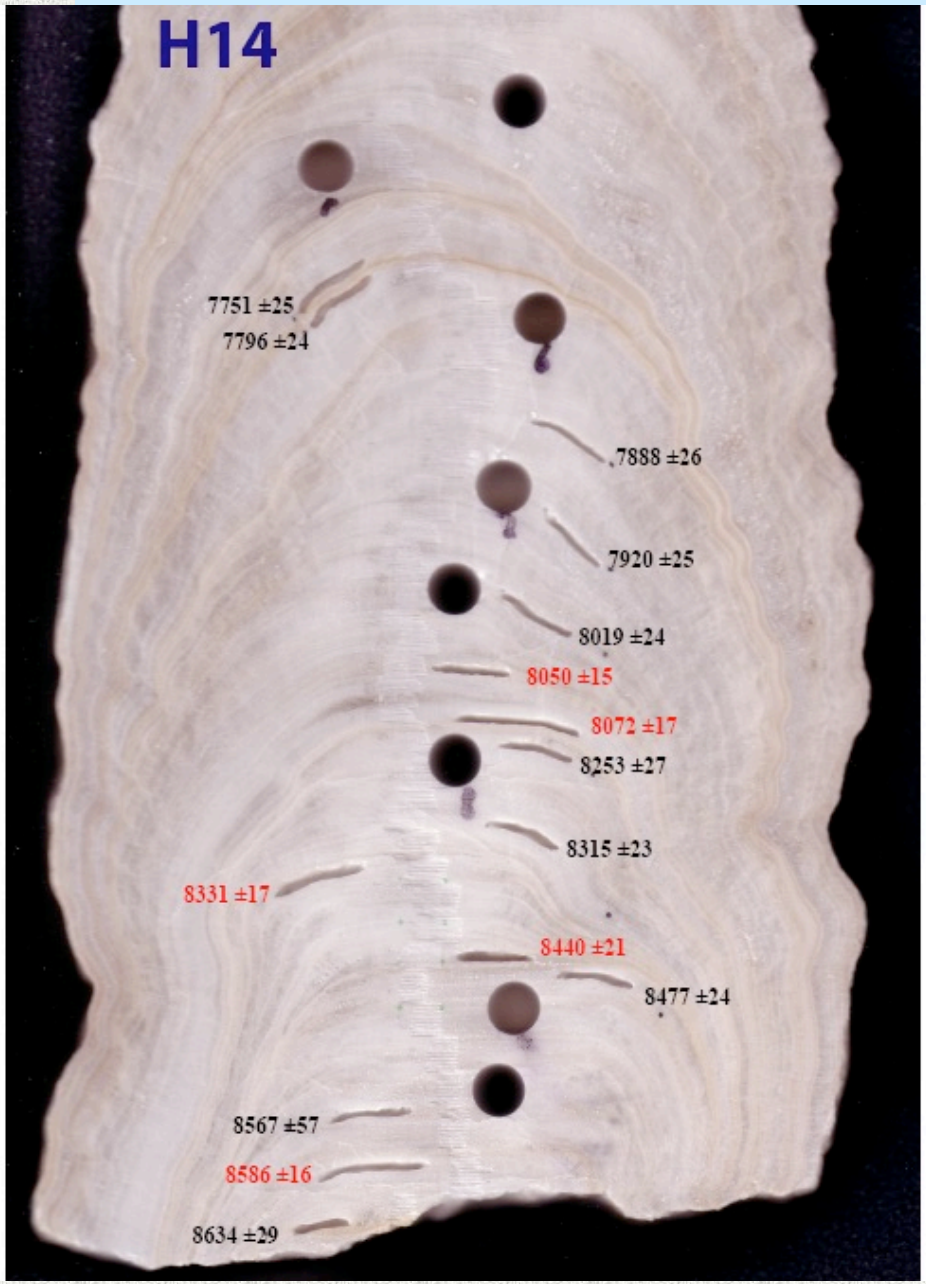

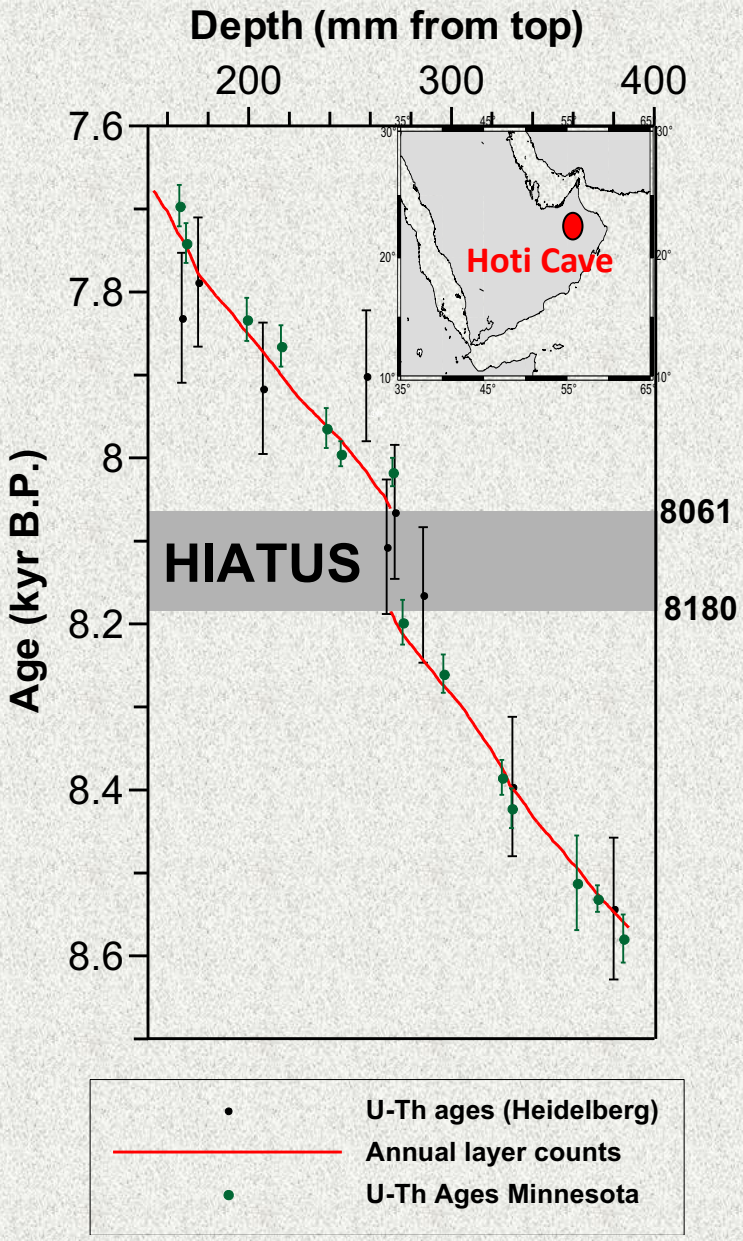

Source: *Dominik Fleitmann (Personal communication)*

Relación temporal entre los eventos de Dansgaard-Oeschger (DO) y los Máximos Isotópicos Antárticos (AIM).

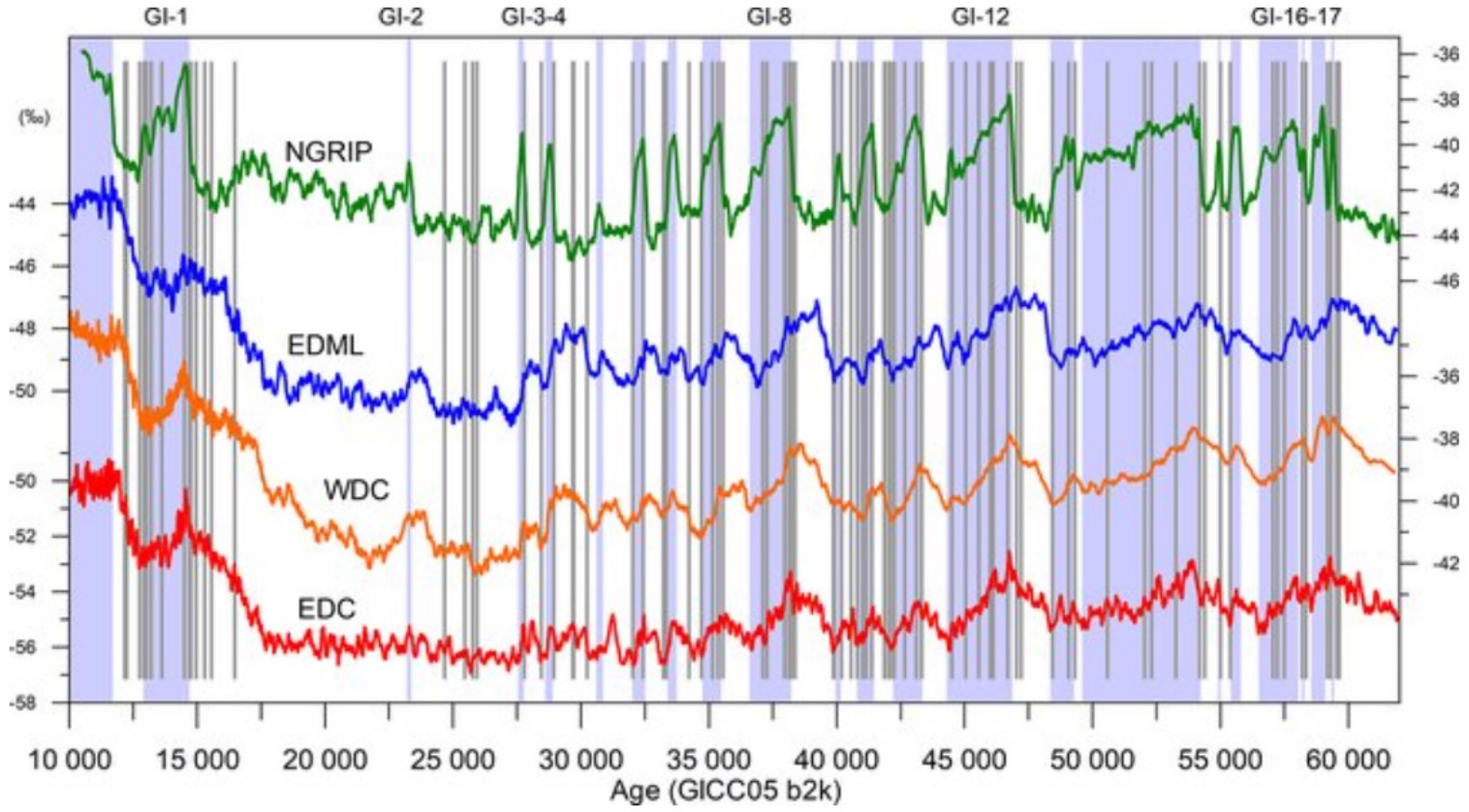

AMOC= Atlantic Meridional Overturning Circulation

Circulación Meridional de Retorno del Atlántico Norte

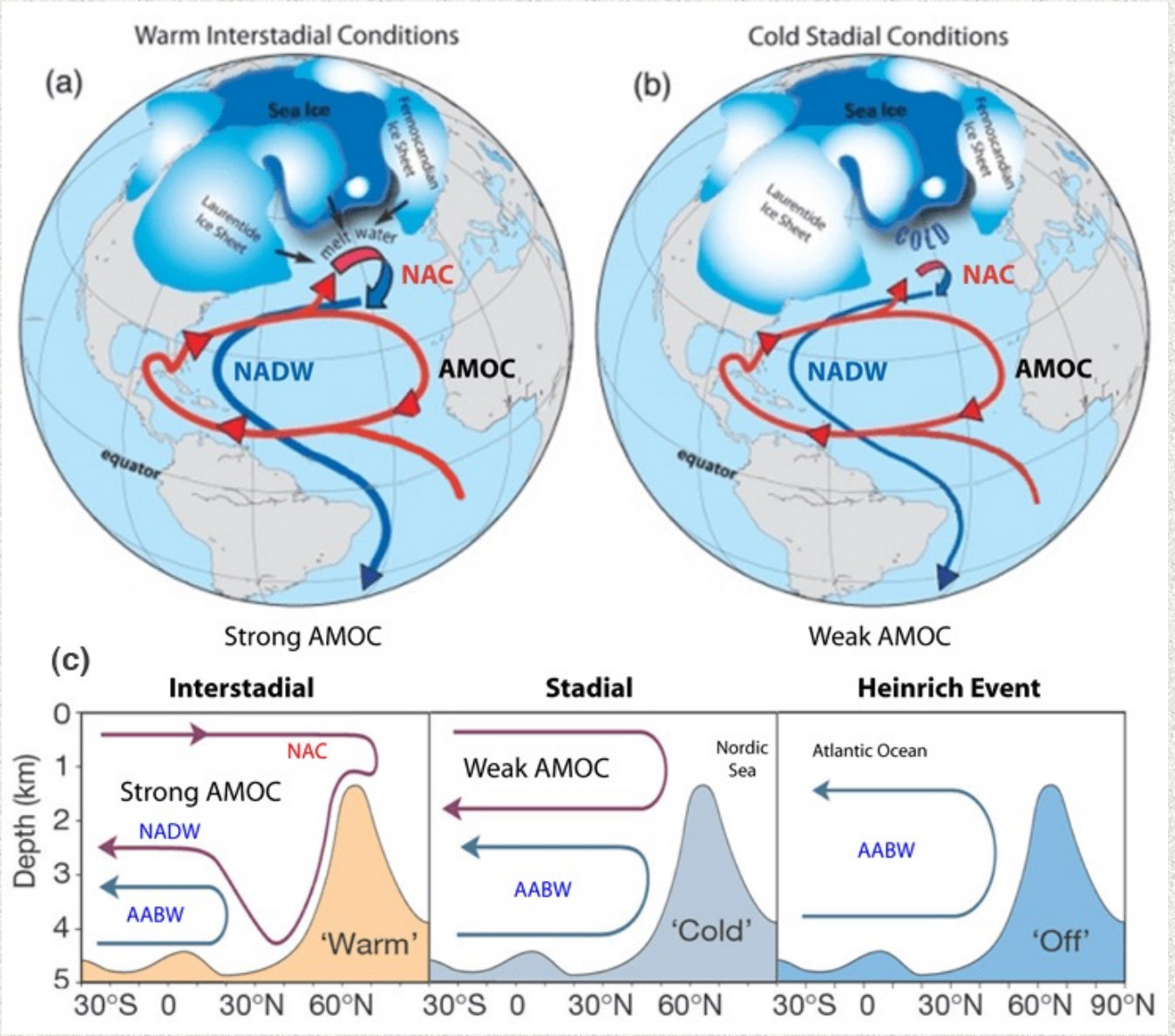

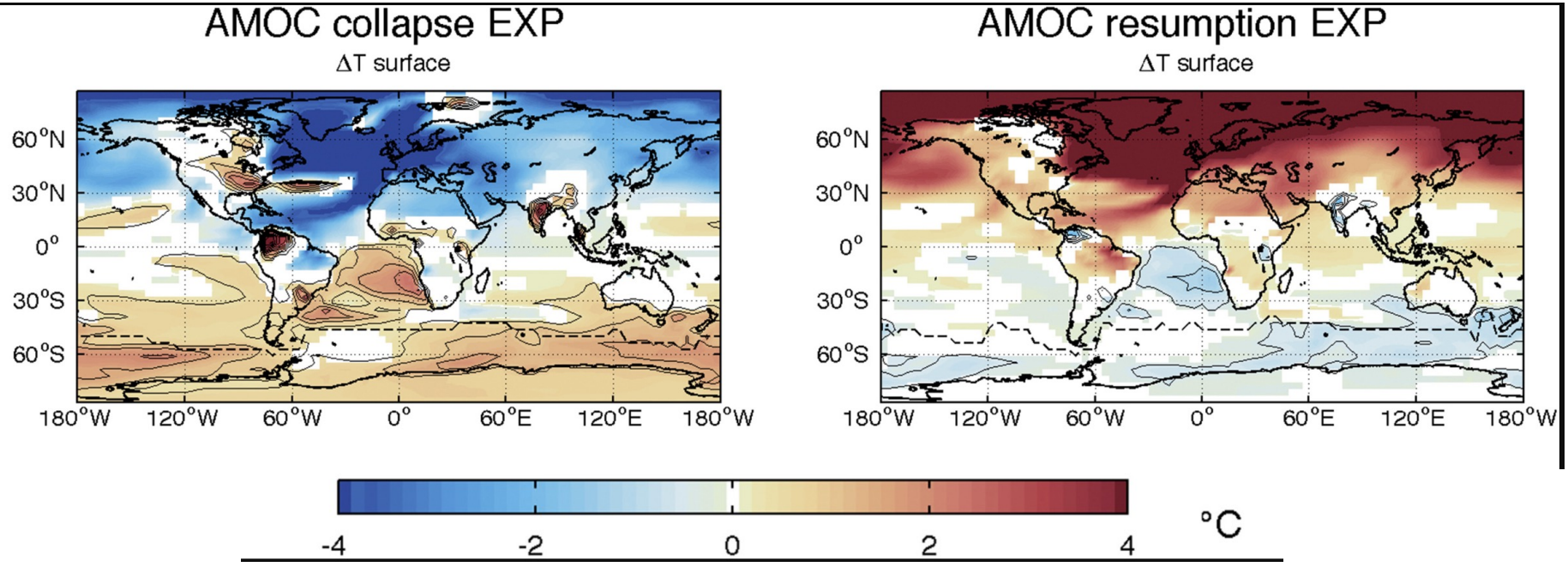

La hipótesis del balancín oceánico bipolar (Bipolar seesaw) térmico fue propuesta por Stocker y Johnsen (2003) como el "modelo termodinámico más simple posible" para explicar la relación temporal entre los eventos de Dansgaard-Oeschger (DO) y los Máximos Isotópicos Antárticos (AIM).

Source: Joel B. Pedro et al., QSR 2018

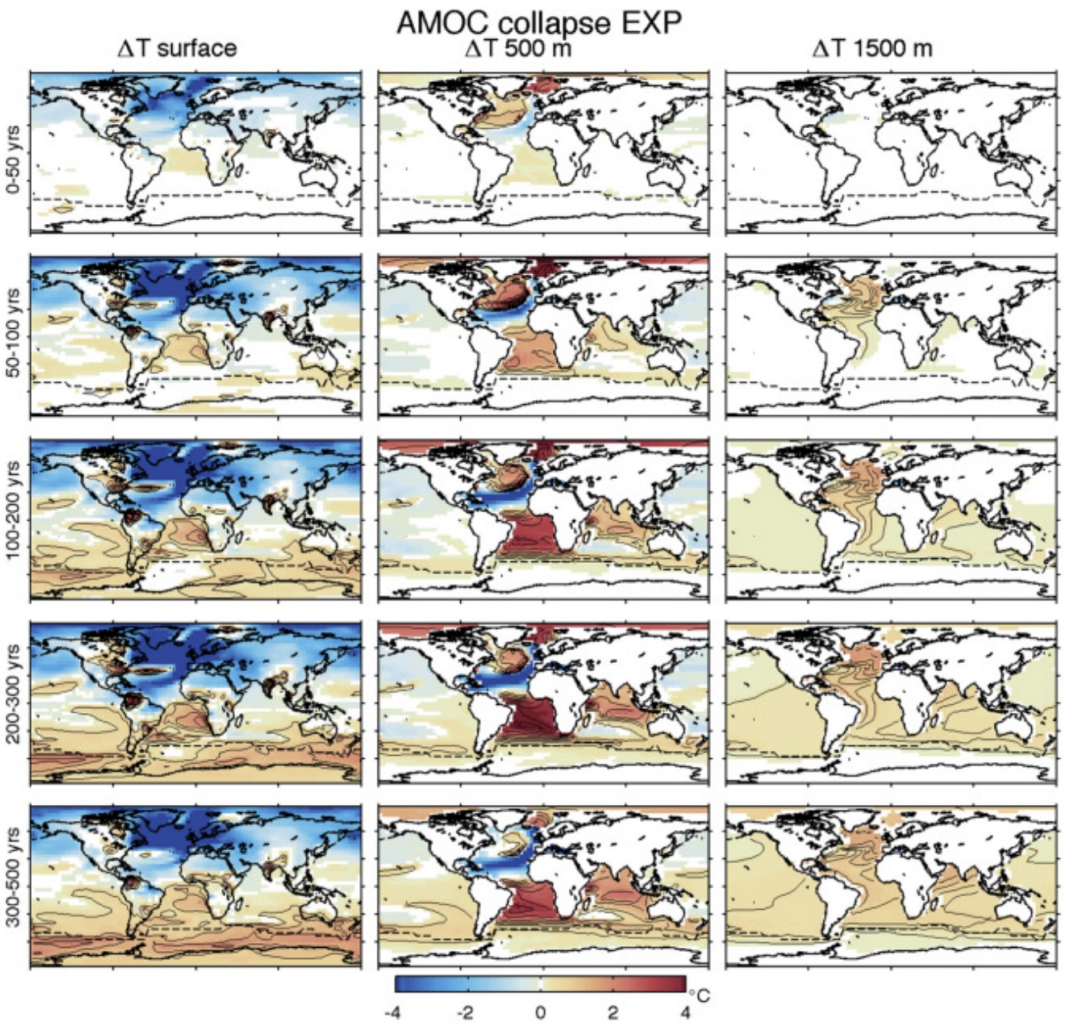

Source: Joel B. Pedro et al., QSR 2018

- The global ocean, not the Southern Ocean, accumulates heat when the AMOC collapses.
- Eddies gradually mix the heat anomalies across the Antarctic Circumpolar Current, melting sea ice.
- Ice-albedo feedback amplifies surface warming, increasing heat flux to Antarctica.

Forcing can be considered on several timescales:

Orbital –Milankovic (eccentricity/obliquity/precession)
~100,000; 40,000; 23,000/19,000 years

Millennial
solar irradiance
thermohaline oscillations ("internal" variability?)

Decadal-to-interannual
volcanic
ENSO/NAO/PDO ("internal" variability?)

Feedbacks? Vegetation/hydrological changes; snow/sea-ice cover

Puyehue, Chile: June 2011

UMASS AMHERST
Geosciences

CLIMATE SYSTEM RESEARCH CENTER

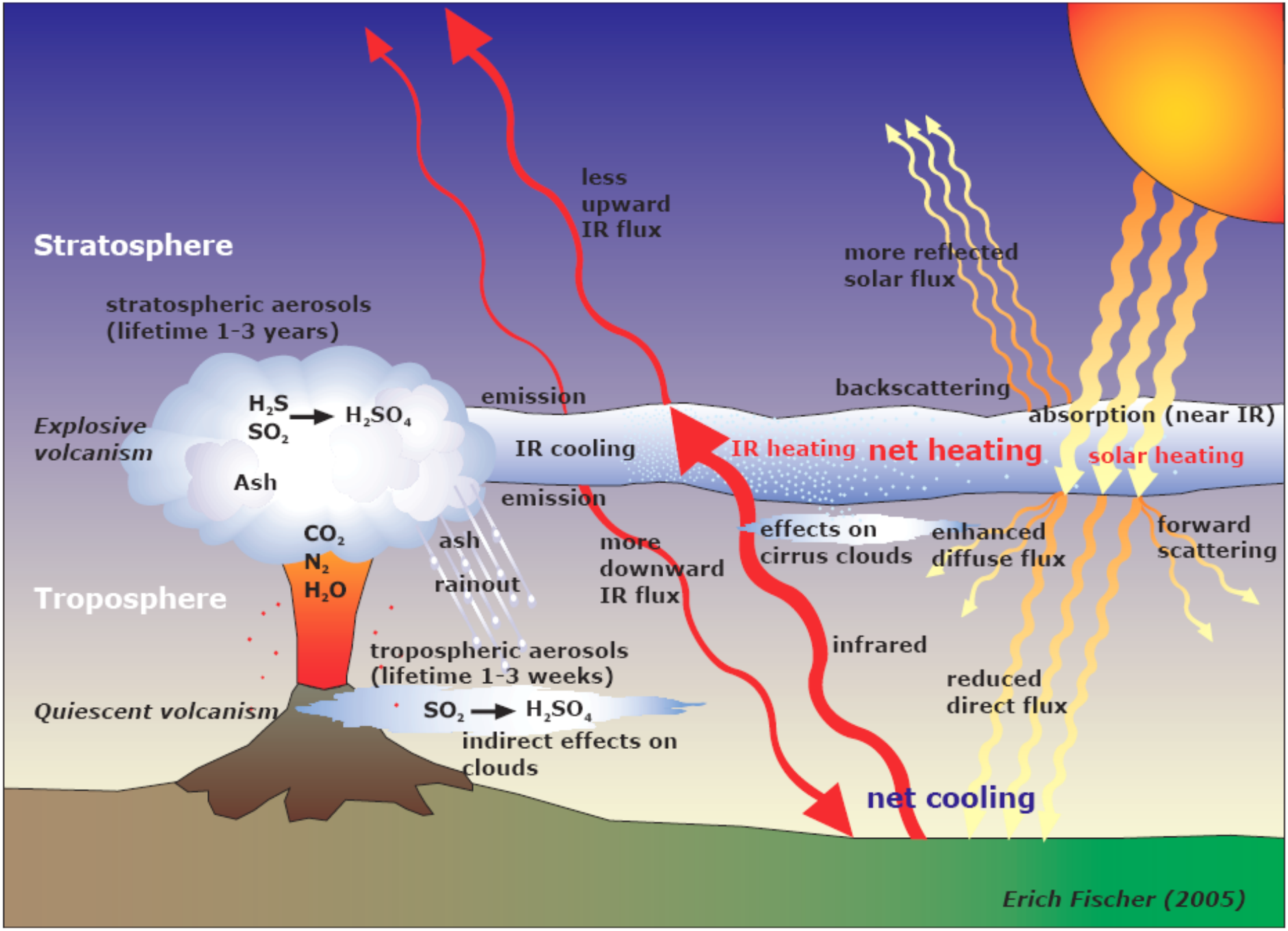

Source: *Robock, 2000*

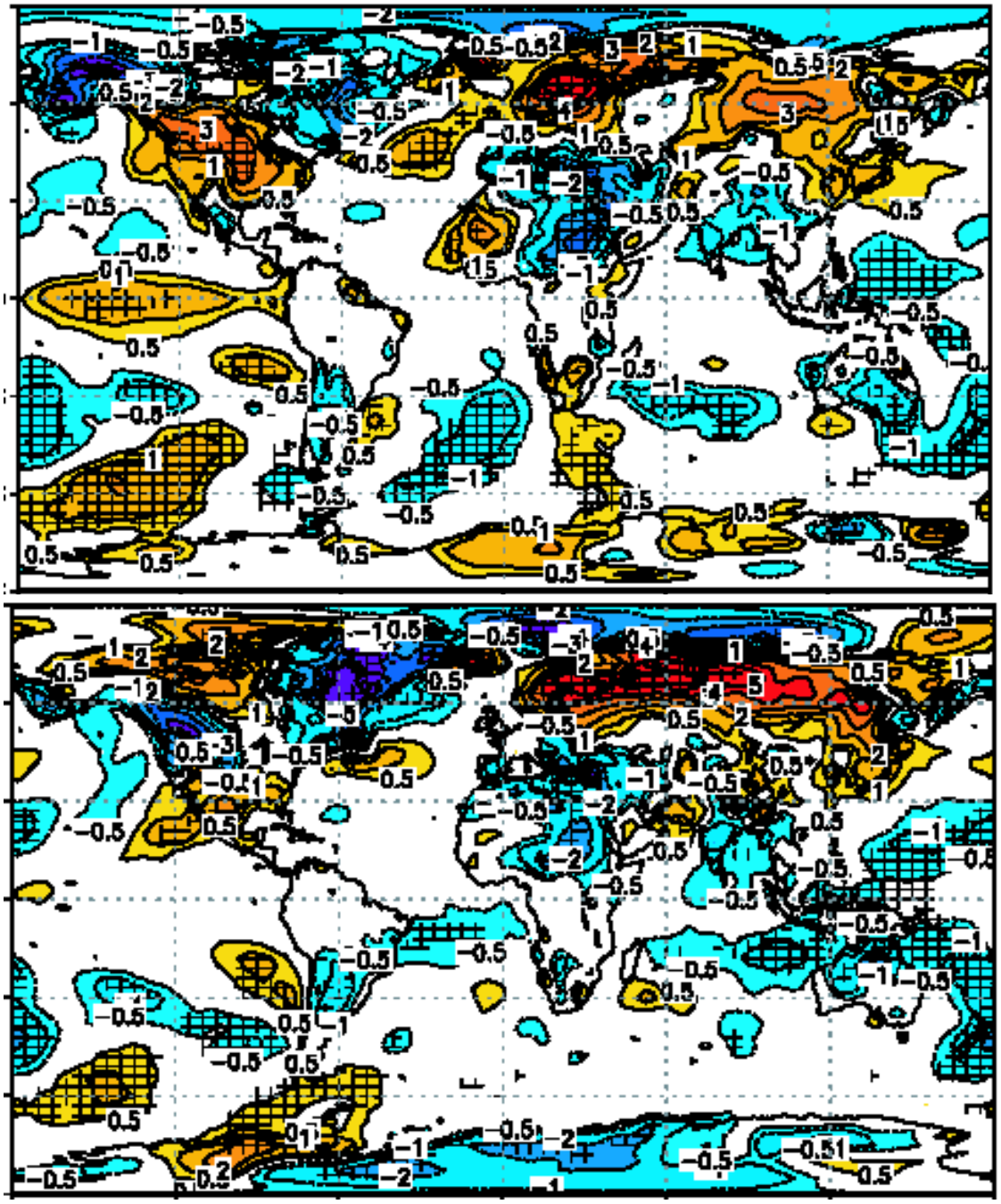

Pinatubo volcanic effect

NCEP (DJF) surface temperature anomalies 1991/92 & 1992/93 (relative to 1985-90)

Source: *Stenchikov et al., 2002*

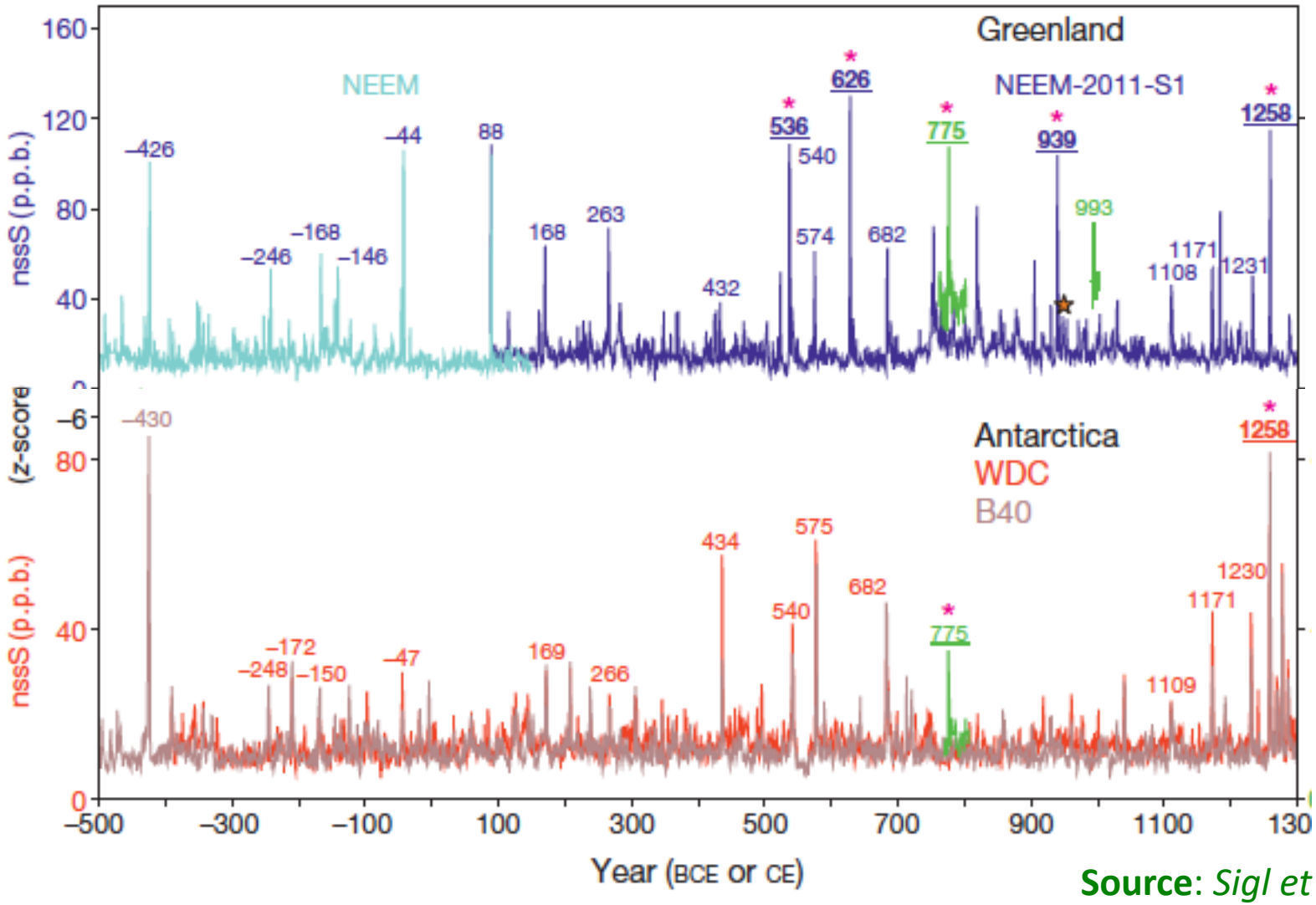

Source: *Sigl et al., 2015*

UMASS AMHERST
Geosciences

CLIMATE SYSTEM RESEARCH CENTER

Tree-ring chronology temperature reconstruction

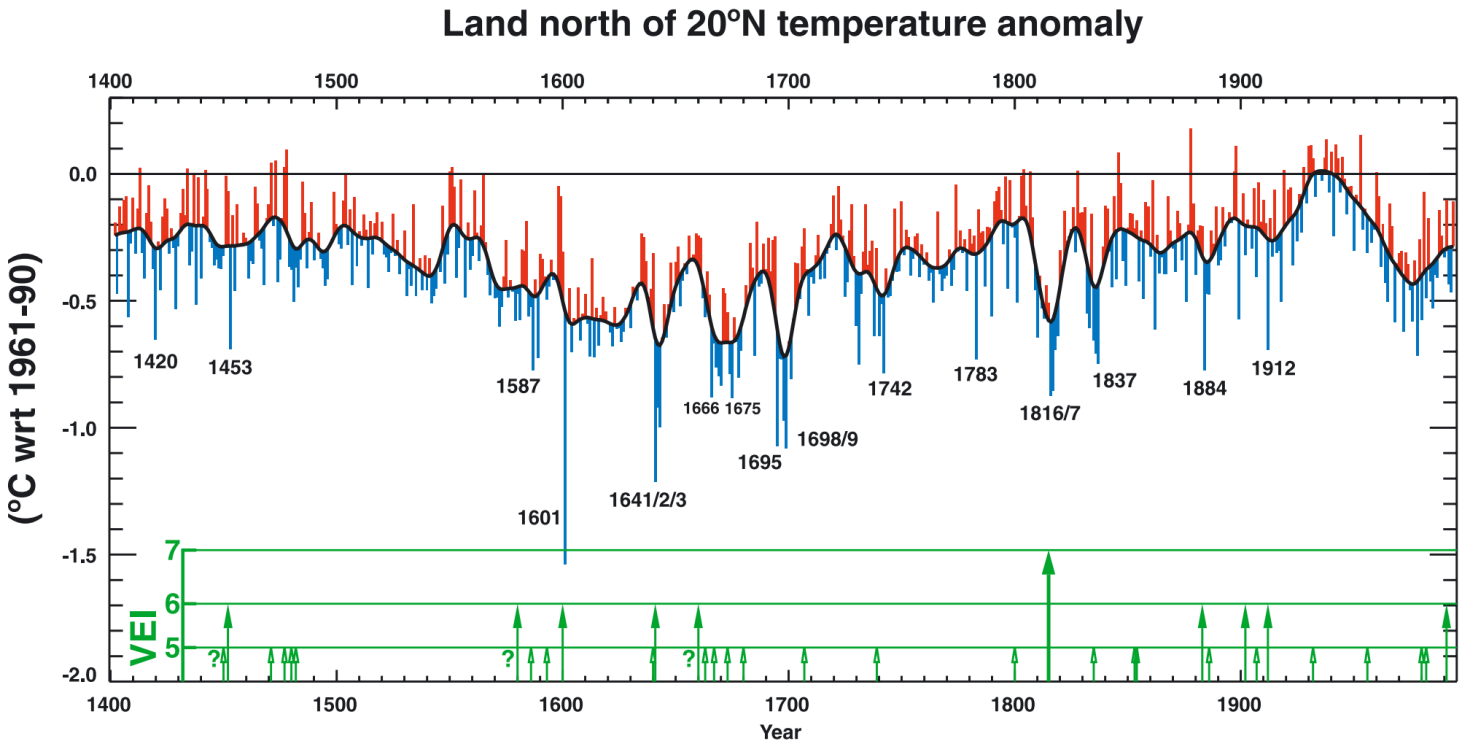

Fig. 5. Estimates of warm-season temperature (°C anomalies from the 1961–1990 mean) for land areas north of 20°N. The smoothed curve is the 25-year low-pass filtered reconstruction produced using the Age-Band Decomposition approach of Briffa et al. (2001). The Volcanic Explosivity Index (VEI) is indicated by the arrows at the bottom; '?' marks those eruptions whose date is uncertain.

Source: *Briffa et al. 2004*

Stalagmite H12 $\delta^{18}O$-profile: Hoti Cave, Oman

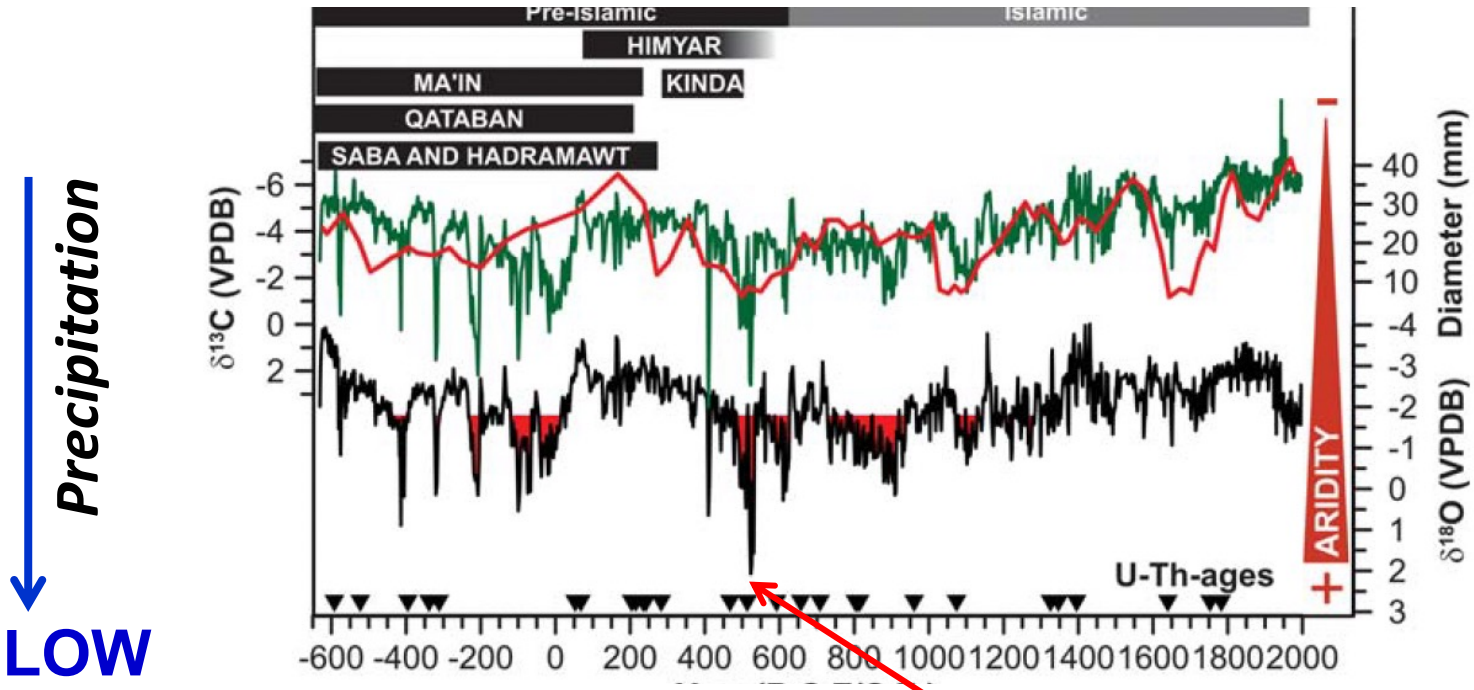

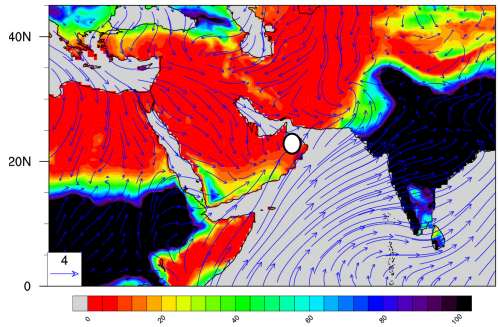

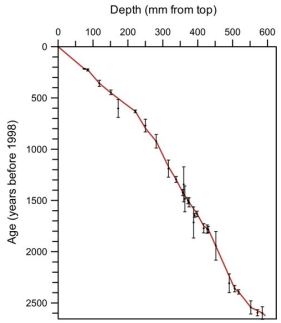

~A.D. 525±20

Source: *Fleitmann et al.Science 2022*

UMASS AMHERST Geosciences

CLIMATE SYSTEM RESEARCH CENTER

Summer monsoon rainfall in Central China

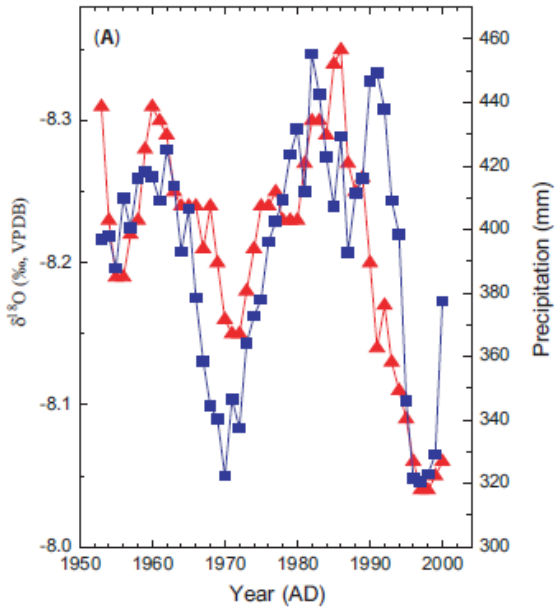

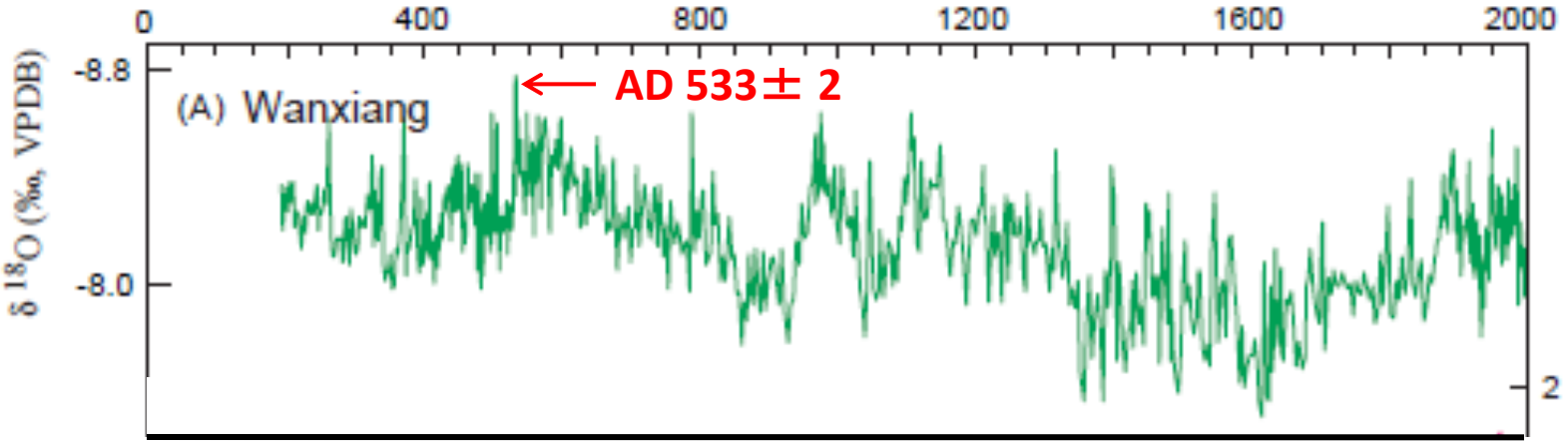

Wetter?

Source: *Zhang et al., 2008*

Global volcanic aerosol forcing and Northern Hemisphere temperature variations for the past 2,500 years

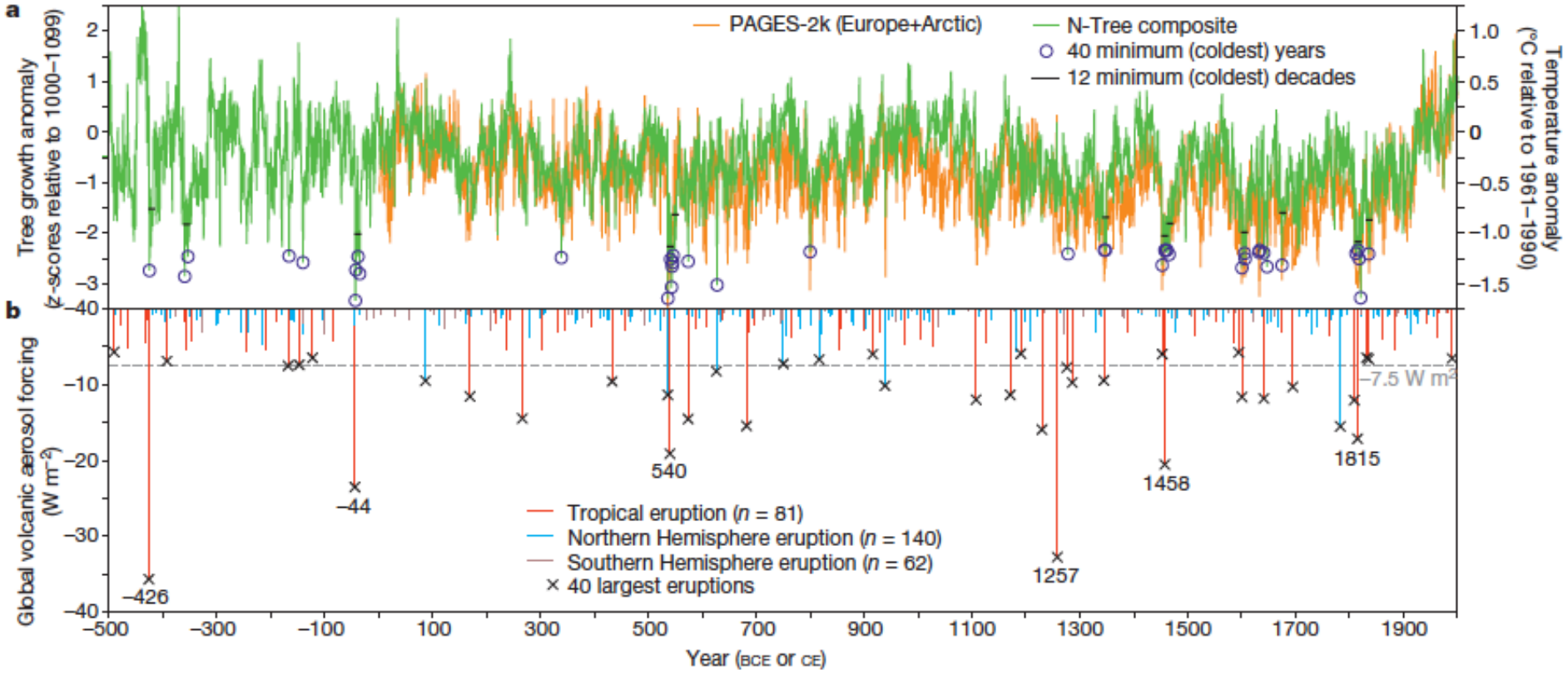

Source: *Sigl et al., 2015*

UMASS AMHERST
Geosciences

CLIMATE SYSTEM RESEARCH CENTER

Anthropogenic Increase: Records Over the Last Millennium

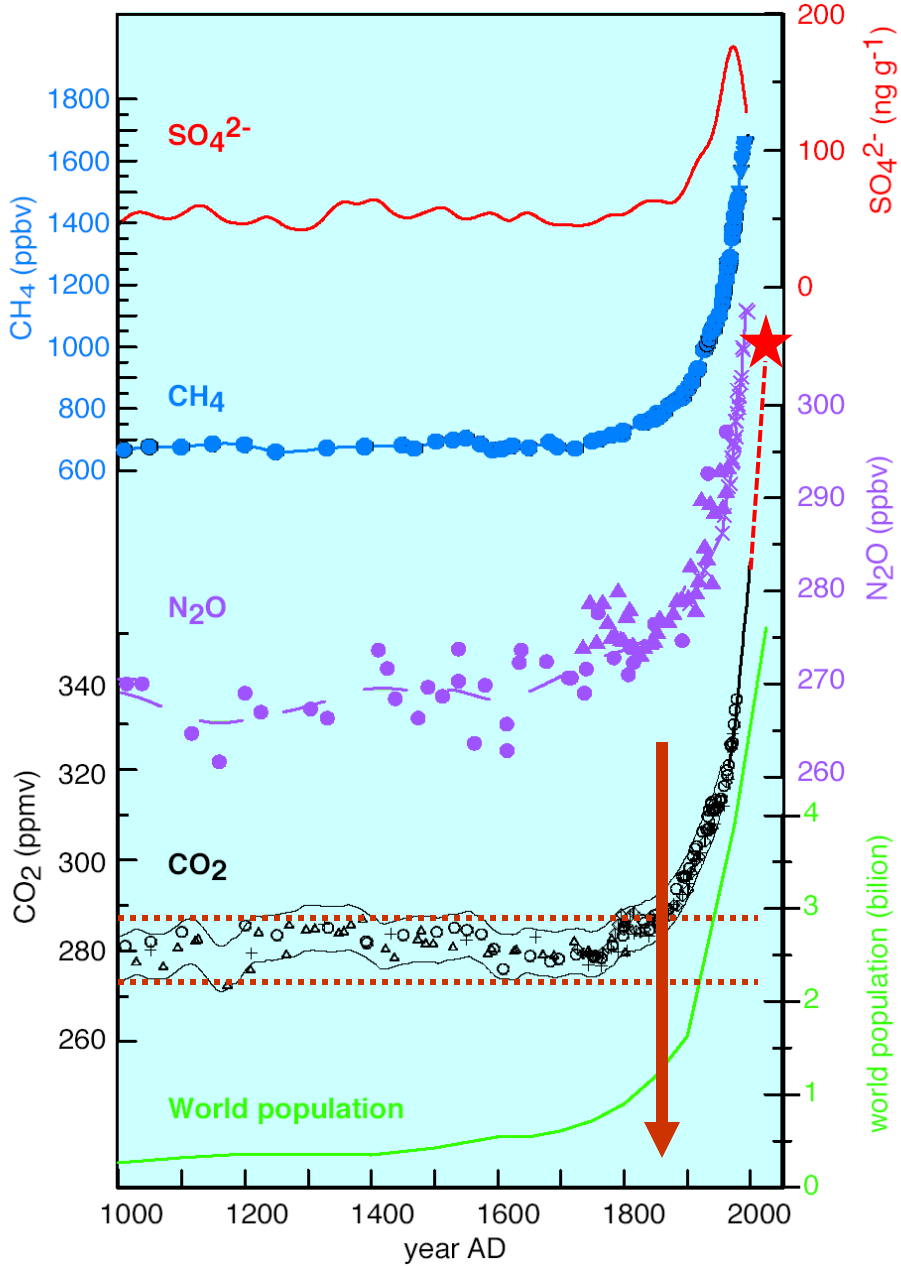

The Anthropocene

Source: *Raynaud et al., 2003*

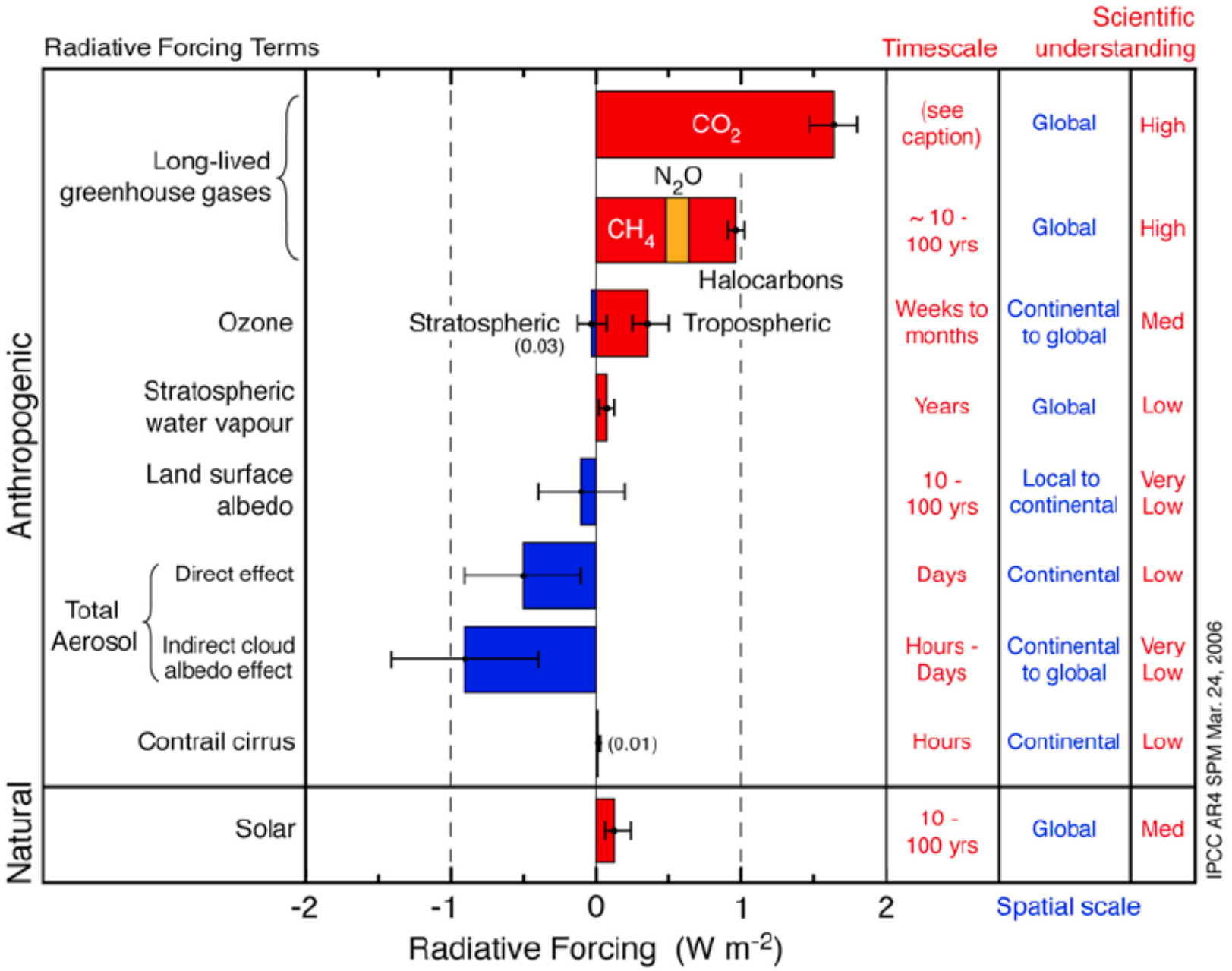

Source: *IPCC 4th Assessment Report, 2006*

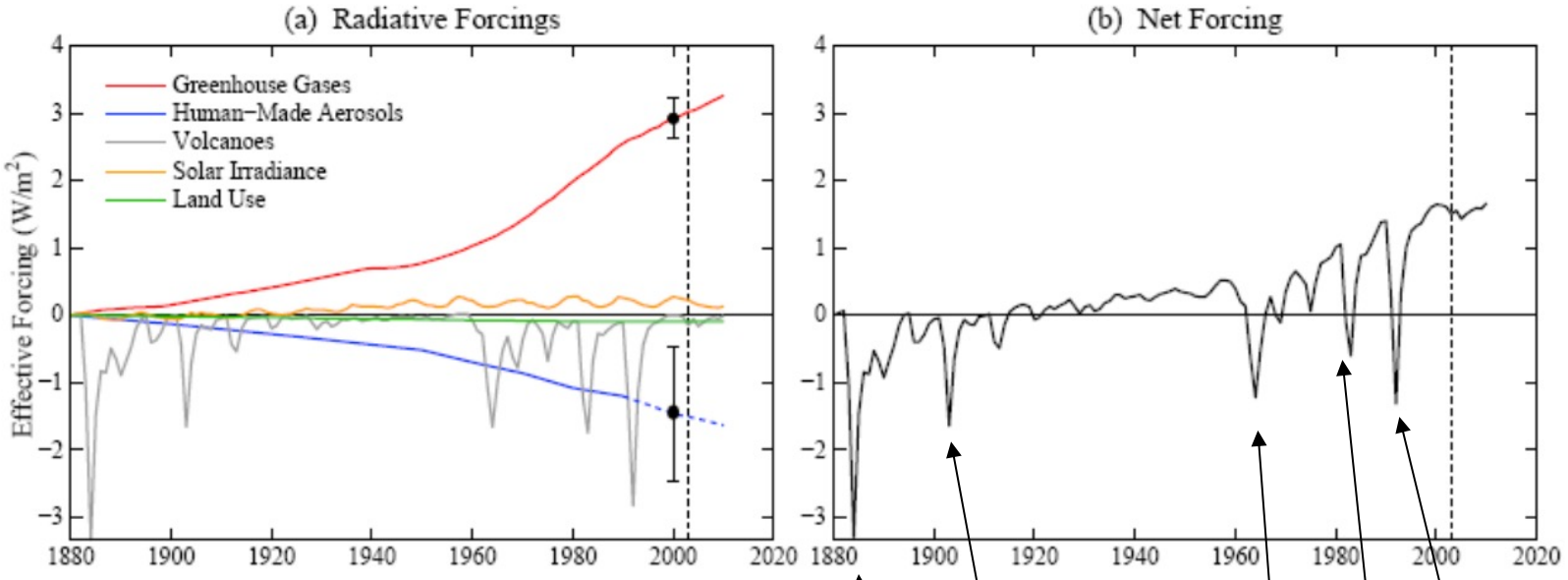

Fig. 1. Climate forcings employed in this paper. Forcings through 2003 (vertical line) are the same as used by Hansen et al. (2007), except the tropospheric aerosol forcing after 1990 is approximated as −0.5 times the GHG forcing. Aerosol forcing includes all aerosol effects, including indirect effects on clouds and snow albedo. GHGs include O_3 and stratospheric H_2O, in addition to well-mixed GHGs. These data are available at http://www.columbia.edu/~mhs119/EnergyImbalance/Imbalance.Fig01.txt.

Krakatoa

Santa María

Agung

Chichonal

Pinatubo

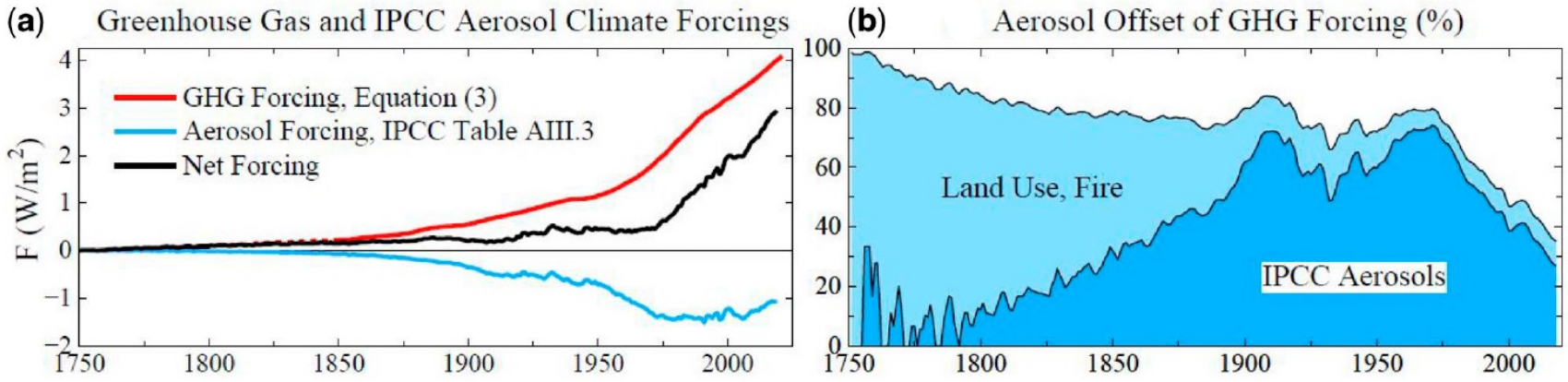

Figure 17. (a) Estimated greenhouse gas and aerosol forcings relative to 1750 values. (b) Aerosol forcing as percent of GHG forcing. Forcings for dark blue area are relative to 1750. Light blue area adds 0.5 W/m^2 forcing estimated for human-caused aerosols from fires, biofuels and land use.

Temperaturas medias globales basadas en datos continentales y oceanicos

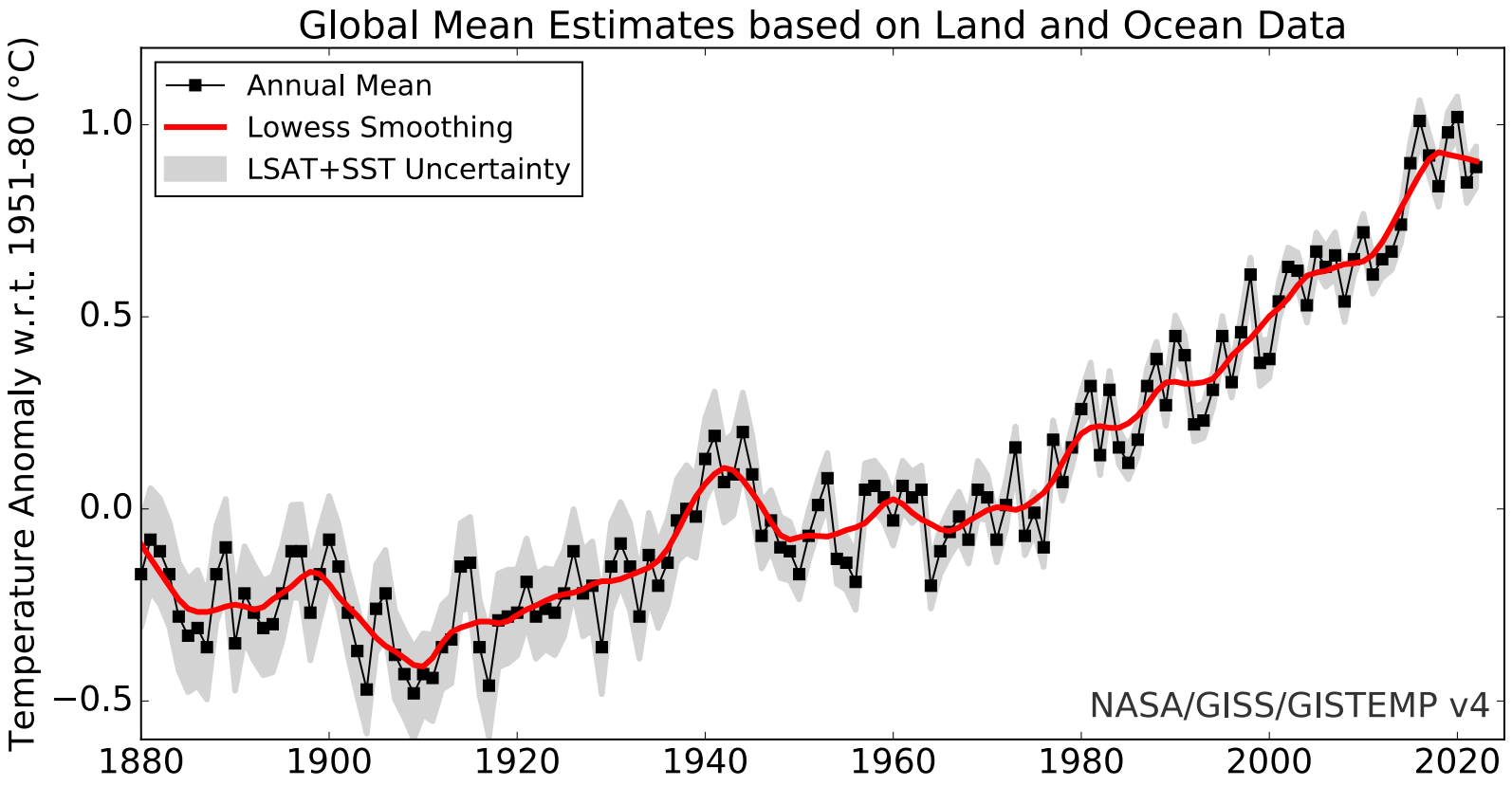

Reference period: 1951-1980

Source: NASA GISS

UMASS AMHERST

CLIMATE SYSTEM RESEARCH CENTER

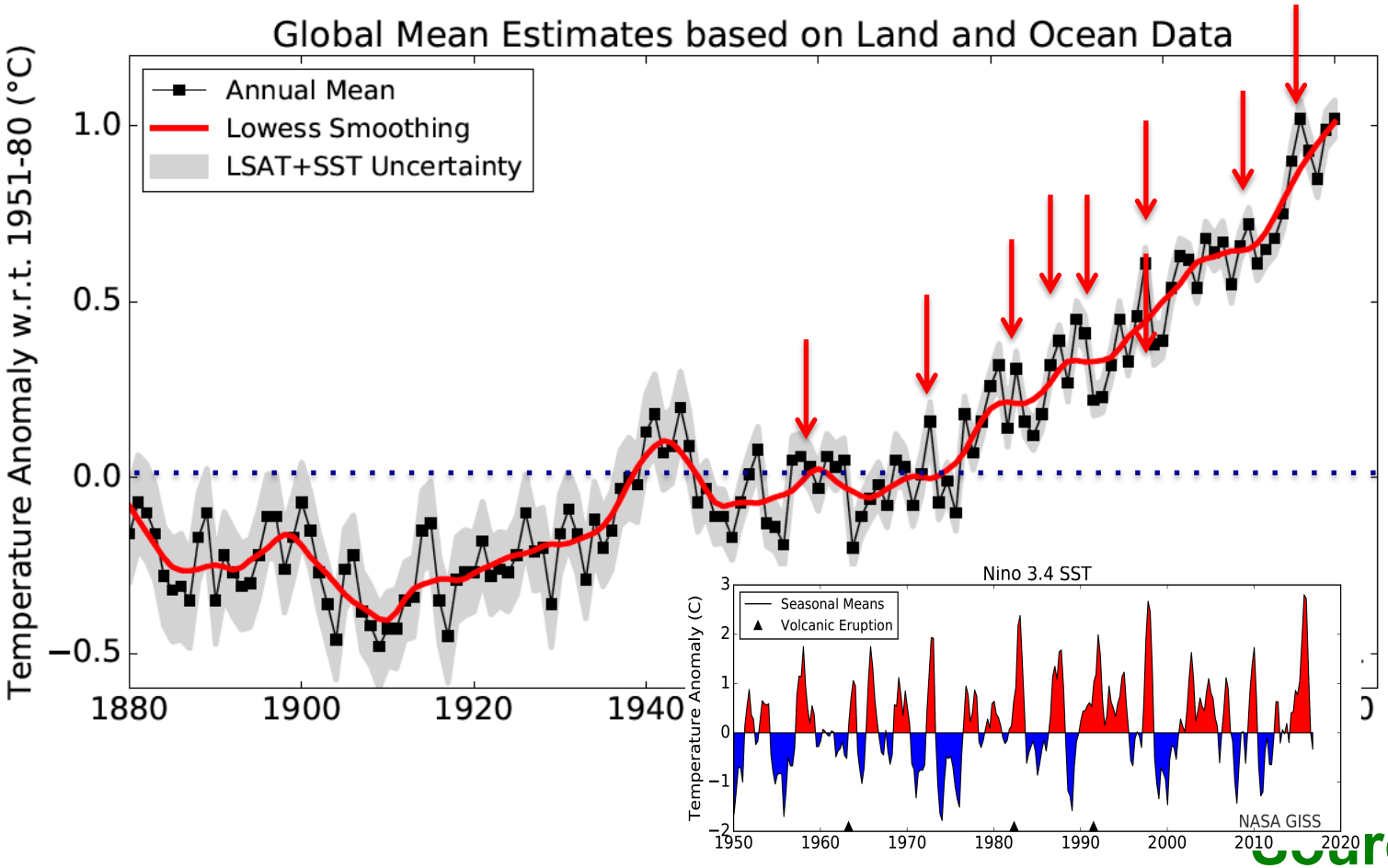

El Niño

La Niña

Source: NASA GISS

UMASS AMHERST

CLIMATE SYSTEM RESEARCH CENTER

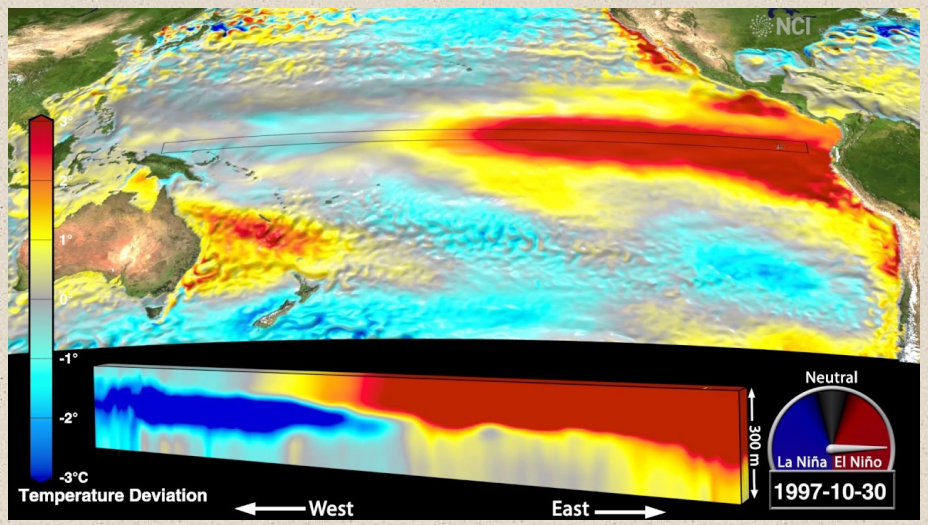
NCI
3°
1°
0
-1°
-2°
-3°C
Temperature Deviation
West
East
300 m
Neutral
La Niña
El Niño
1997-10-30

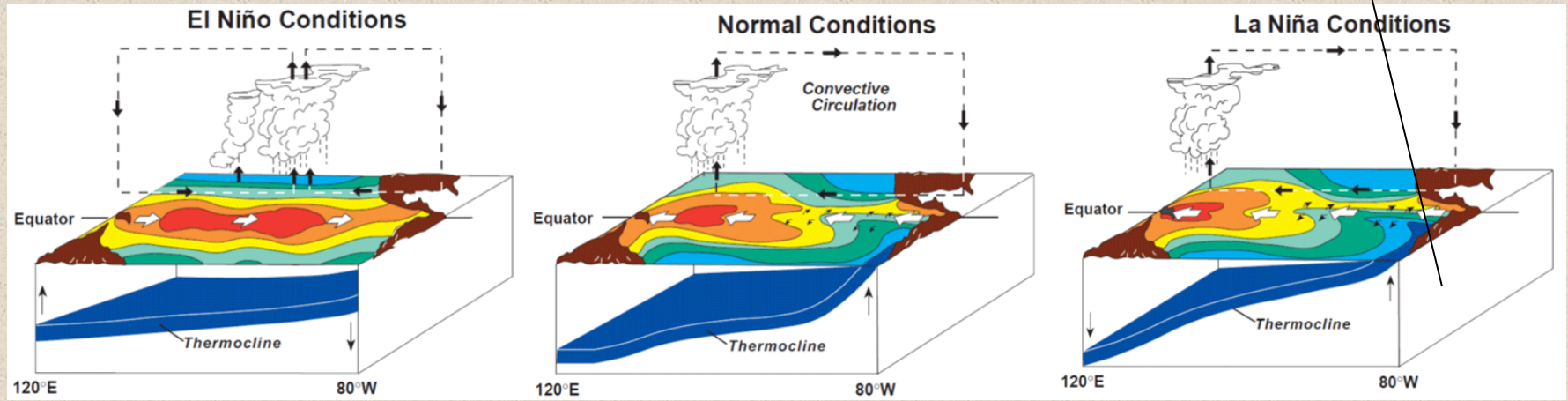
El Niño Conditions
Equator
Thermocline
120°E
80°W
Normal Conditions
Convective Circulation
Equator
Thermocline
120°E
80°W
La Niña Conditions
Equator
Thermocline
120°E
80°W